Introduction to Atom Probe Tomography: characterization of nanostructures

Alain Portavoce
CNRS, Aix-Marseille University, IM2NP, case 142, 13397 Marseille, France

PULSE School: Epitaxy updates and promises, Porquerolles, 14-18 September 2015

Outline

- Introduction
  - nanotechnology ⇒ nano-characterizations!
- Electric Field-mediated evaporation
- Atom Probe Tomography experiments
  - APT measurements
  - 3D reconstruction
- Sample preparation
- APT data analysis
- APT: some issues

Introduction

Nanotechnology

- Ultra-thin films
- Nanocrystalline materials
- Nano-wire
- Nano-islands
- …

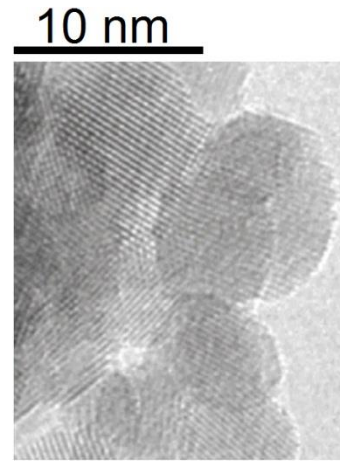

Nanocrystalline
Si films

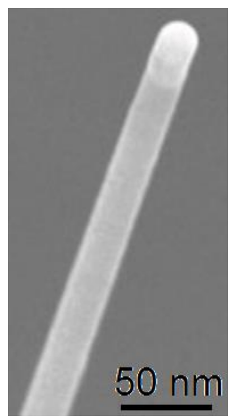

Si nano-wires

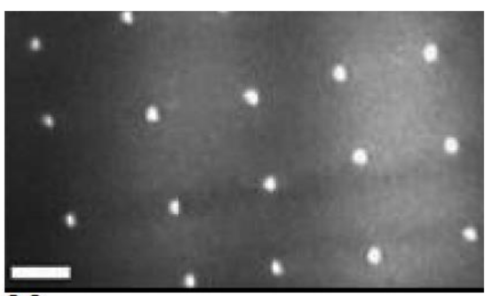

100 nm Ge quantum dots

Applications

- Microelectronic
- Solar cells
- …

Introduction

Nano-materials + nano-objects (10 to 100 nm)
⇒ 3D characterizations (nano-grains, dots, wires…)

- ➢ Composition /stress
- ➢ Defects in nanostructures (dislocations, clusters…)
- ➢ Interfaces
- ➢ Variations versus directions (3D)

Nano-characterizations

- Structure
2D analysis: HRTEM, HRSEM…; 3D analysis: STM, AFM…)

- Composition
2D analysis: STEM, nano-AES,…; 3D analysis?
⇒ APT = 3D chemical analysis at the atomic scale

Introduction: microelectronics

Nanocrystalline layers

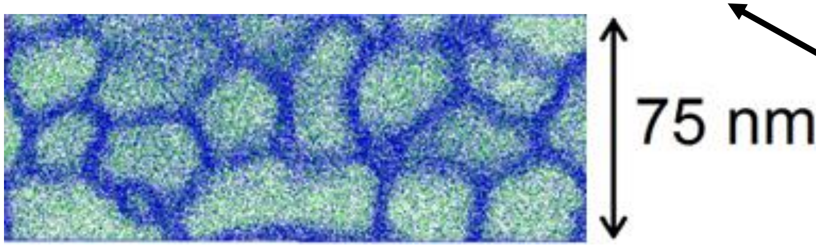

APT measurements
Pt segregation in Ni_2Si GBs

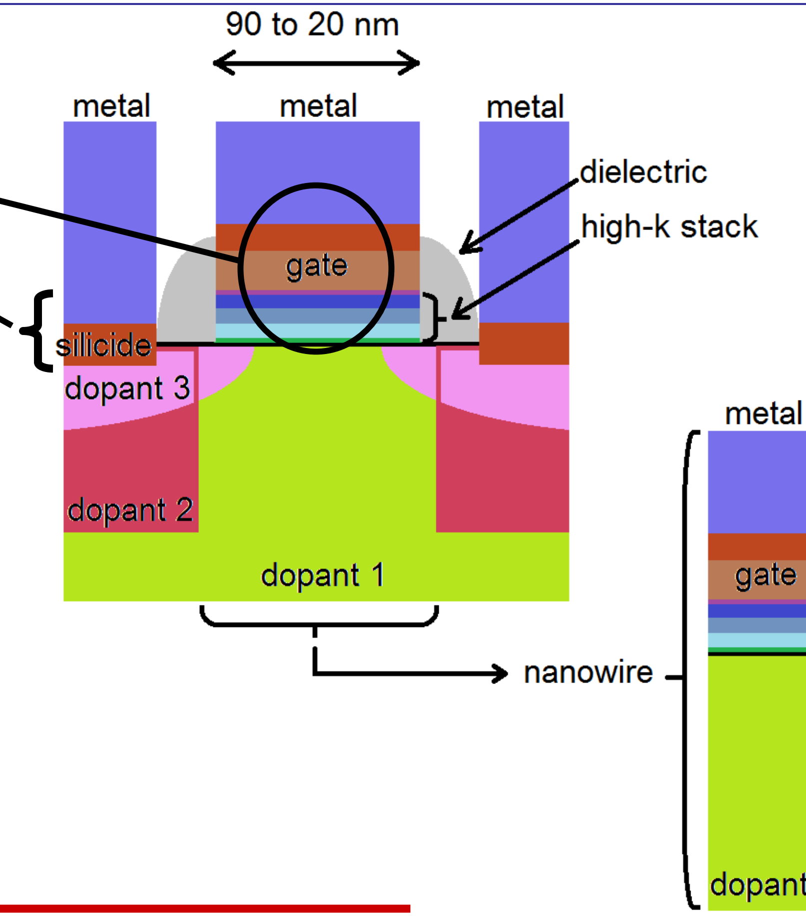

Nanotechnology

- Reduction of material volume and film thickness
- Increase of the number of interfaces (+ stress)

Im2np
Institut Matériaux Microélectronique Nanosciences de Provence
UMR 6242 CNRS, Universités Paul Cézanne, Provence et Sud Toulon-Var

Introduction

Atom Probe Tomography Microscopy

- Chemical analysis of 3D volumes
- Atomic scale
- No need of composition calibrations
- Composition of interfaces and defects (dislocations, clusters…)
- Can be directly compared to 3D simulations at the atomic scale (Molecular Dynamics, Monte Carlo)

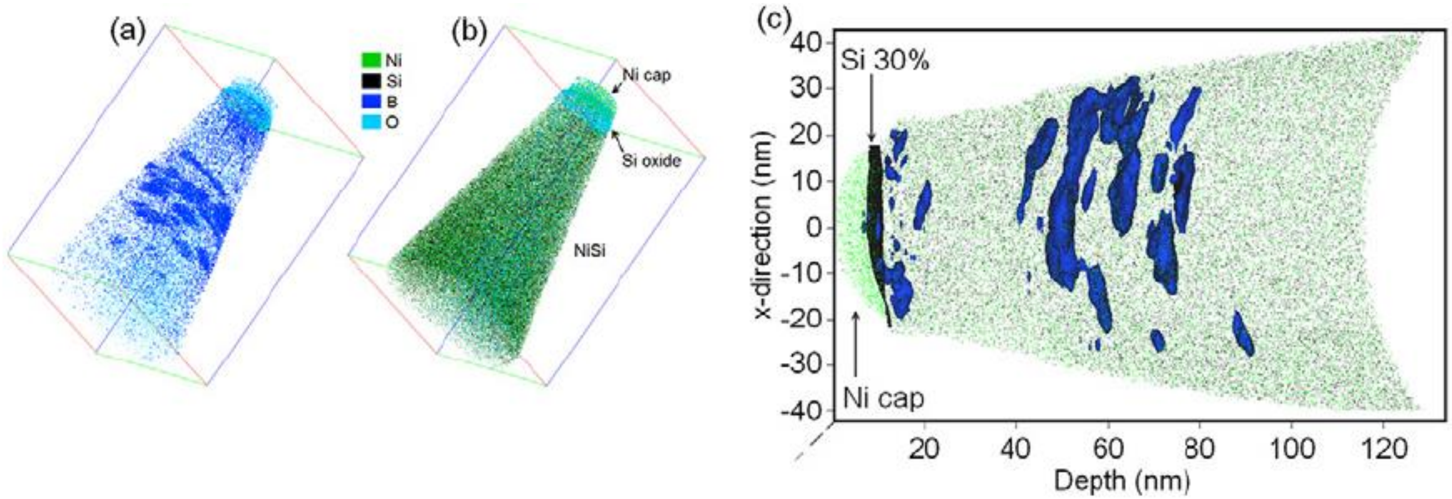

Punctual electrical charge

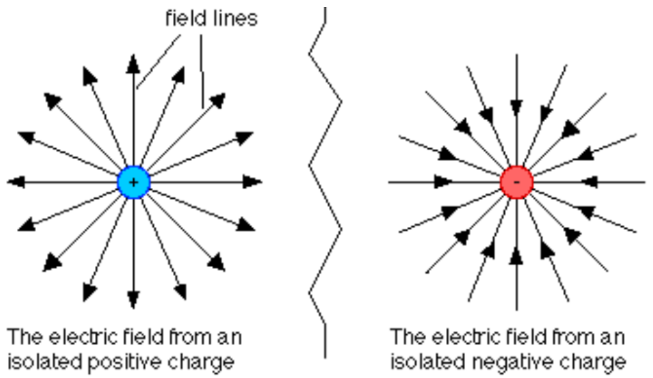

$$\vec{F} = \frac{q}{4\pi\varepsilon_0 r^2}\hat{r} \qquad V = \frac{q}{4\pi\varepsilon_0 r} \qquad F = \frac{V}{r}$$

$$\vec{f}_e = q'\vec{F} \qquad U = q'V = q'Fr$$

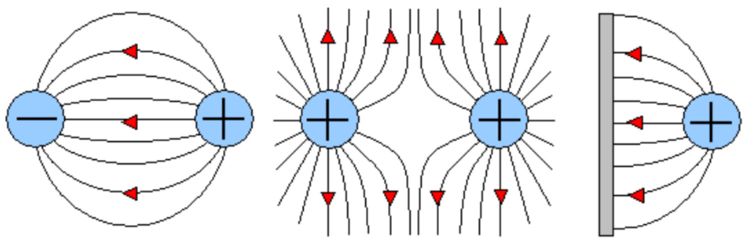

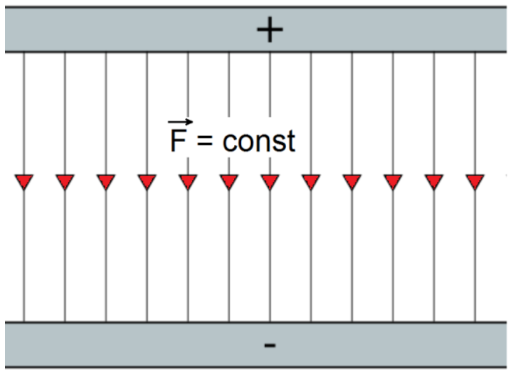

Punctual charge q in vacuum

F(r) = electrical field at the distance r from the charge q
V(r) = electrical potential at the distance r from the charge q
U(r) = electrical potential energy at the distance r from the charge q
f_e = electrical force applied on an other charge q' at a distance r from q

Field effect

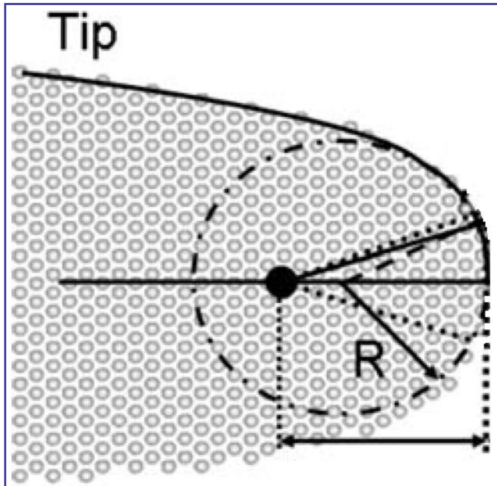

$$F = \frac{V}{k_f R}$$

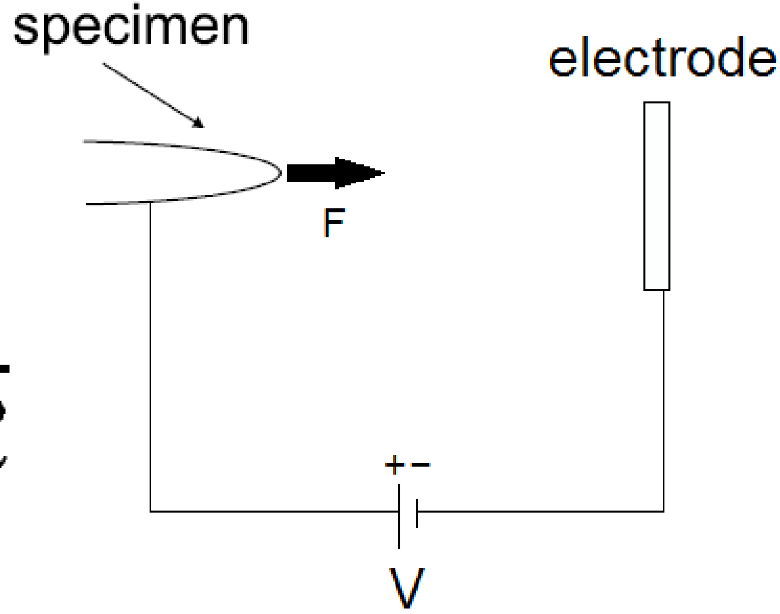

V = 10 kV, K_f = 5, R = 50 nm
$\Rightarrow F$ = 400000 kV/cm^2

Size effect on electrical field

V = applied voltage between the tip and the electrode
R = curvature radius of the tip (~ 50 nm)
K_f = considers the influence of the specimen/detector geometry ~ 2-7
F = electrical field on the surface tip

Atom probe tomography (APT)

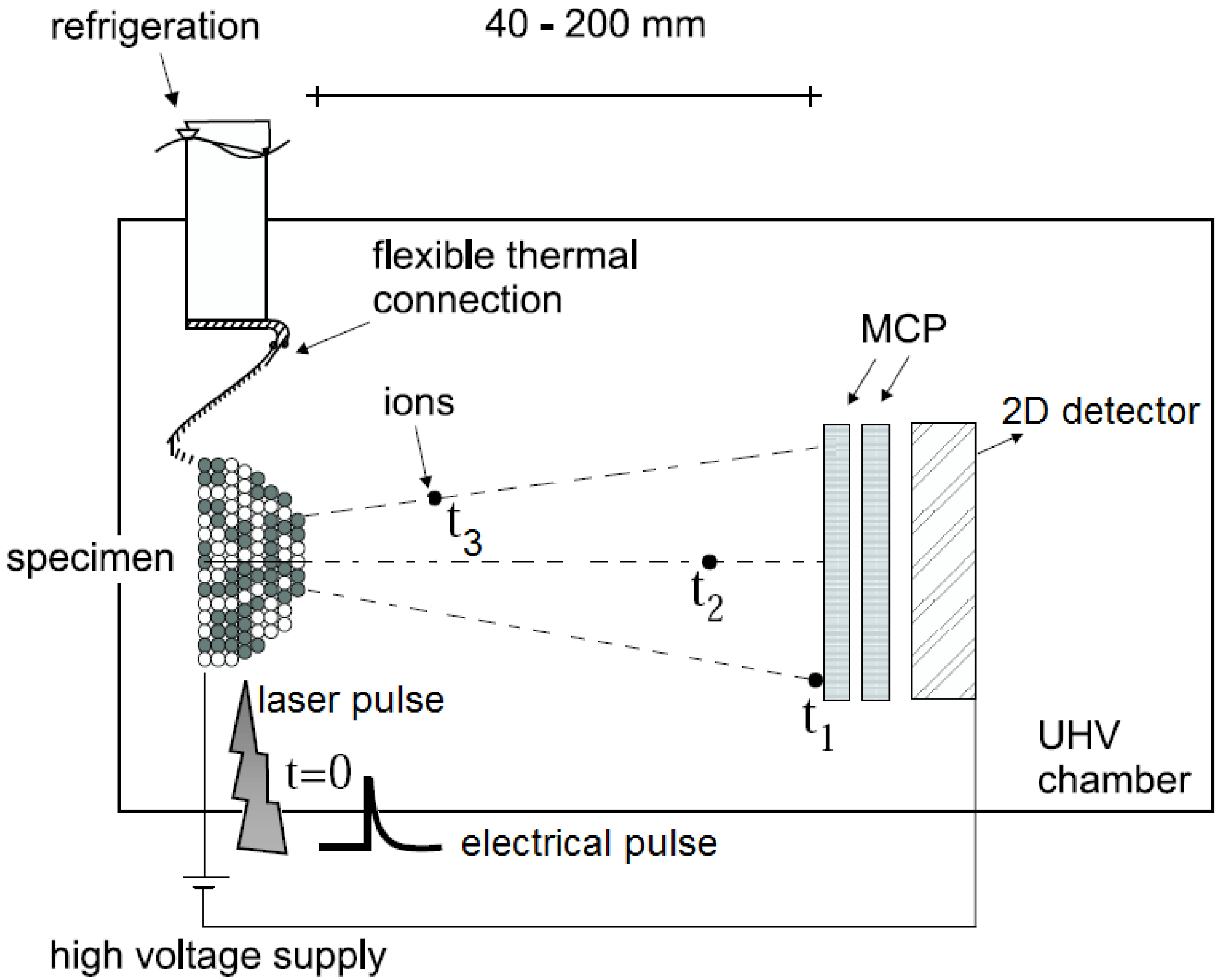

Ion evaporation: energy barrier

1/ Break the chemical bonds = Λ

2/ Ionize the atom n times = $\sum I_n$

3/ The n electrons back in the tip = $-n\Phi$

$$Q_0 = \Lambda + \sum_{j=1}^{n} I_j - n\Phi$$

Q_0 ~ 10th eV

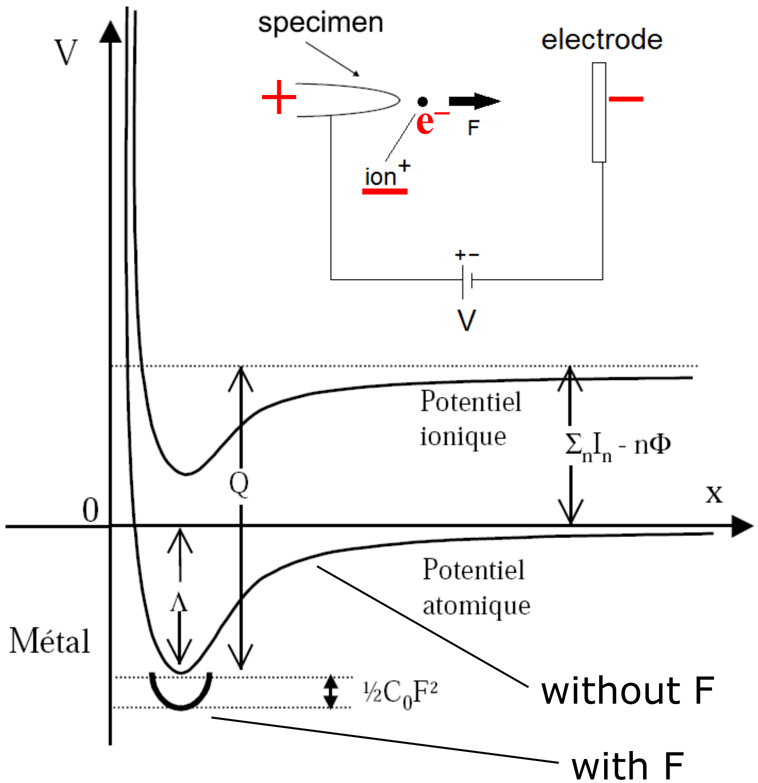

Electrical field mediated evaporation: thermally activated

Λ = heat of sublimation = total chemical bound energy of an atom of the tip
I_n = ionization energy of the nth electron
$\sum I_n$ = ionization energy of the free atom
Φ or φ_e = work function of the emitting surface

Field evaporation

The electrical field F allows to reduce the barrier $Q_0 \Rightarrow Q_n$

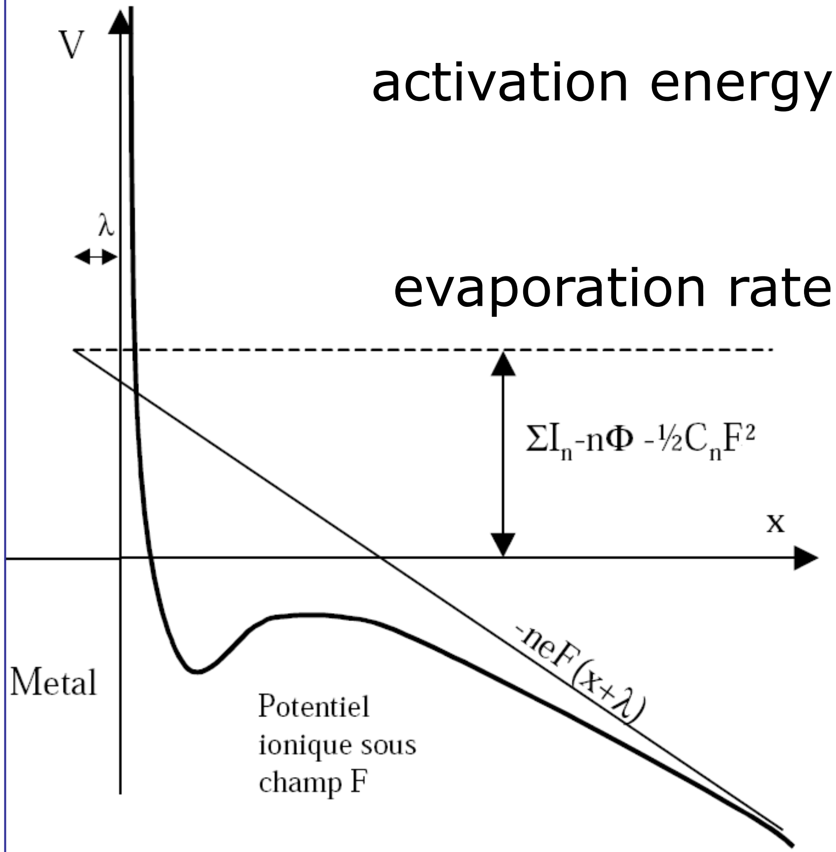

activation energy $\Rightarrow Q_n = \Lambda + \sum_n I_n - n\varphi_e - f(F_{dc})$

$$f(F_{dc}) = \gamma F_{dc}$$

evaporation rate $\Rightarrow \phi = \upsilon \exp(-Q_n/k_B T)$

The expression of the function $f(F_{dc})$ depends on models, but close to the threshold of evaporation, a linear behavior was experimentally observed $\Rightarrow f(F_{dc}) = \gamma F_{dc}$, with γ a material-dependent parameter

required time for evaporation $\Rightarrow \tau_{evap} = \tau_0 \exp(Q_n/k_B T)$

Field evaporation: Athermal model

$$Q_n = 0 \Leftrightarrow F_n \sim \left(\frac{4\pi\varepsilon_0}{n^3 e^3}\right) \times \left(\Lambda + \sum_{j=1}^{n} I_j - n\Phi\right)^2$$

$$F_n \sim \left(\frac{4\pi\varepsilon_0}{n^3 e^3}\right) \times Q_0^{\ 2}$$

Very low T (20-100 K) $\Rightarrow$ field evaporation only with $Q_n = 0$

Low temperature $Q_n \rightarrow 0$ to obtain elec. field mediated evaporation

F_n = evaporation field at zero activation energy = electrical field needed in order to cancel the activation energy!

Laser-pulsed APT: Thermal field evaporation

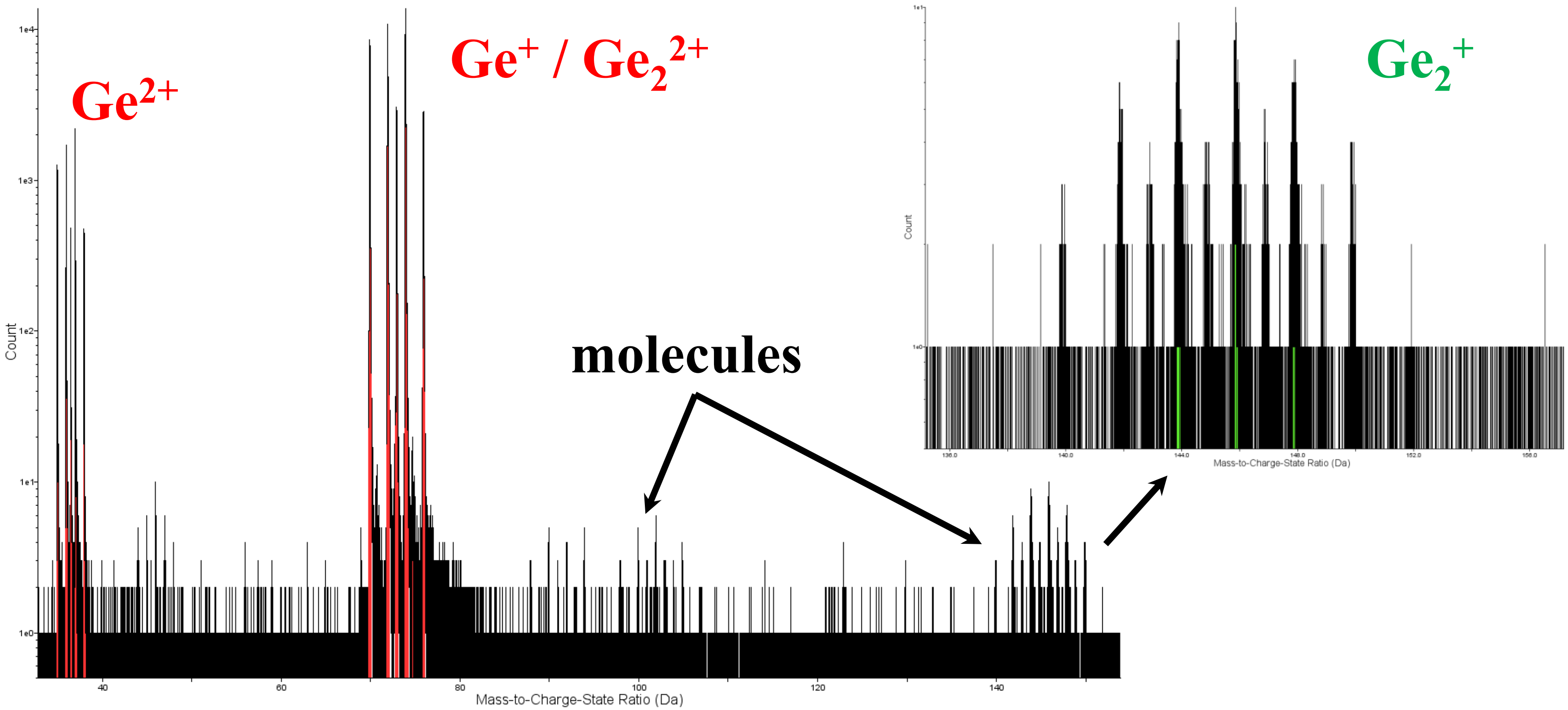

0.4 nJ and 20 K for Ge(001) substrate

- Detect Ge^{2+} and Ge^{1+} with a ratio Ge^{2+}/Ge^{1+} ~ 0.2 (influence of Ge_2)
- Ge_2 molecules are observed in the mass spectrum
- Background noise ~ 1

Laser-pulsed APT: Thermal field evaporation

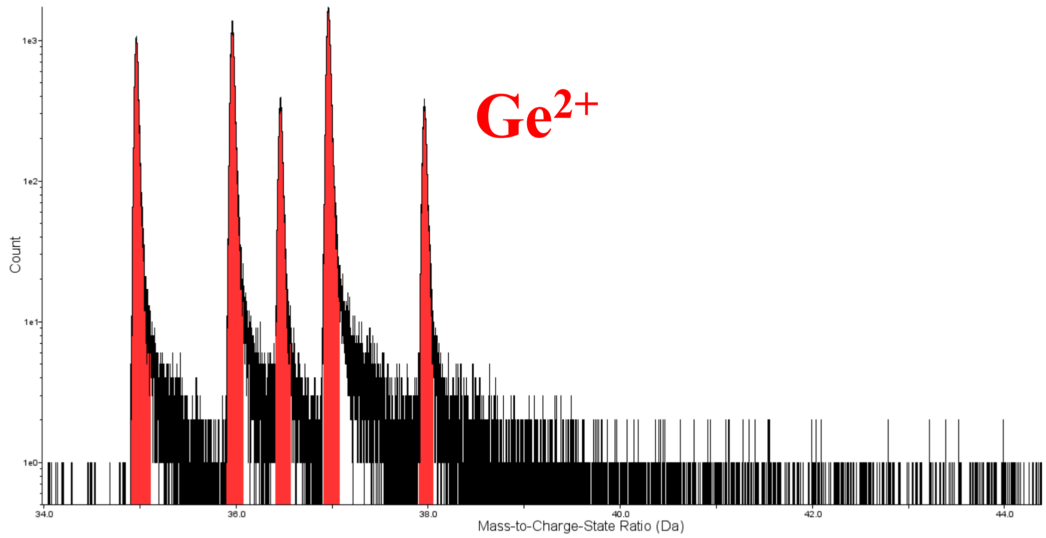

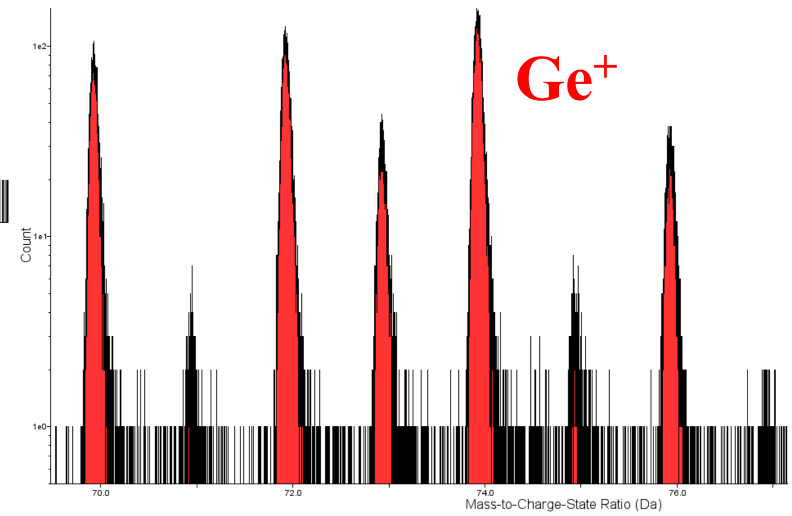

0.07 nJ and 20 K for Ge(001) substrate

- Detect Ge^{2+} and Ge^{1+} with a ratio Ge^{2+}/Ge^{1+} ~ 10
- No molecules in the mass spectrum
- Background noise ~ 1

Laser-pulsed APT: Thermal field evaporation

Ge(001) substrate

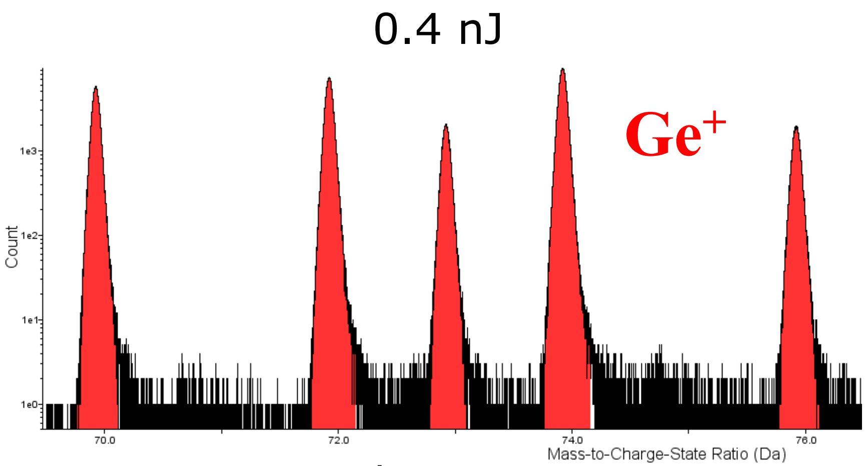

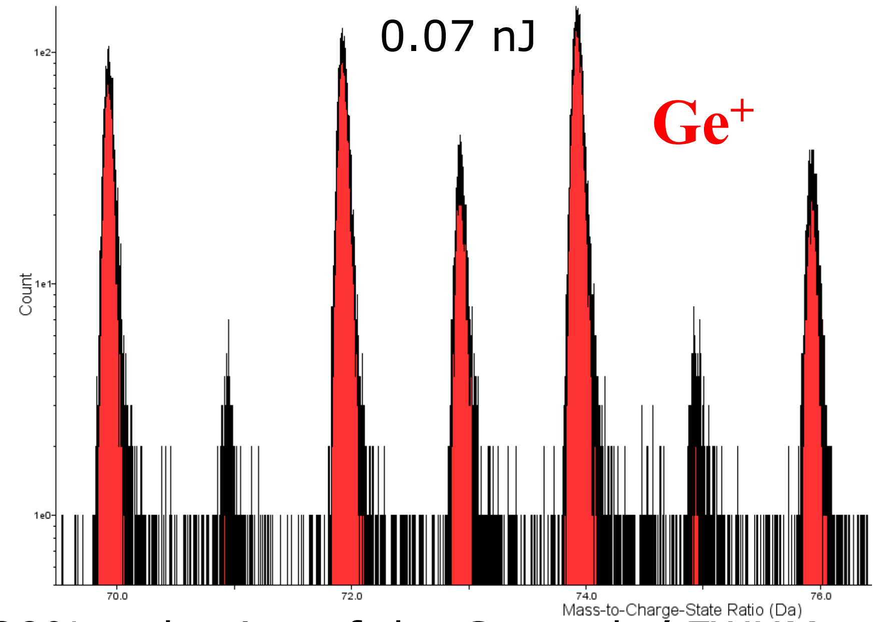

Laser power reduction 0.4 → 0.07 nJ ⇨ 20% reduction of the Ge peaks' FWHM

If the temperature/laser power increases

- The width of the mass spectrum peaks increases(loss of resolution)
- The ratio X^{2+}/X^{1+} changes: X^{2+} decreases while X^{1+} increases
- Molecules can appear in the mass spectrum (complexification)

⇒ Usually APT experiments occur in the thermal field evaporation regime

Post ionization

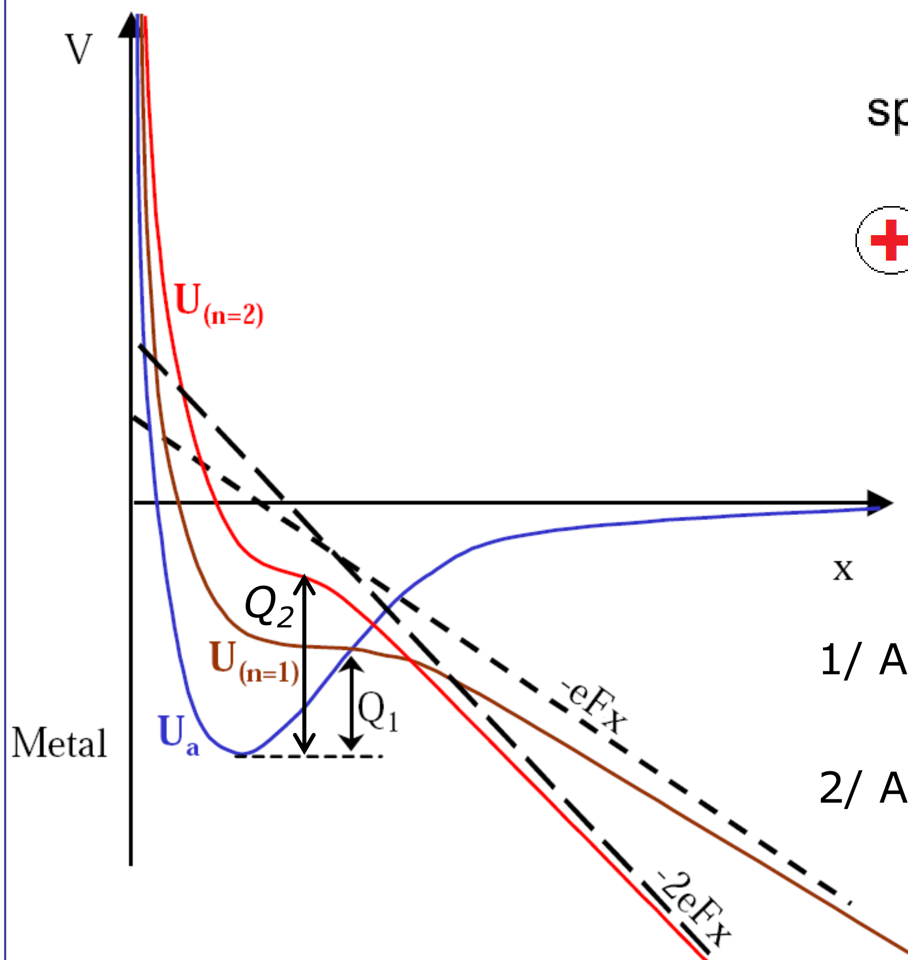

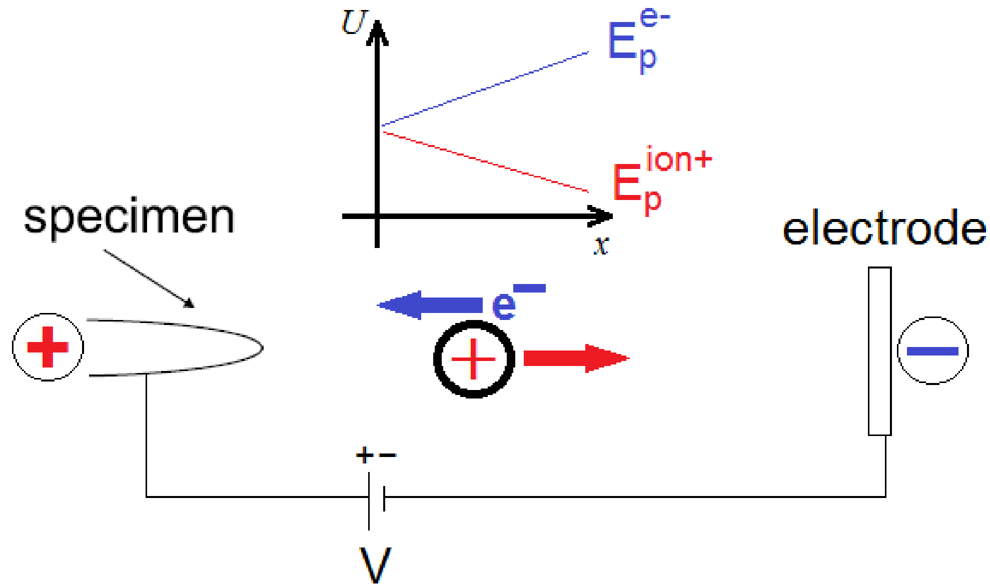

1/ Atom evaporation with the charge +1 $\Rightarrow Q_1$

$Q_1 < Q_2$

2/ Atom post-ionization getting the charge +2

Post ionization

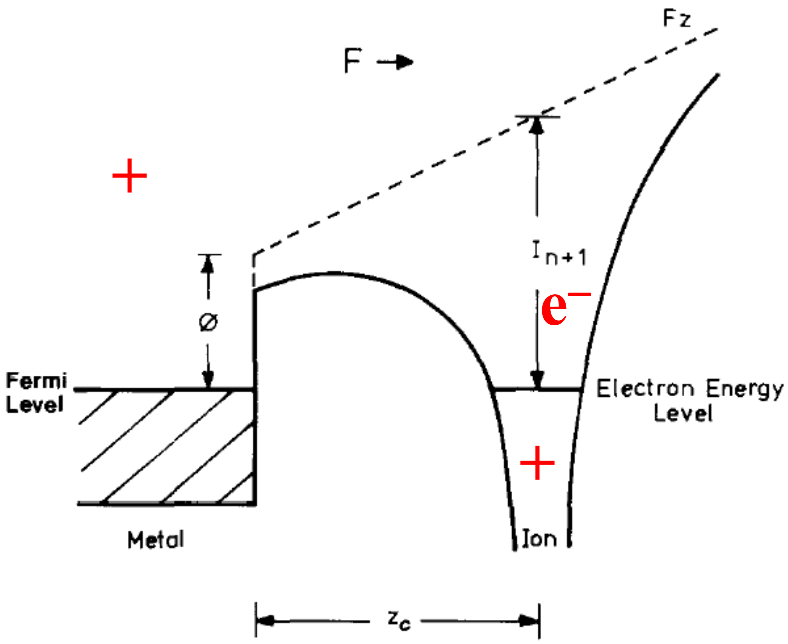

$$Fz_c = I_{n+1} - \phi$$

1/ atom pulled from the surface: lose 1 or more electrons

2/ ion reach Z_c: 1 or several post-ionizations

3/ ion flight

One dimension tunneling model ⇒ at 0 K (no laser pulsing)

F = electrical field
Z_c = post ionization critical distance between the ion and the tip surface
∅ = zero field electron work function of the surface
I_{n+1} = ionization potential of the n times charged ion

Post ionization

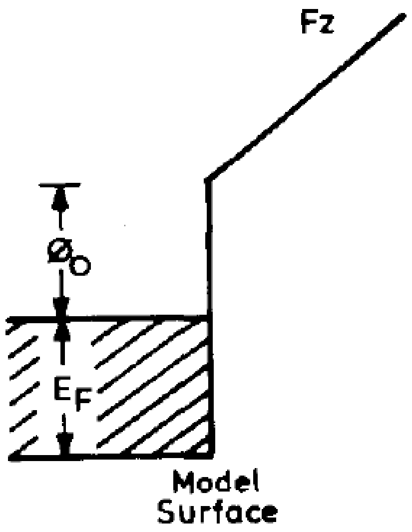

Equations' notation

ħ = m_e = e = 1 (m_e = electron mass)
Energy unit: the hartree (27.2 eV)
Length unit: the Bohr radius (0.053 nm)
unit of field strength: 514.2 V nm^{-1} or 51.42 V $Å^{-1}$
In the equations the field strength is in V nm^{-1}

$$V_{\text{model}} = -Z/r - Fr\cos\theta$$

Model I

V_{model} = tunneling potential of the considered electron
$-Ze/r$ = electrostatic potential at distance r from the ionic nucleus
Z = effective nuclear charge seen by the tunneling electron
r: measured from the nucleus of the ion
θ = the field direction

The energy level of the least tightly bound electron in the ion is not shifted from its zero field value of $-I_{n+1}$

Post ionization

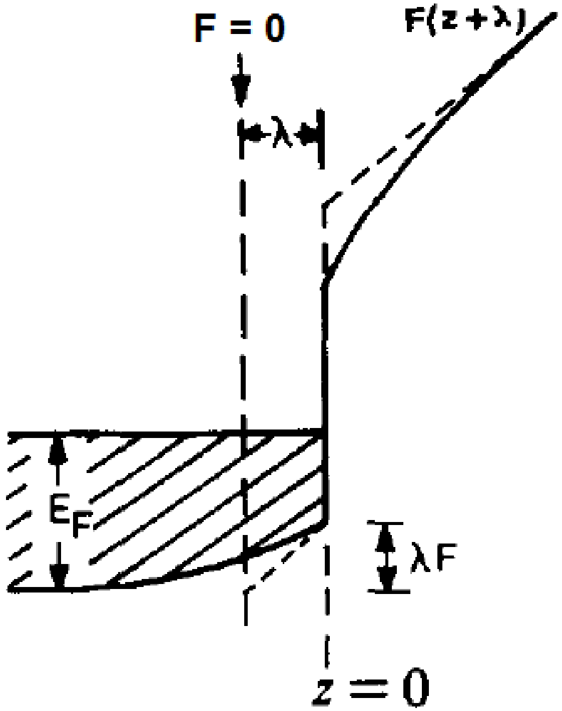

Model II

λ = screening penetration length of the electric field beyond the surface

The energy level of the least tightly bound electron in the ion is shifted from its zero field value: due to the field effect (ΔE_{Stark}) and due to the ion and electron image potentials (ΔE_{image})

Post ionization

$$V_{\text{model}}(z_0, r) - E(z_0) = I_{n+1} - \Delta E_{\text{Stark}} - Z(z_0)/r - Fr\cos\theta$$

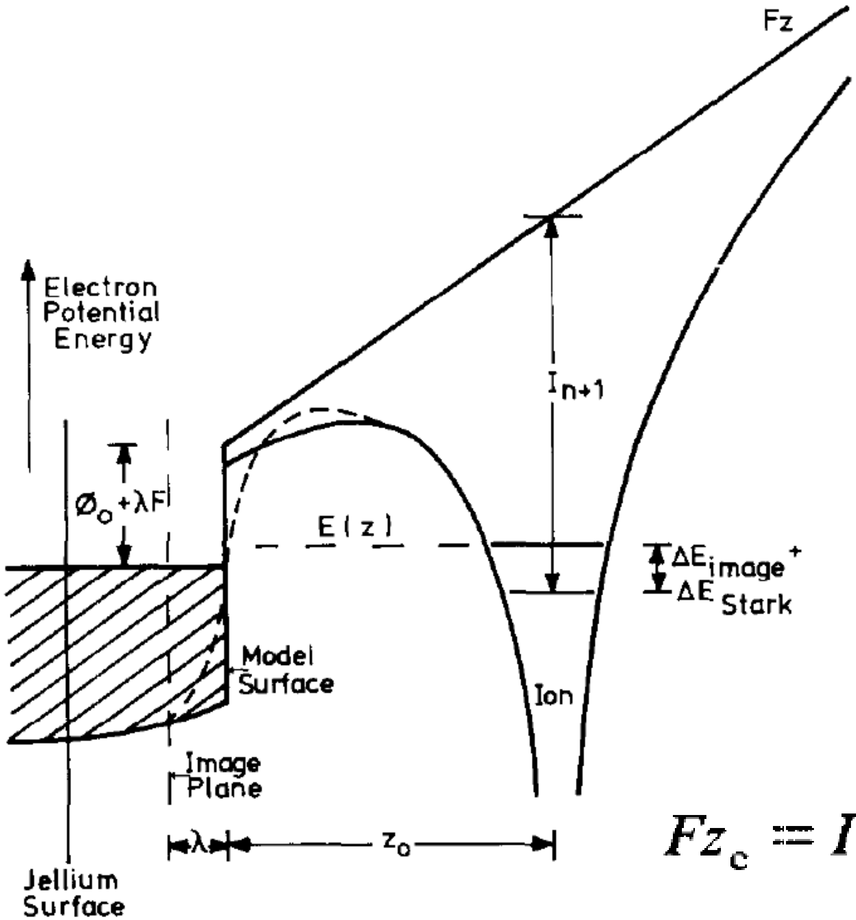

$$V_{\text{model}}(z_0, r) - E(z_0) = 0$$

$$Fz_c = I_{n+1} - \Delta E_{\text{Stark}} - \Delta E_{\text{image}} - \phi_0 - \lambda F$$

Post ionization

- Post-ionization occurs at or near the evaporation fields of most, if not all, metals
- Field evaporation may occur as a two-stage process
- Post ionization does not influence the initial evaporation and does not affect the rate at which evaporation occurs at a given field strength
- The total number of evaporated ions is dependent on the initial field evaporation, while their charge state is dependent on post-ionization
- T and F (depends on the shape of the tip) at the very top of the tip are unknown during experiments, thus, the ratio between 2+ et 1+ peaks in the mass spectrum can be a good indication of evaporation conditions (repeatability)

Post ionization

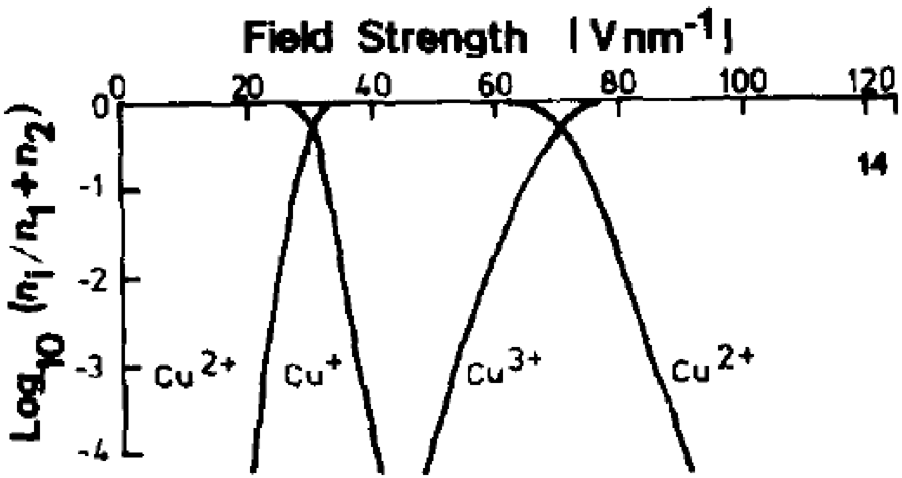

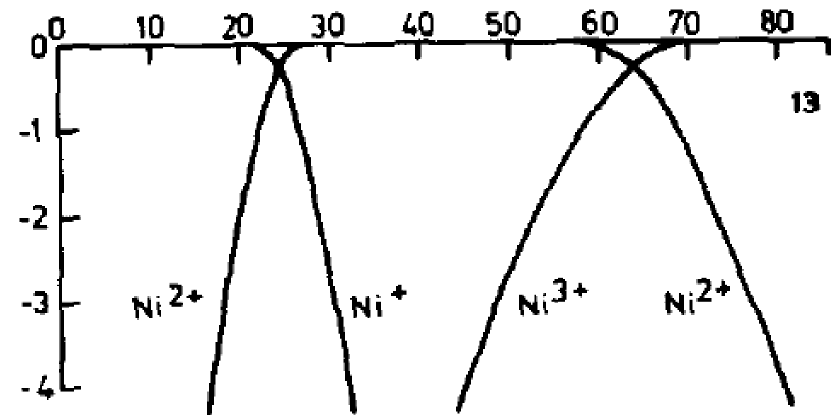

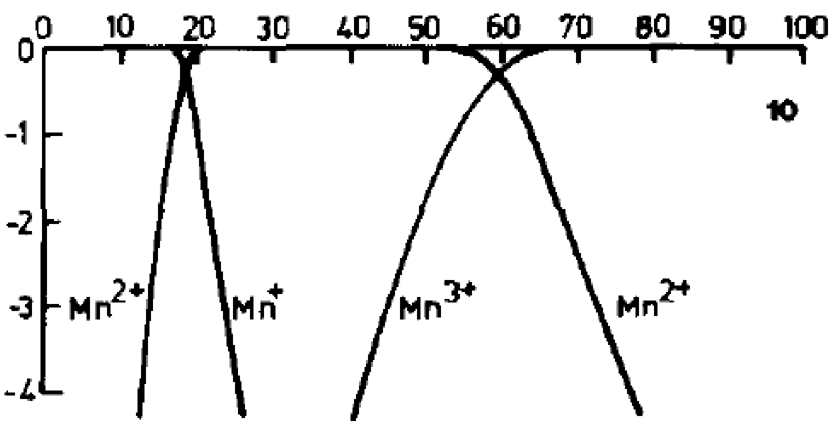

Calculated field ⇒ ratio of ions of different charges

Experimentally ⇒ evaporation field can be deducted from the ratio of ions of different charges

Post ionization

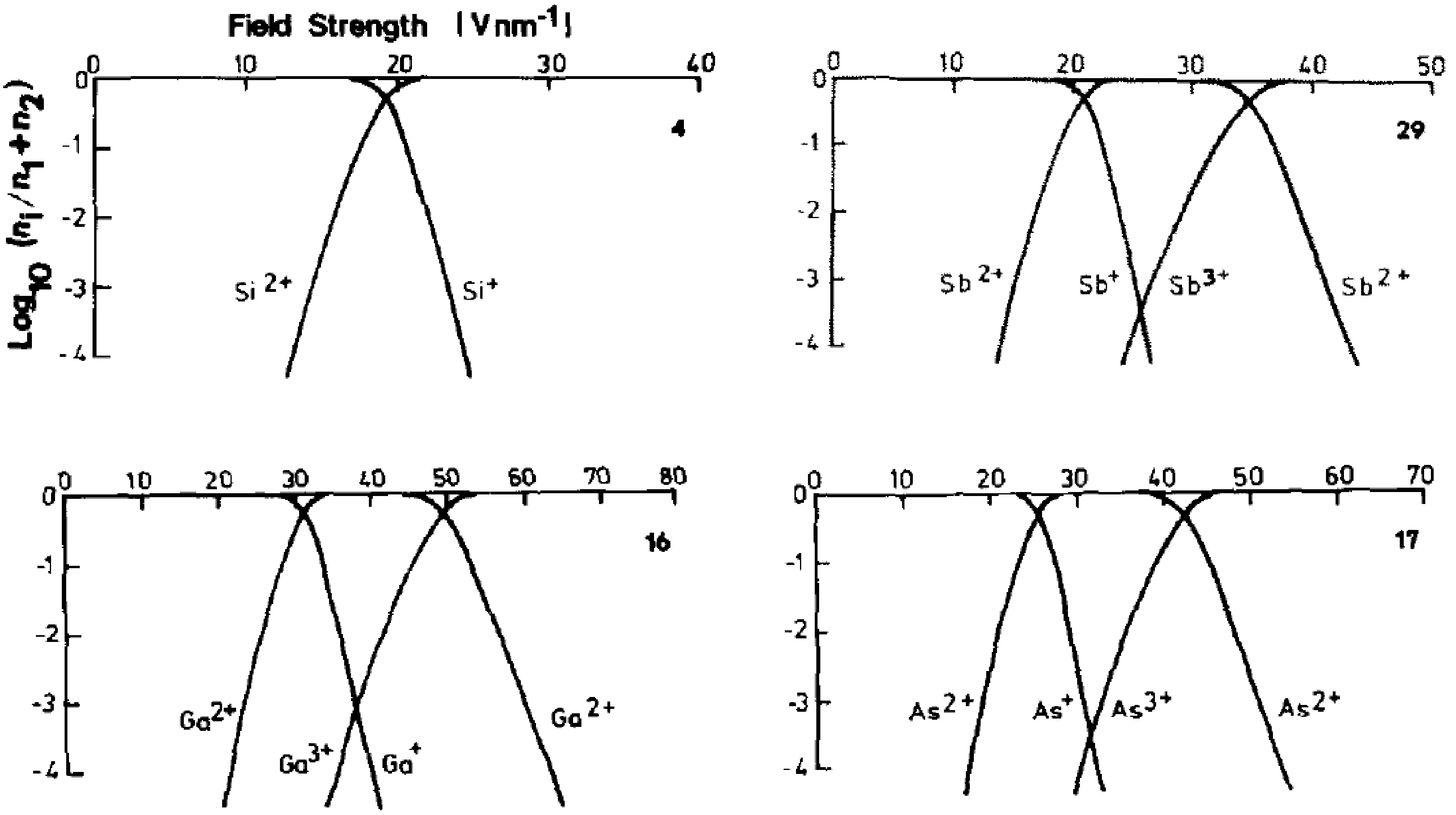

Atom probe tomography (APT)

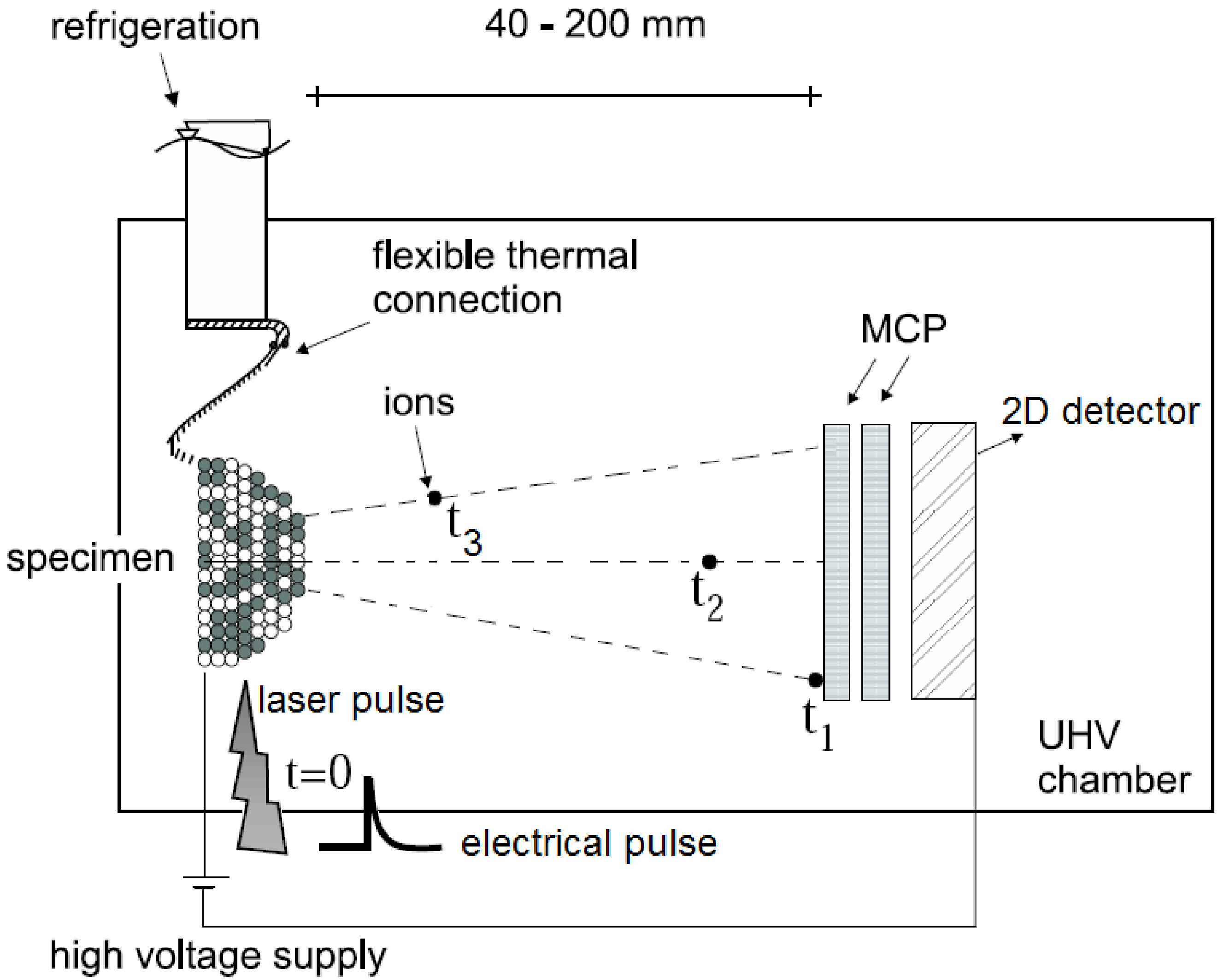

APT: electrical or laser pulses

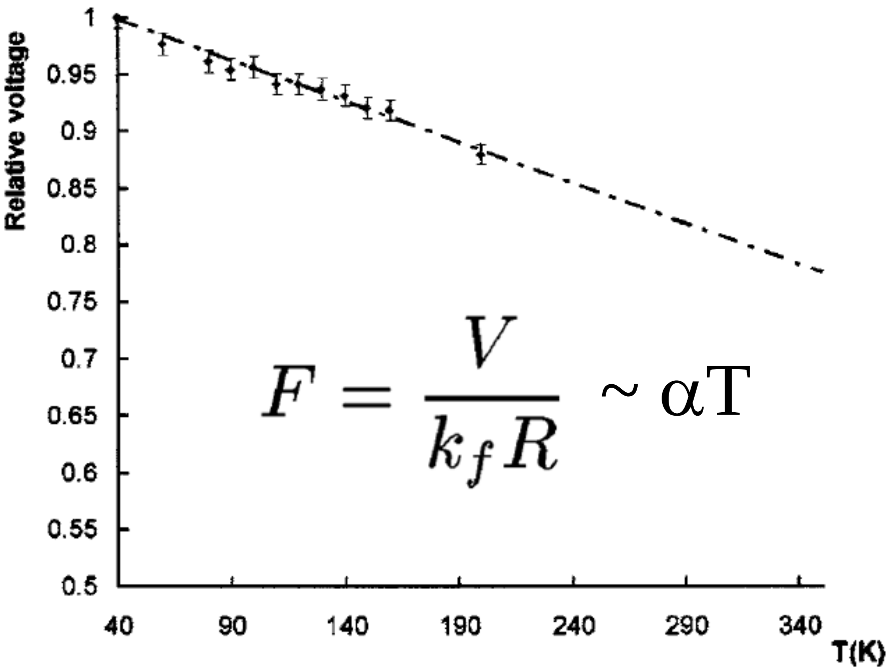

$$F = \frac{V}{k_f R} \sim \alpha T$$

Relative evaporation voltage as a function of emitter temperature for a tungsten sample. The detection rate is 0.005 atom/pulse.

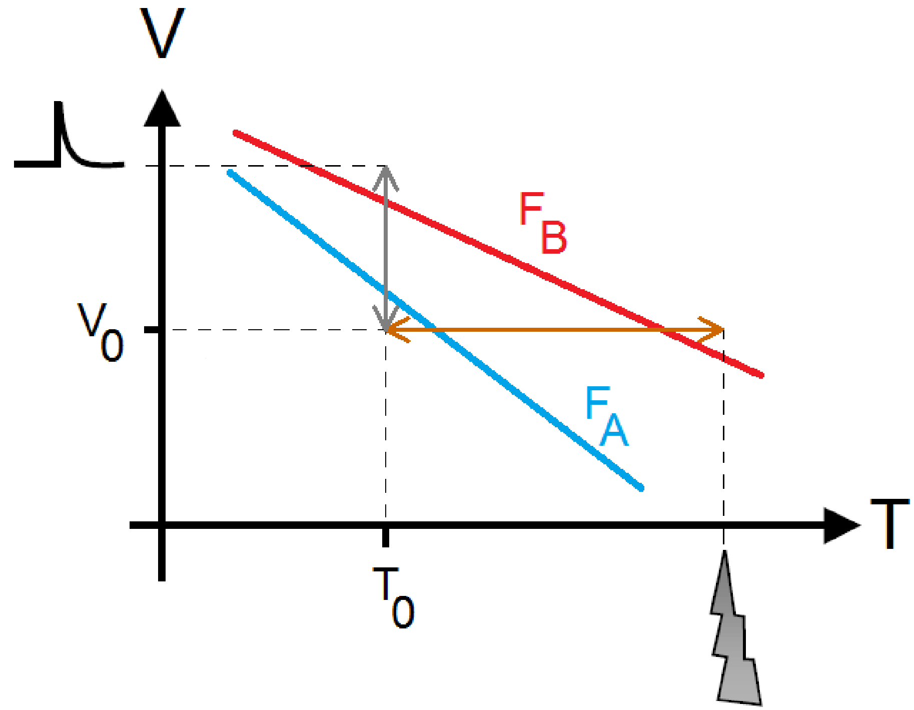

Electric- or laser-mediated ion evaporation

Electrical pulses: conductive materials
Laser pulses: semiconductors and dielectrics

APT: ion identification

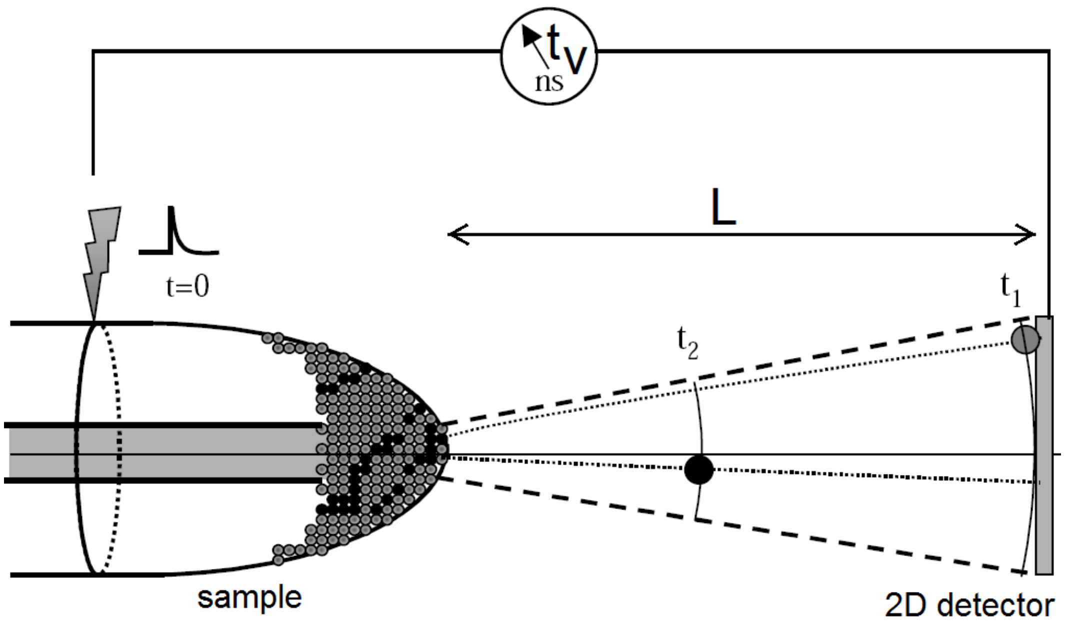

$$\frac{M}{n} = 2eV \cdot \frac{t_v^{\,2}}{L^2}$$

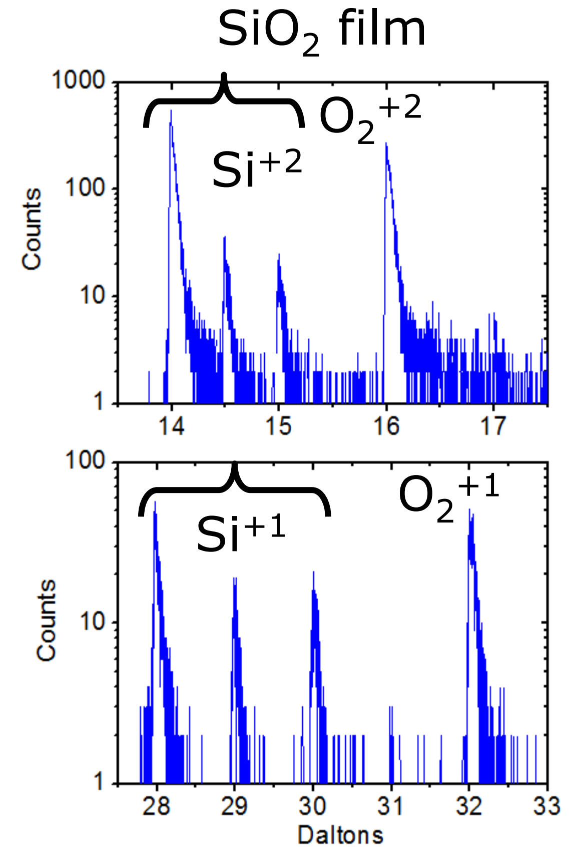

Time of flight mass spectrometry

M = ion mass, n = ionization degree, L = flight distance, e = elementary charge, t_v = time of flight, V = electrical potential applied on the tip

APT: 2D detection in real space

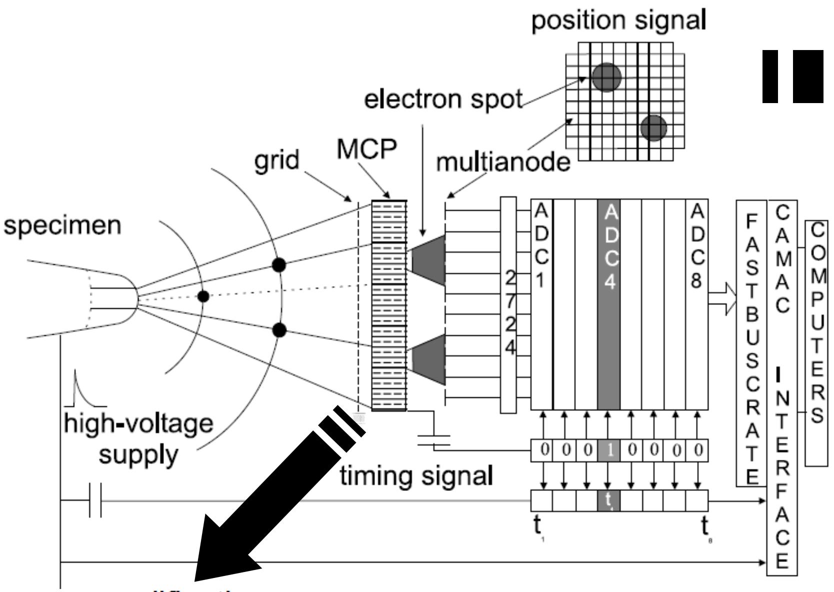

Delay lines X and Y

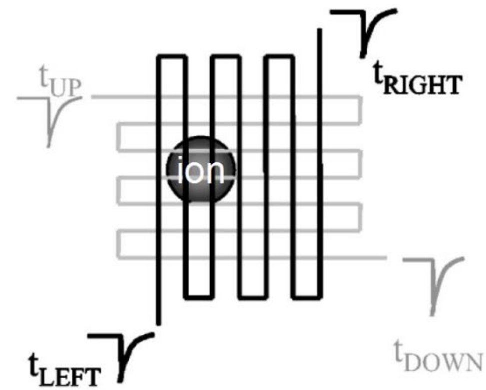

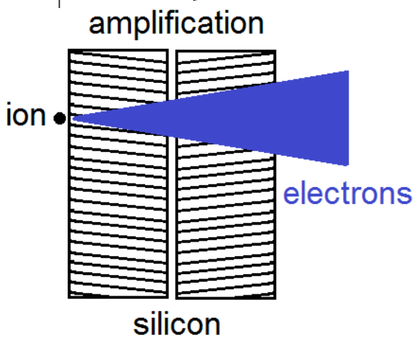

40 mm diameter MCPs in a chevron configuration

$X = V_x \times (t_{LEFT} - t_{RIGHT})/2$

$Y = V_y \times (t_{DOWN} - t_{UP})/2$

Cu $\Rightarrow V_x = V_y \sim 1.4$ ns mm^{-1}

Delay line detector

- Single ion hit on micro channel plate ⇒ electron cloud (~ 50% of ions)
- Electron cloud on delay lines ⇒ X:Y coordinates

Im2np
Institut Matériaux Microélectronique Nanosciences de Provence
UMR 6242 CNRS, Universités Paul Cézanne, Provence et Sud Toulon-Var

APT measurements

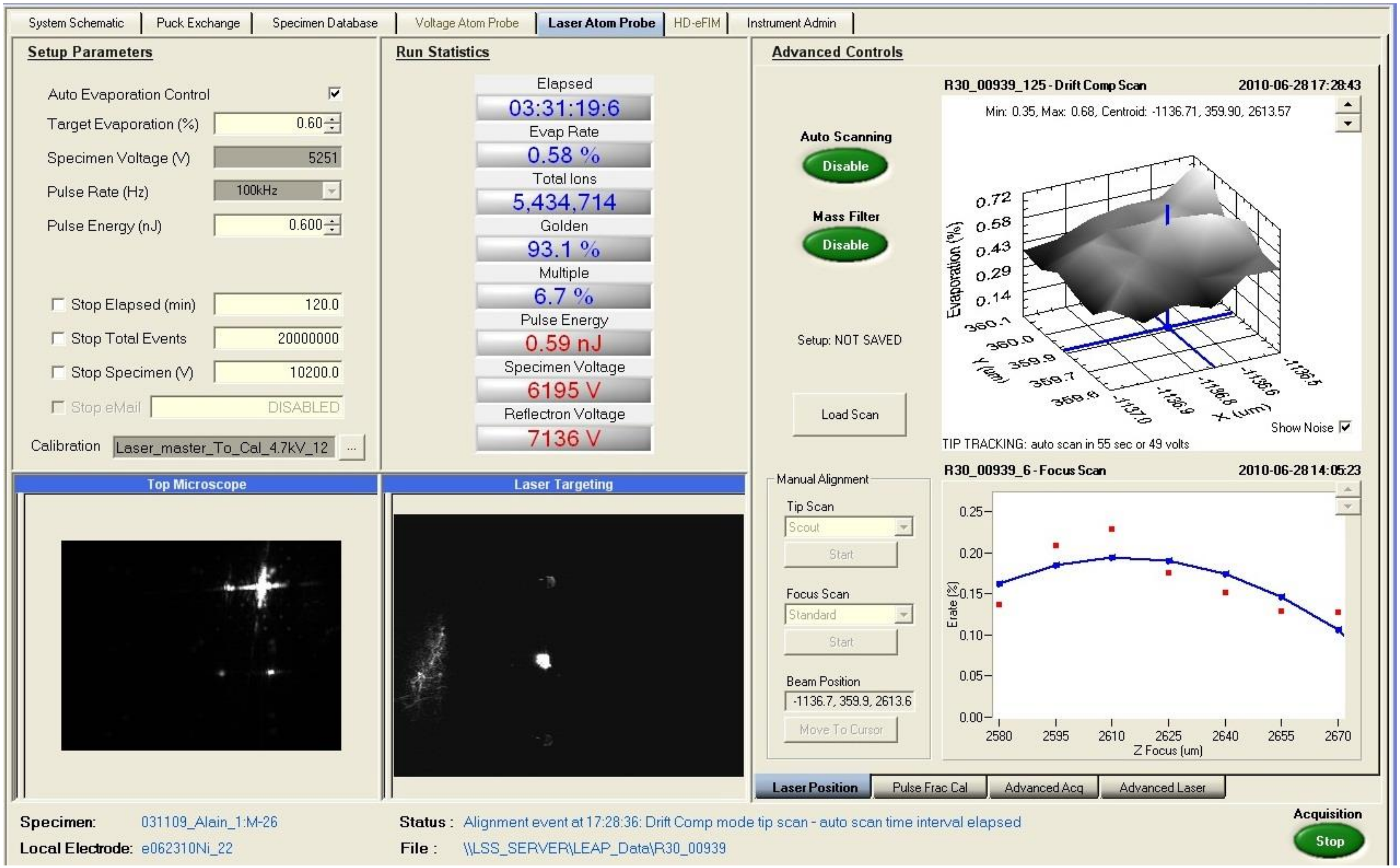

P = 1.4 × 10^{-11} Torr, T = 20-80 K, Pulse rate = 100-250 kHz, evap. rate = 0.2-1%, laser power = 0.01-3 nJ

APT measurements

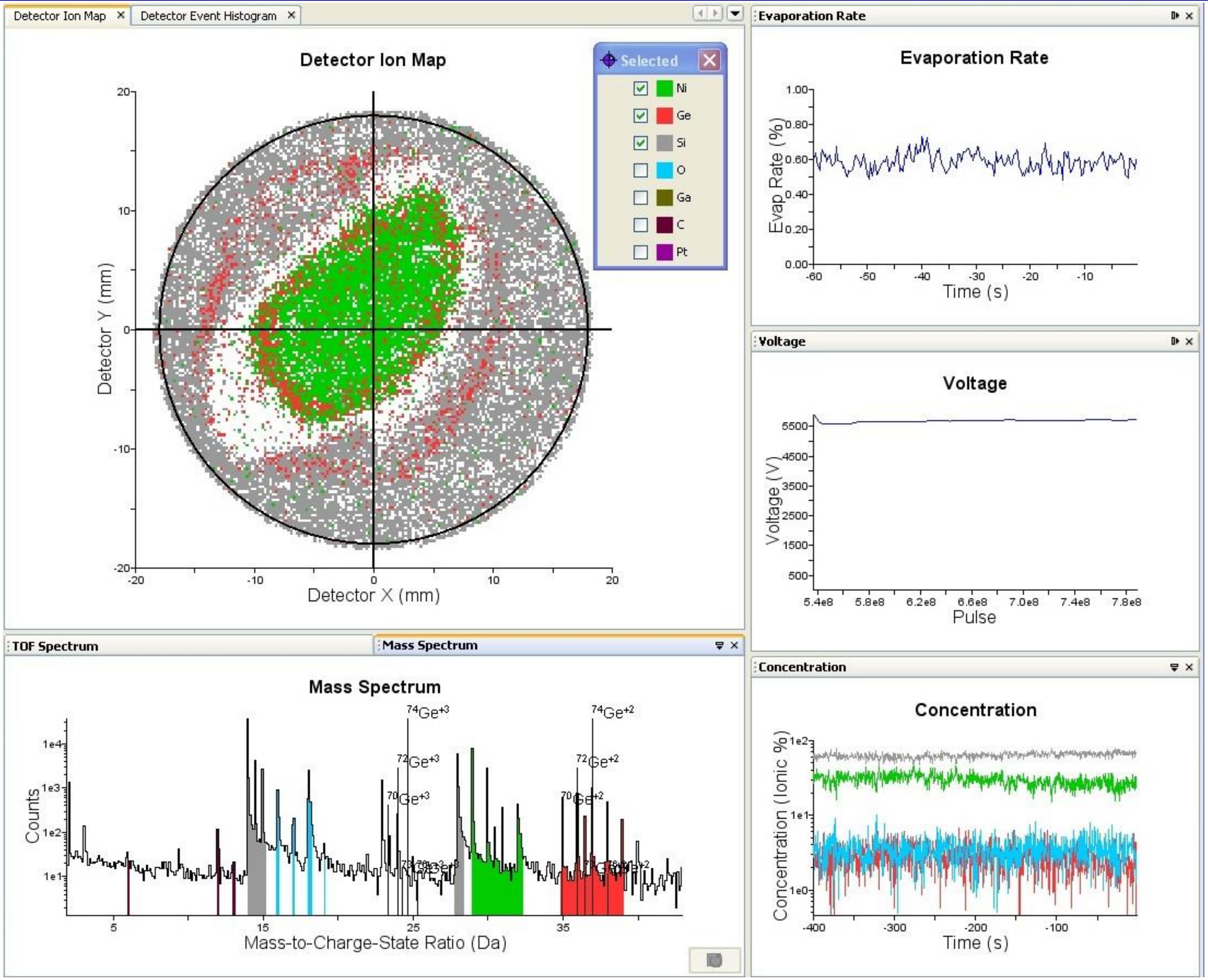

APT: 3D reconstruction

- APT microscopy "Raw" data = sequence of hit records

⬇

Hit number, $X_{Detector}$, $Y_{Detector}$, Δt_{Pulse}, $V_{Specimen}$

- Reconstruction = process that transforms Raw data into the 3D volume (of the tip) containing the atoms

⬇

Ion number, X_{Tip} , Y_{Tip} , Z_{Tip} , Mass

APT: Stereographic projection

Gault et al., Ultramicroscopy 111 (2011) 448

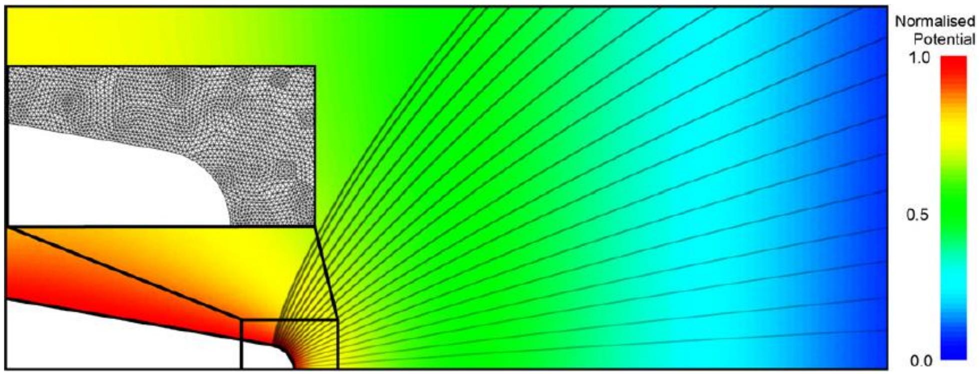

Electrostatic simulations of the potential around the tip (shank angle = 10°) and of the ion trajectories

Gault et al., JAP 105 (2009) 034913

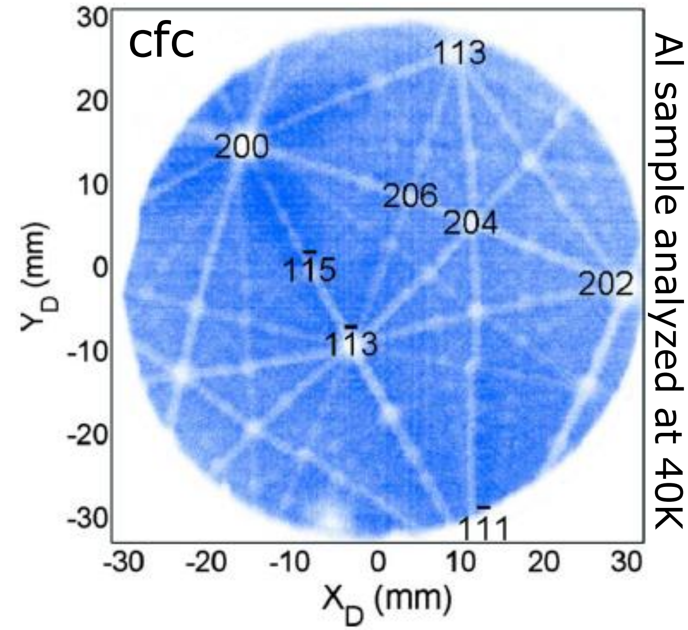

Ion trajectory

- Experimental distance d_{pole} between the observed crystallographic poles corresponds to the stereographic projection of the sample crystal structure with a constant center
- m can be determined experimentally considering the ratio between crystallographic angles observed in APT data (θ = arctan d_{pole} /L_0)

APT: 3D reconstruction

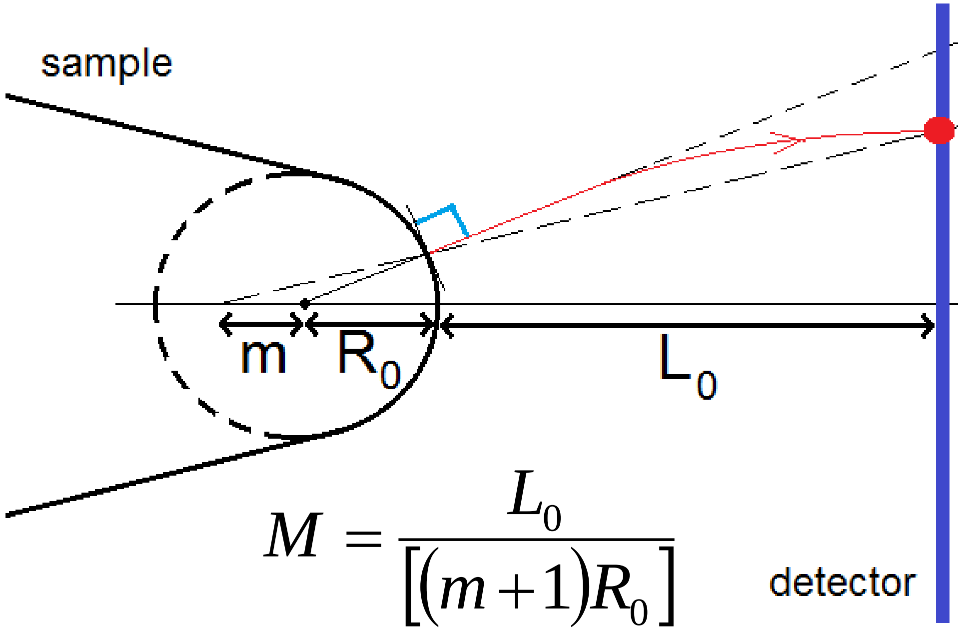

$$M = \frac{L_0}{[(m+1)R_0]}$$

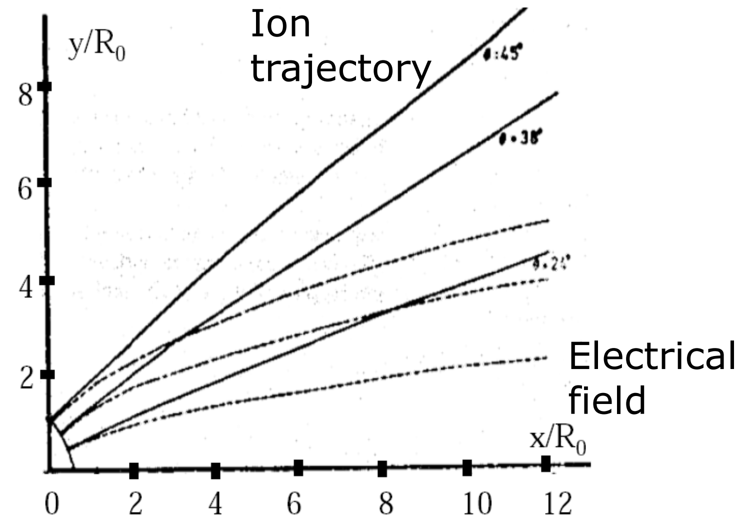

Ion trajectory

- Almost stereographic projection with constant center
- Magnification (M) proportional to the ratio between the tip-to-detector distance (L_0) and the tip radius of curvature (R_0) ⇒ few cm and M > 1M
- Compression due to tip shape + elec. Field ⇒ m compression factor

APT: voltage reconstruction

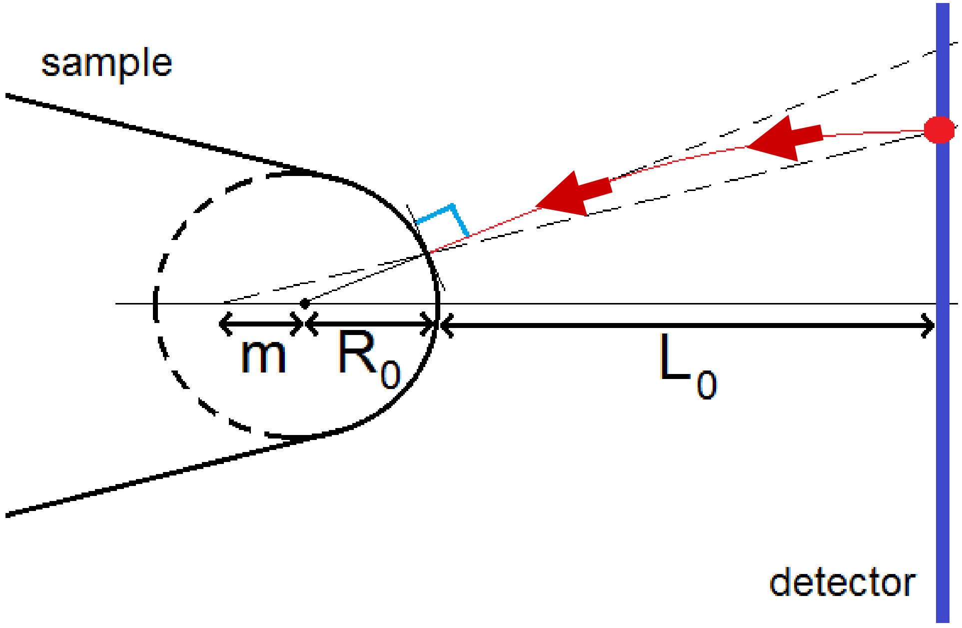

$$M = \frac{L_0}{\left[(m+1)R_0\right]}$$

↓

Reversed projection

↓

$$X_{tip} = \frac{X_d}{M} \qquad Y_{tip} = \frac{Y_d}{M}$$

- Knowing the ion tip-to-detector trajectory (stereographic projection corrected by a compression factor), we can deduce the reverse ion trajectory (detector-to-tip)
- Ion with straight trajectory ⇒ direct relationship between each position (X_{tip}, y_{tip}) on the tip surface and the position (X_d, Y_d) on the detector

APT: voltage reconstruction

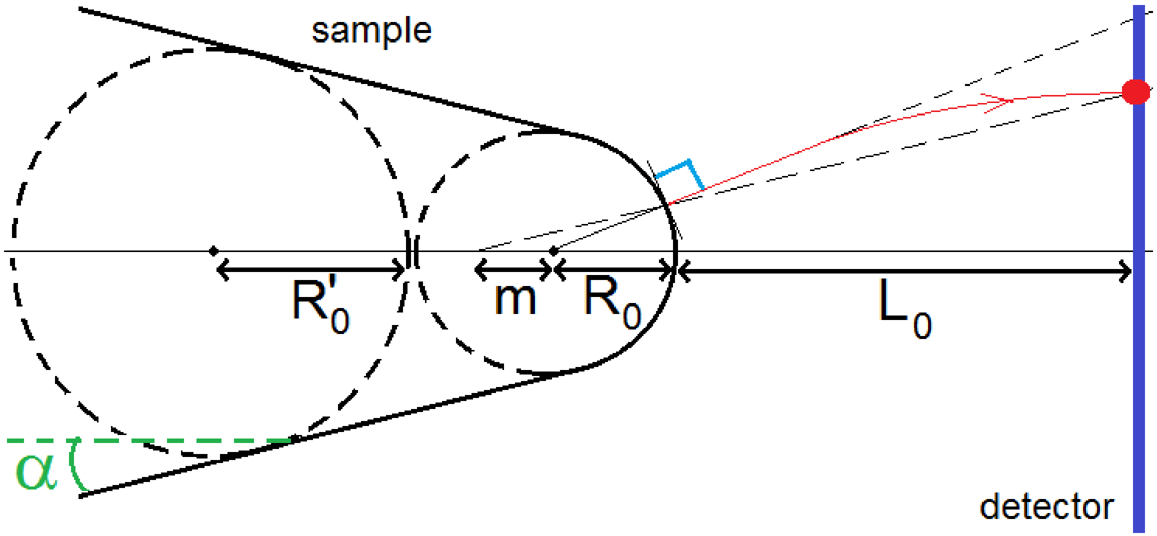

$$M = \frac{L_0}{[(m+1)R_0]}$$

Field effect equation

$$F = \frac{V}{K_f R_0} \Rightarrow R_0 = \frac{V}{K_f F}$$

- During the specimen evaporation, the radius of the tip progressively increases, since the shank angle α of the tip is > 0
- The variations of the tip radius can be determined using the relation between the elec. field, the elec. potential and the radius

Evap. field factor K_f = const for a given material (evap. equilibrium shape)
F = const for a given material + conditions of evaporation (evap. rate)

APT: voltage reconstruction

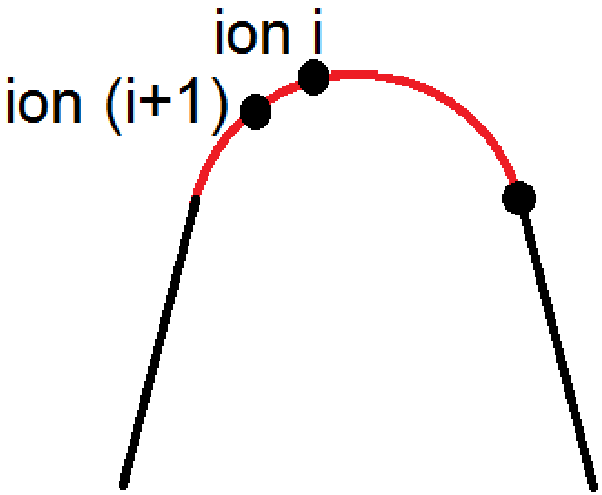

$$z_{tip}^{(i+1)} = z_{tip}^{i} + dz$$

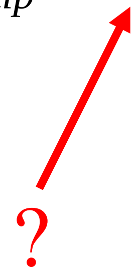

$$V_S = \frac{N\Omega}{\eta} \Rightarrow V_a = \frac{\Omega}{\eta}$$

$$V_a = \frac{\Omega}{\eta} = S_{tip} dz \Rightarrow dz = \frac{\Omega}{\eta S_{tip}}$$

- Assume that the volume V_a of a detected atom is removed equally across the tip surface S_{tip} = the volume of a single atom is spread over the entire tip surface
- Not all the atoms are collected $\Rightarrow$ η = detector efficiency
- The depth location dz of an atom in the tip can be determined knowing the volume Ω of the considered atom, and knowing the surface of the tip

APT: voltage reconstruction

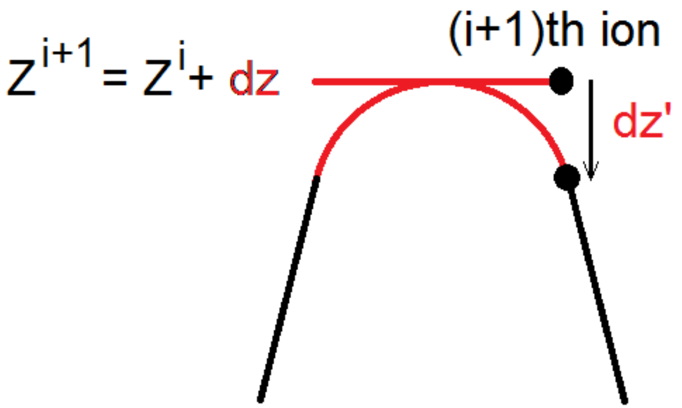

$$Z^{i+1} = Z^i + dz + dz'$$

$$S_{tip} = \frac{S_d}{M^2} \Rightarrow dz = \frac{\Omega L_0^2 K_f^2 F^2}{\eta S_d (m+1)^2 V^2} = f(V)$$

$$dz' = R_0\left(1 - \sqrt{\left(X_{tip}^2 + Y_{tip}^2\right)/R_0^2}\right)$$

- The evaporated surface of the tip can be determined knowing the surface of the detector S_d and the magnification M
- The atomic positions in-depth are progressively built in the plane normal to the specimen apex
- In order to reconstruct atomic positions at the specimen surface, a term dz' is added to account for the curvature of the tip = projection of the ion orthogonally onto the spherical cap beneath the apex plane

APT: shank angle reconstruction

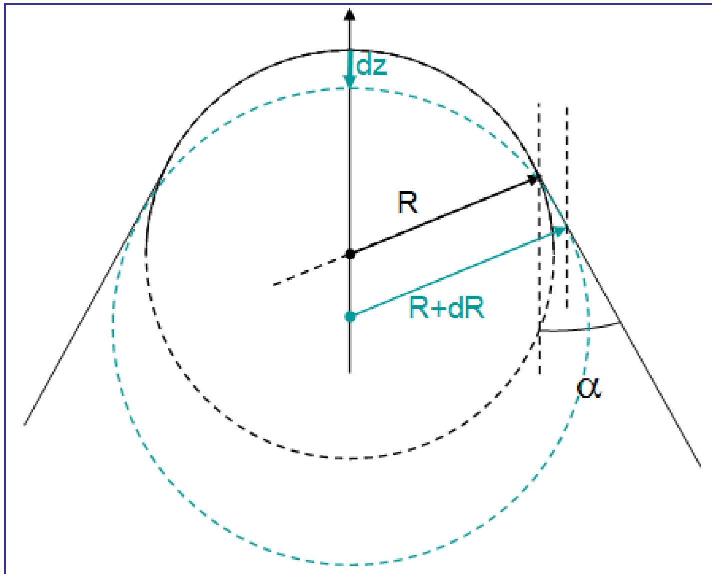

$$\frac{dR}{dz} = \frac{\sin(\alpha)}{1-\sin(\alpha)} = f(\alpha)$$

$$Z^{i+1} = Z^i + dz + dz' \qquad dz = \frac{\Omega L_0^2}{\eta S_d (m+1)^2 R^2} \qquad dz' = R\left(1-\sqrt{\left(X_{tip}^2 + Y_{tip}^2\right)/R^2}\right)$$

- ➢ If the tip shank angle α is constant, the variation of R versus the depth z can be expressed using classical geometry laws (in general 2 ≤ α ≤ 10°)
- ➢ The same method as for voltage reconstruction is used for Z variations

APT: shank angle reconstruction

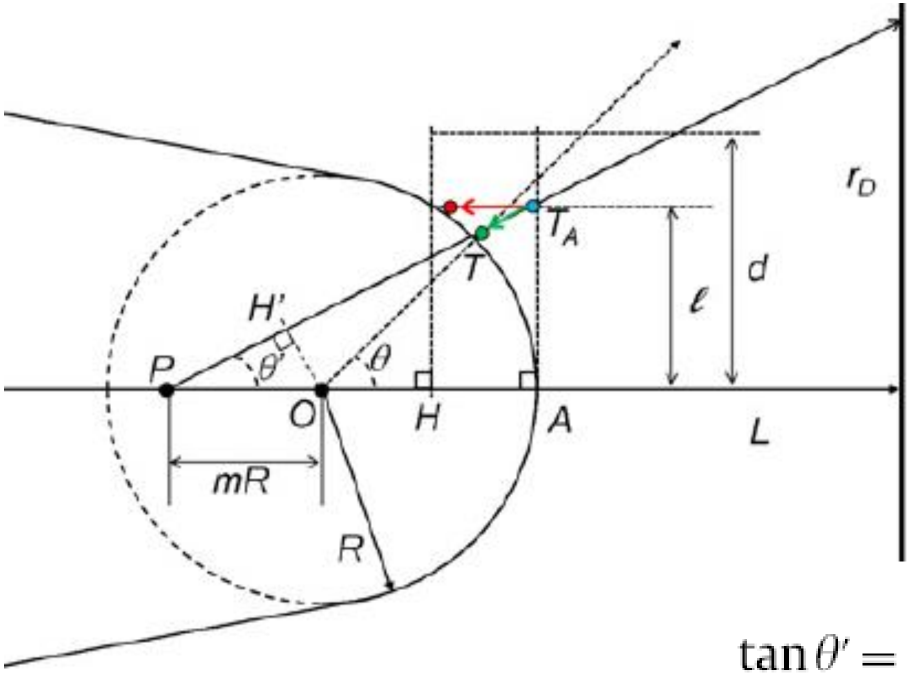

$$PT = s = R\left(m\cos\theta' + \sqrt{1 - m^2\sin^2\theta'}\right)$$

$$\tan\theta' = \frac{d}{L+(m+1)R} = \frac{\sqrt{X_D^2+Y_D^2}}{L+(m+1)R} \approx \frac{\sqrt{X_D^2+Y_D^2}}{L}$$

➢ Use geometrical relations to determine the position of the atoms on the surface of the tip, knowing the distance L between the tip and the detector, the ICF m, the curvature radius R of the tip, and the ion coordinates on the detector (X_D, Y_D)

APT: 3D reconstruction

Gault et al. Mat. Today 15 (2012) 378

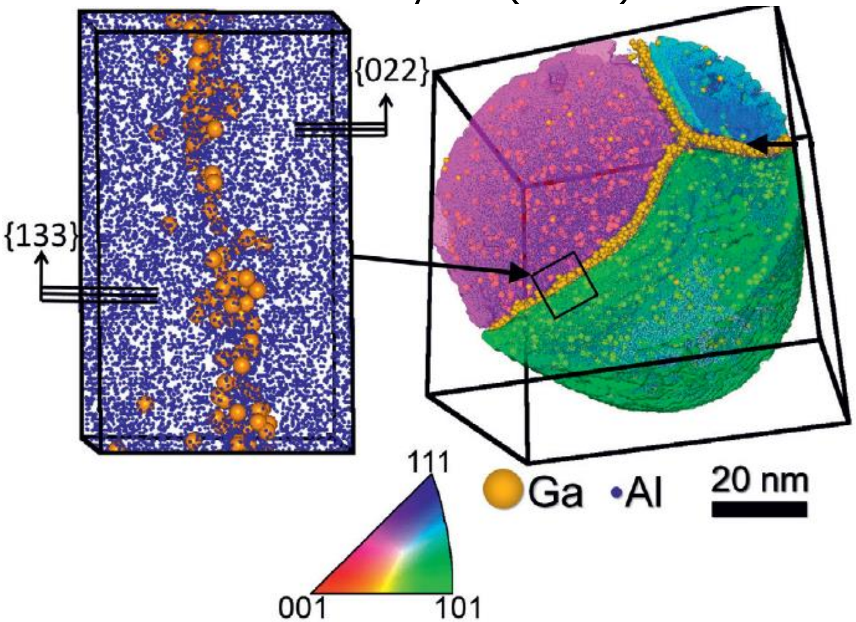

Ga grain boundary segregation in a nano-crystalline Al thin-film. The atomic planes are resolved up to the grain boundaries

3D reconstruction based on:
- Single evaporation field F
- Single curvature radius R
- Single shank angle α

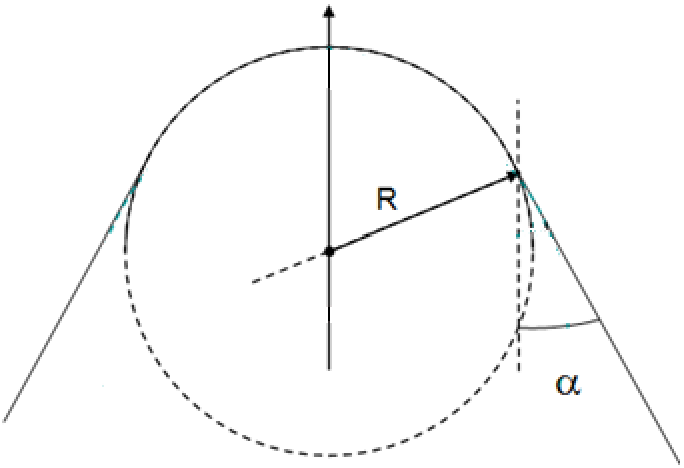

➢ The Reconstruction procedure works well but…generally used in not suitable cases! ⇨ samples made of different materials exhibiting different F, R and α (multilayers, clusters…)

Atom probe tomography

- Magnification ~ 10^6 times = ×10 millions
- Lateral resolution (T < 100 K) ~ 0.05-0.3 nm

$$\delta = \left\{ 16(m+1)^2 . \left(\frac{k_B T . R_0}{eF k_f} \right) + 4 \left(\frac{(m+1)^2 \hbar^2 R_0}{2M . eF k_f} \right)^{1/2} \right\}^{1/2}$$

Thermal term (principal) + Heisenberg incertitude

- Depth resolution < 0.07 nm in best cases
- Field of view ~ 50-250 nm
- Analyzed depth up to 0.5 µm (depends on tip fracture)

APT improvements

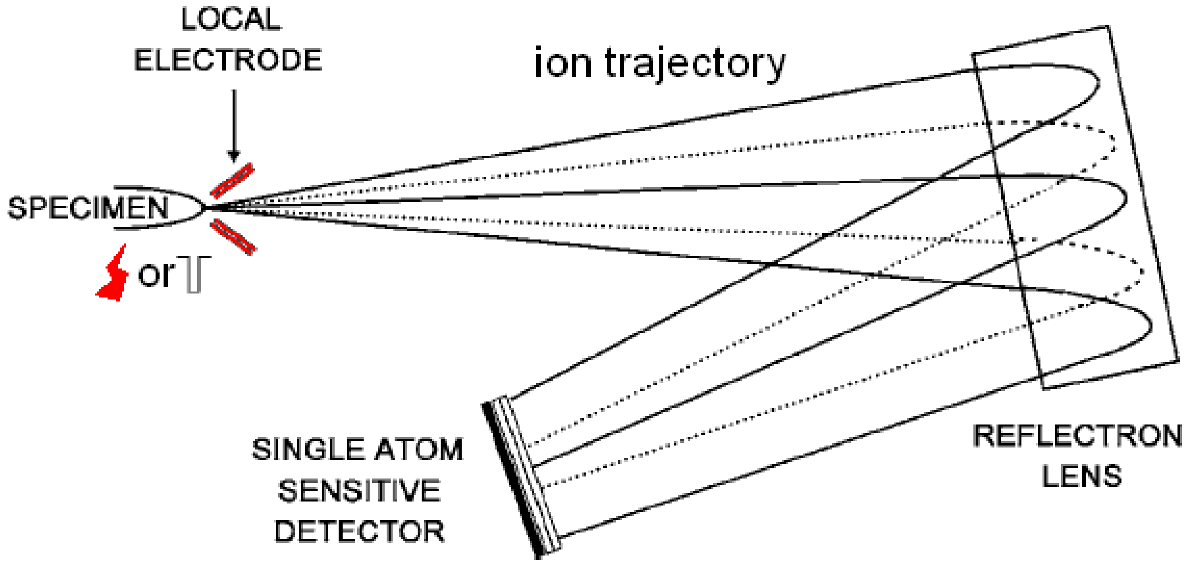

- With the local electrode, the voltage is applied between the sample and the LE, i) allowing to apply a lower voltage on the sample for the same elec. field (decrease of sample fracture probability and improves mass resolution), ii) allows to use arrays of pre-shaped tips improving sample preparation and sample preparation time saving, by giving the capability to select the evaporation of a given tip among several

- The reflectron lens allows to multiply by ~3 the flight path length of ions, allowing to significantly increase mass resolution

APT: sample preparation

- Bulk metallic materials can be prepared by electro-erosion, but for semiconductors and for the main part of nanotechnology materials (nano-layers, nano-wires, quantum dots…) the samples need to be prepared by Ga^{+} focus ion beam (FIB)

- Similar to field evaporation, differences in materials' erosion properties complicate FIB sample preparation

- Need weak ion beam (2-5 kV) to minimize Ga contamination and sample amorphization

APT: sample preparation

1/ Ni sputtering
2/ Pt deposition

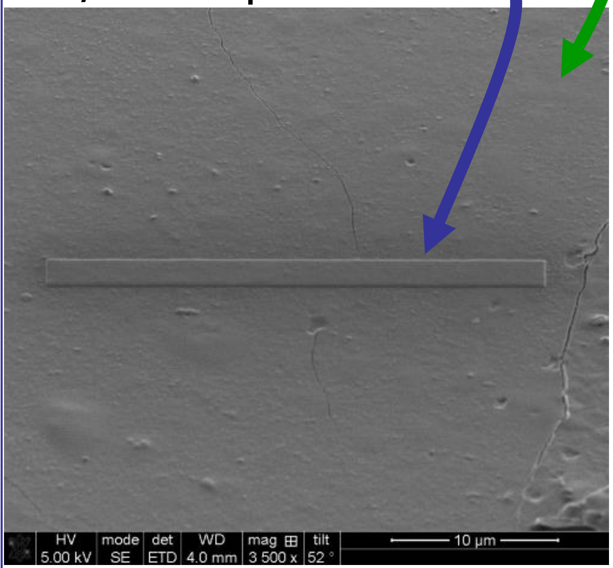

3/ Carve the a sample wedge

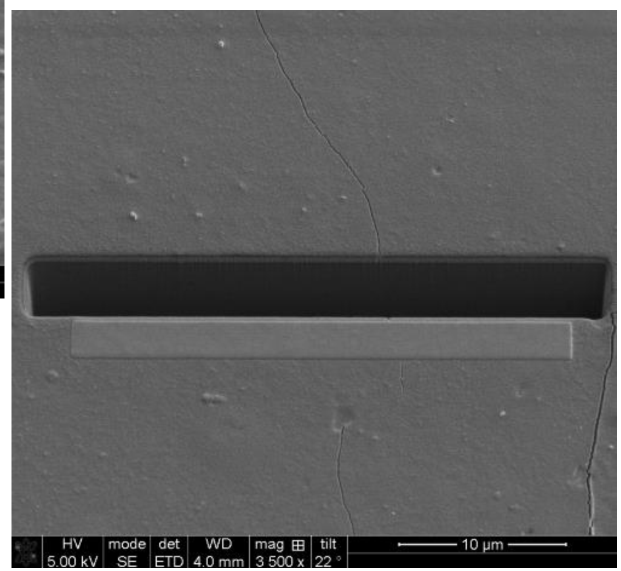

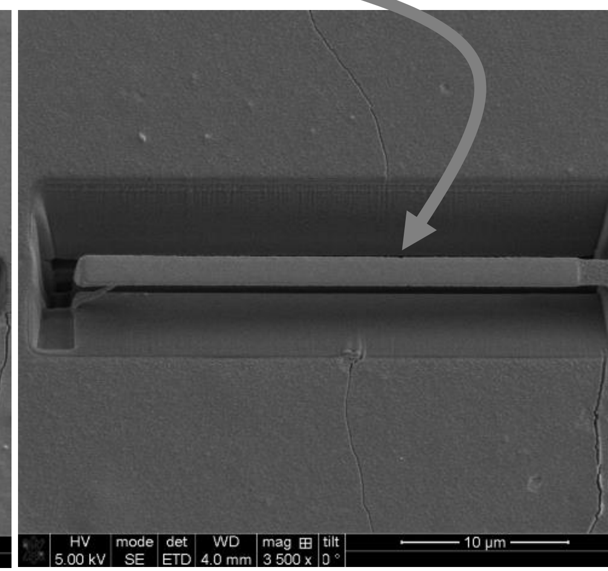

APT: sample preparation

4/ Lift off the wedge

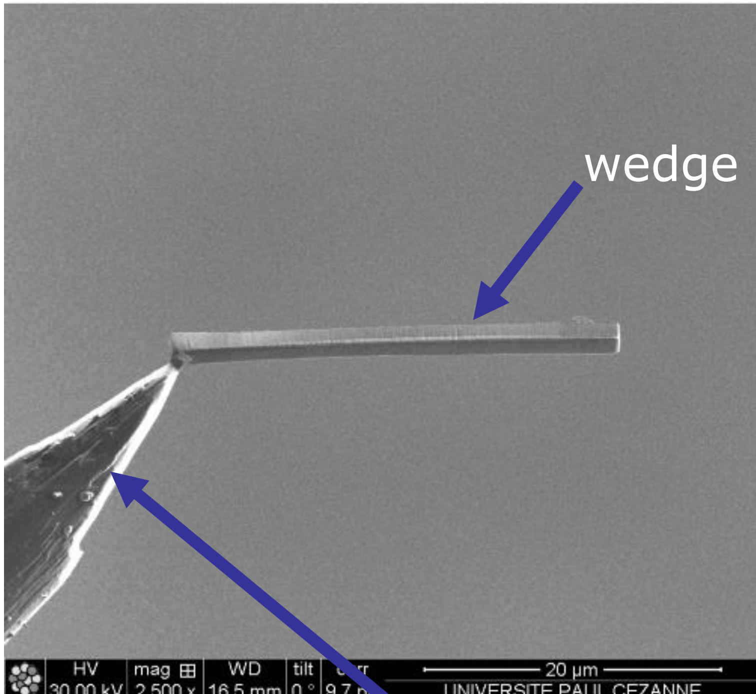

5/ Attach wedge pieces on pre-shaped posts

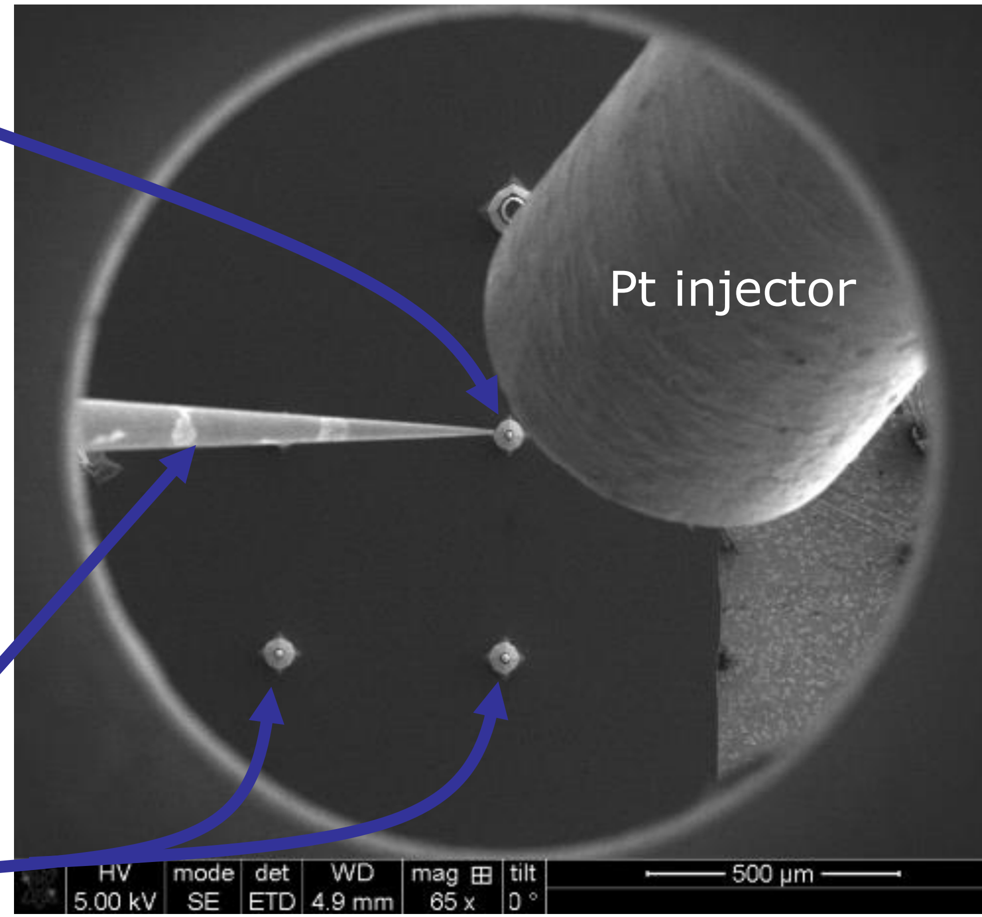

APT: sample preparation

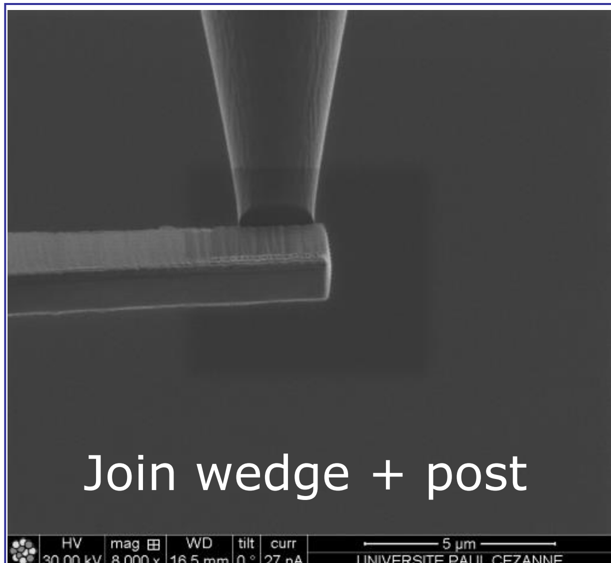

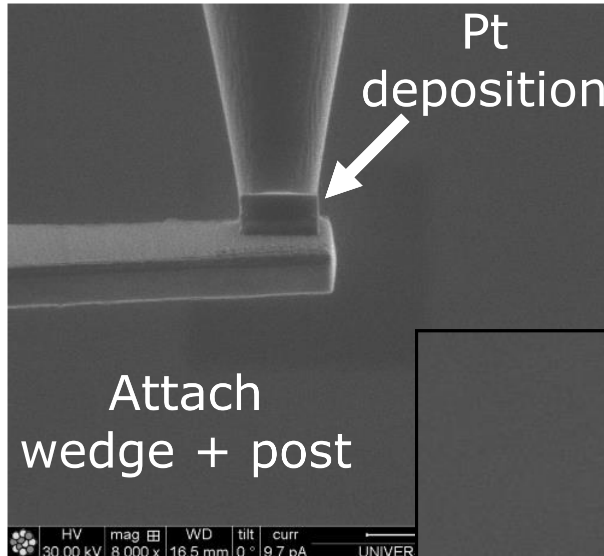

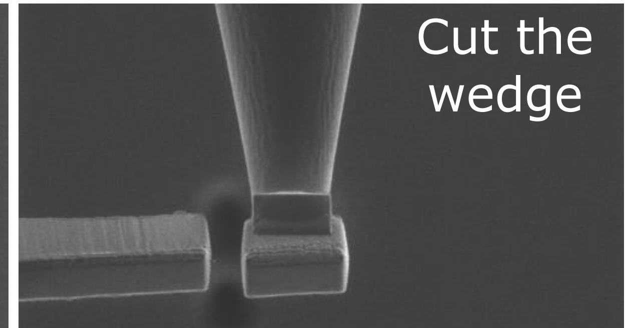

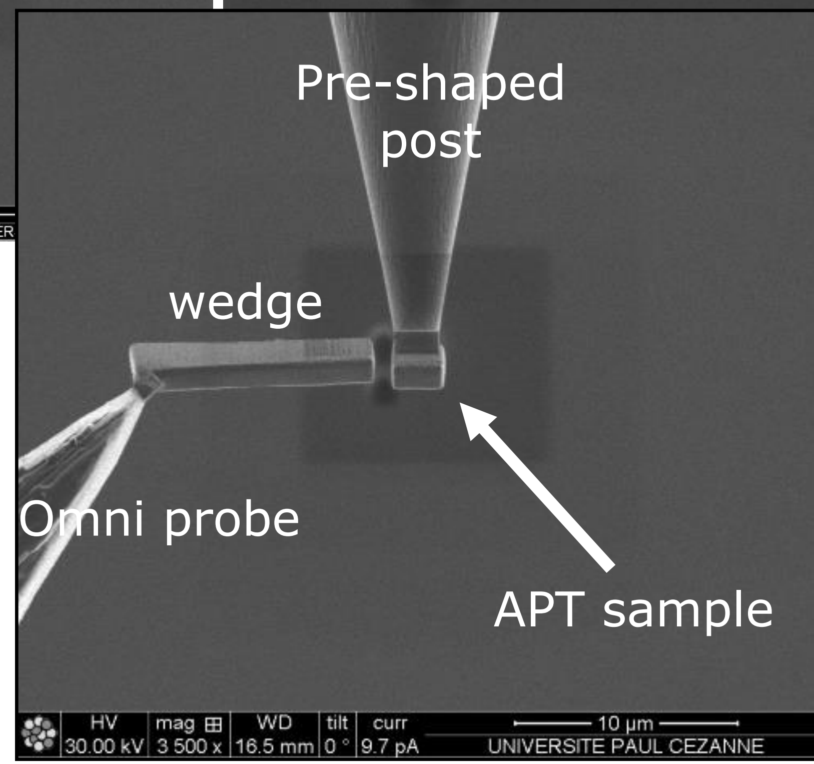

5/ Attach wedge pieces on the pre-shaped posts

Institut Matériaux Microélectronique Nanosciences de Provence
UMR 6242 CNRS, Universités Paul Cézanne, Provence et Sud Toulon-Var

APT: sample preparation

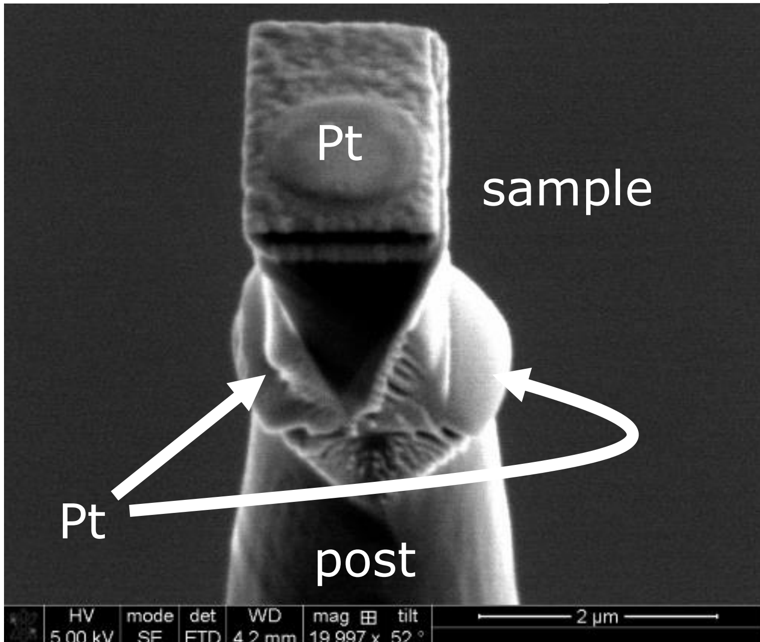

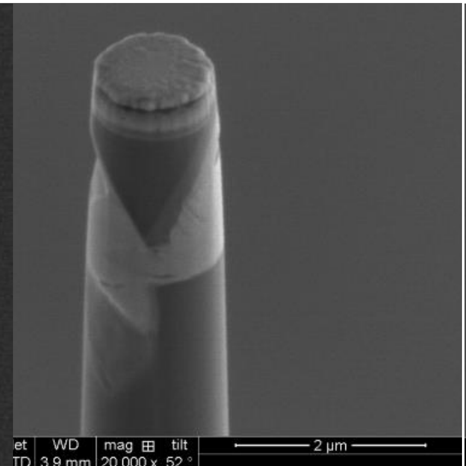

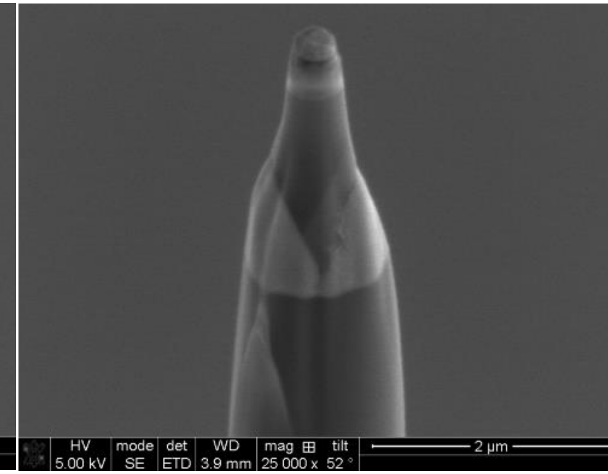

6/ Shape the tips

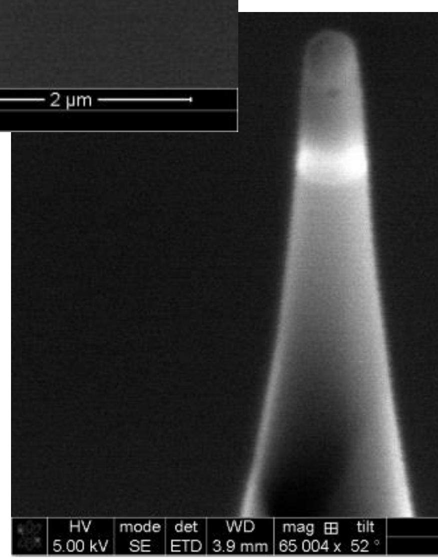

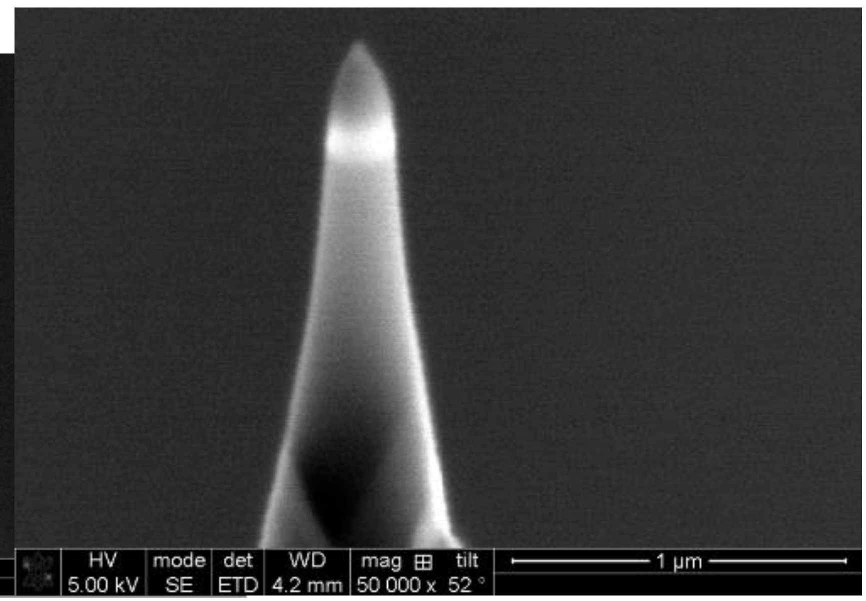

APT: sample preparation

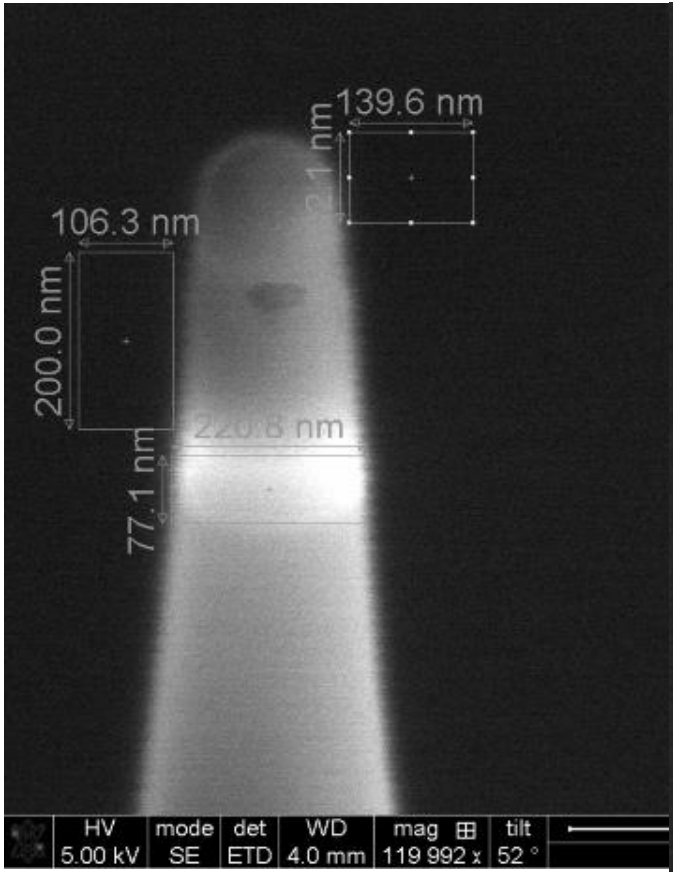

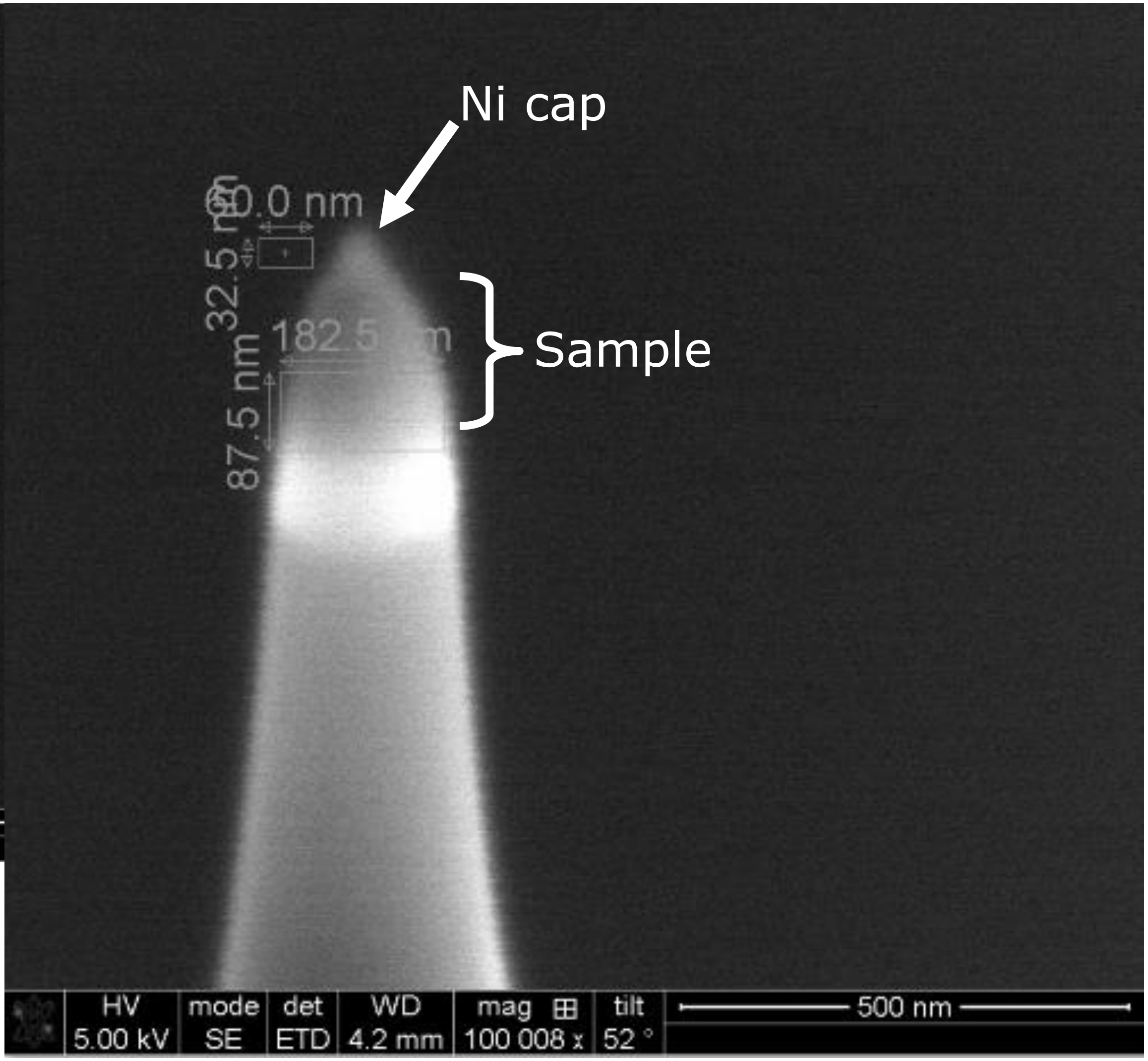

Reconstruction tools

Spatial distribution map (SDM)

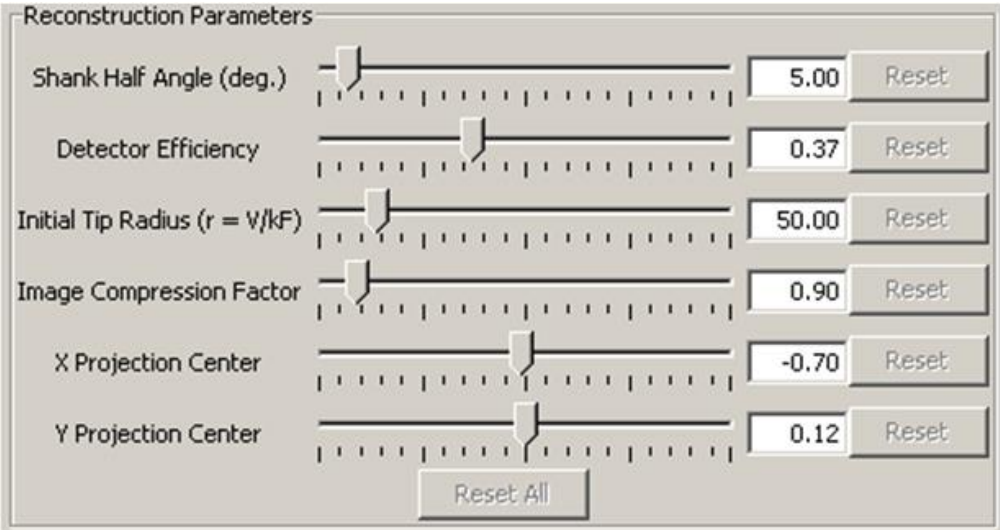

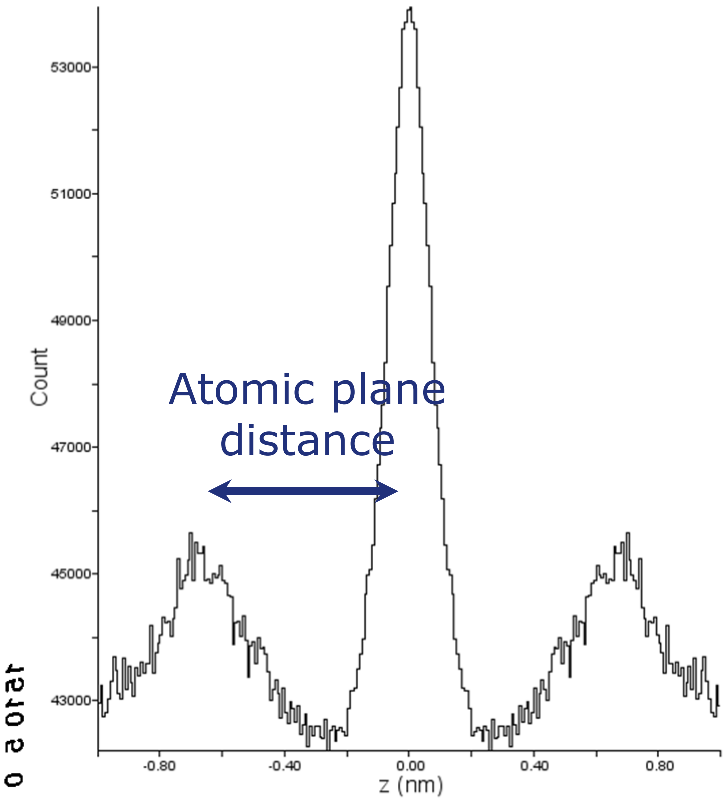

Ge(001) substrate

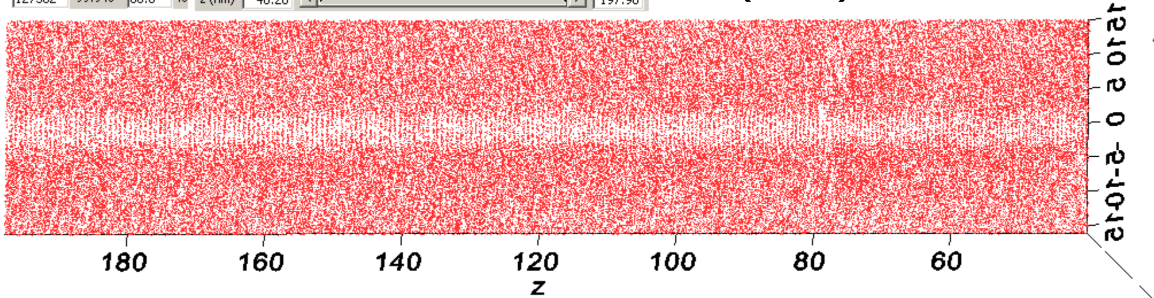

Reconstruction tools

Mass spectrum

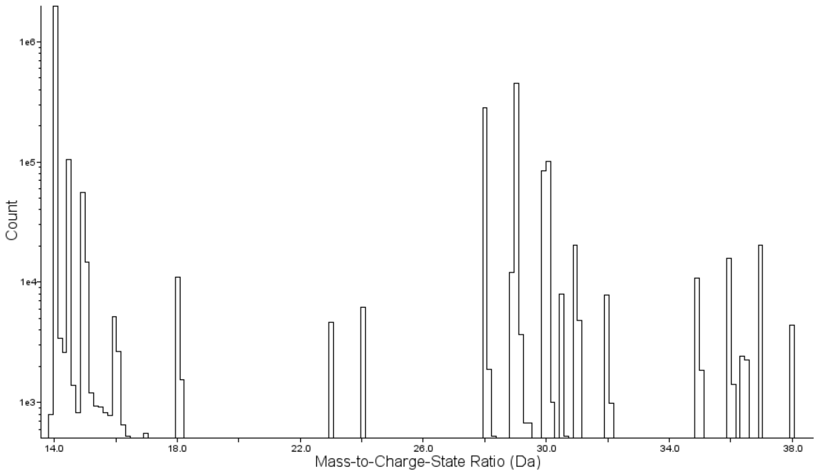

Proportion of isotopes

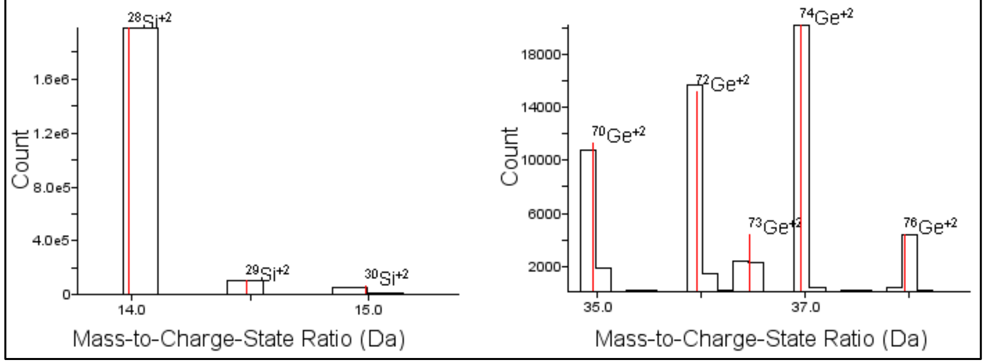

Mass spectrum identification

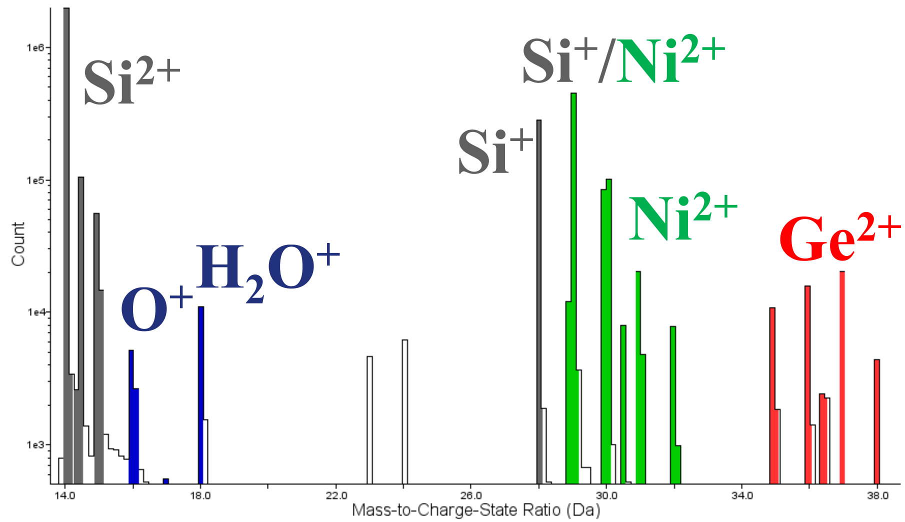

APT data analysis

3D qualitative analysis

Gay dot: Si atom
Green dot: Ni atom
Red dot: Ge atom

Buried Ge islands

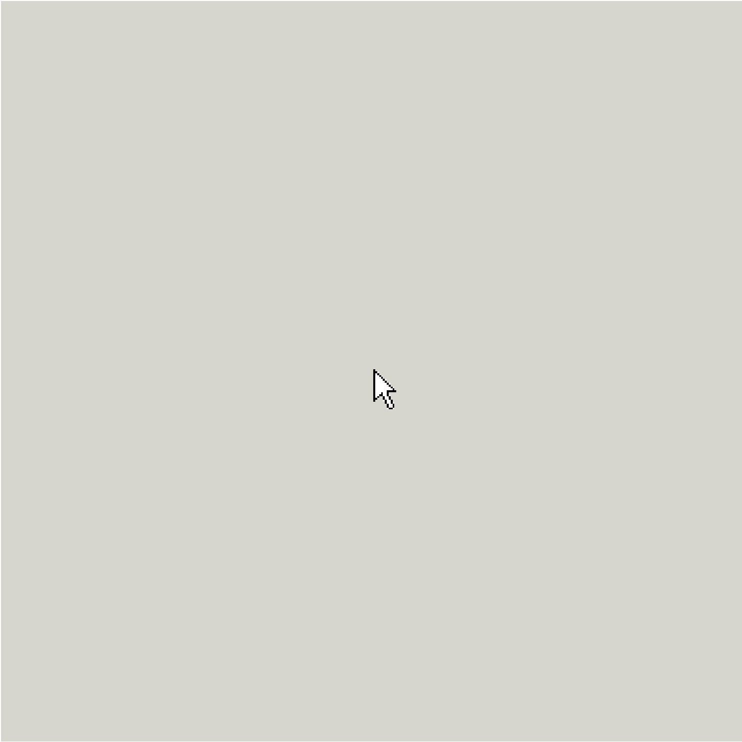

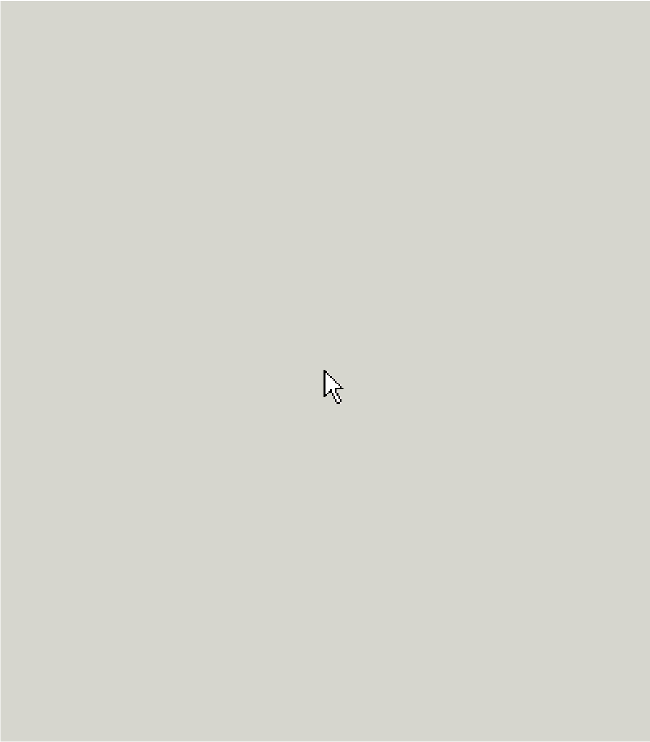

➢ Ion selection, clipping, plan-view and cross-section view

APT data analysis

3D qualitative analysis: Examples

Ge(Mn) nano-columns

TEM

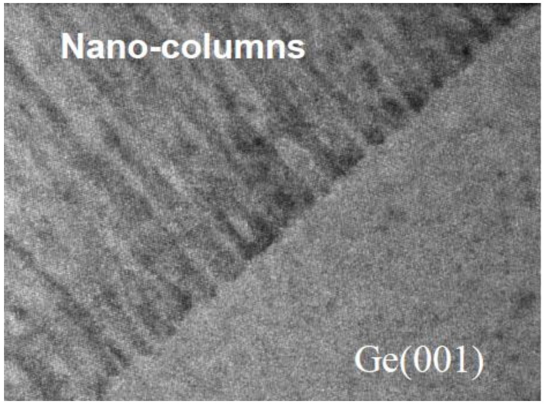

cross-section

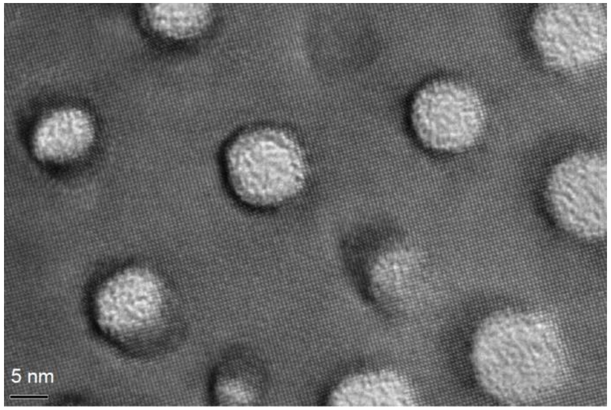

plan-view

APT

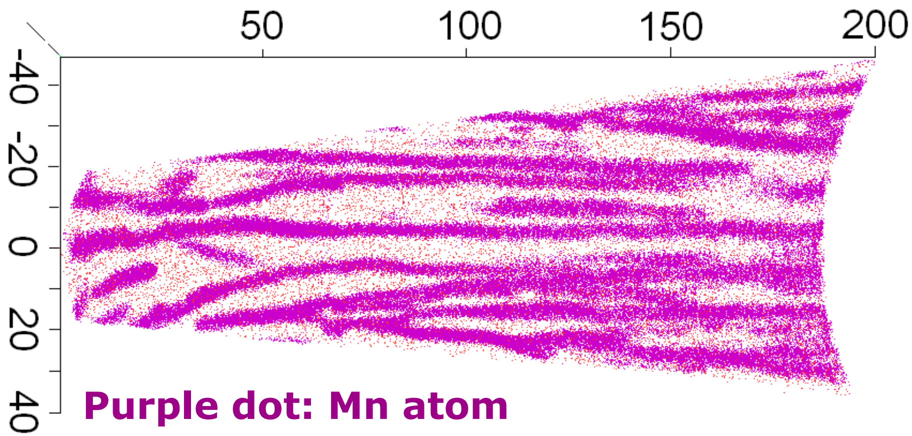

Purple dot: Mn atom

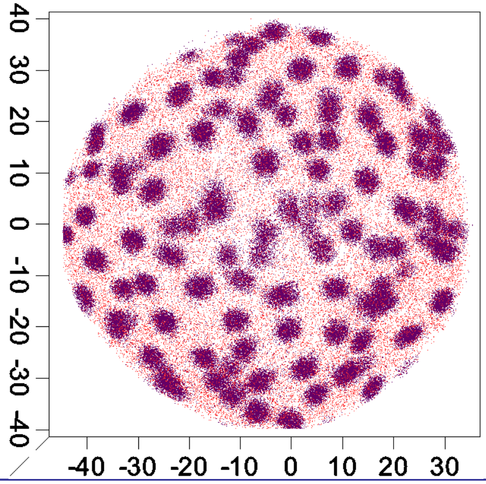

APT data analysis

Quantitative measurements: Region of interest (ROI)

Buried Ge islands

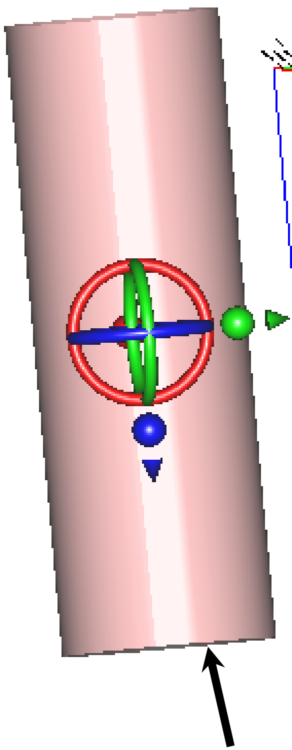

ROI

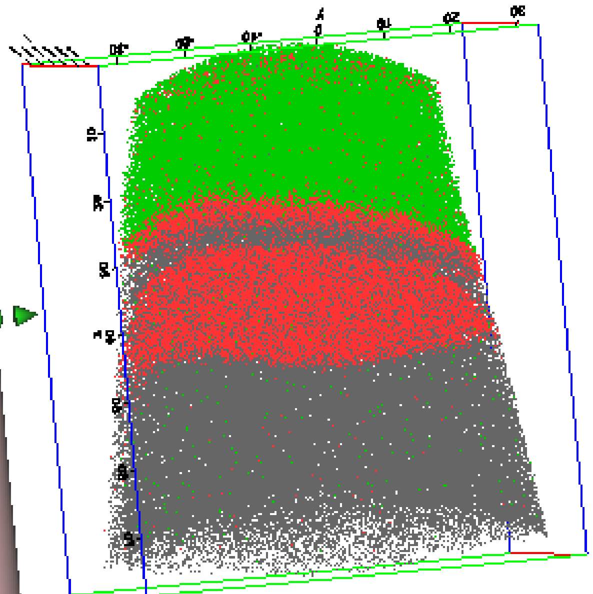

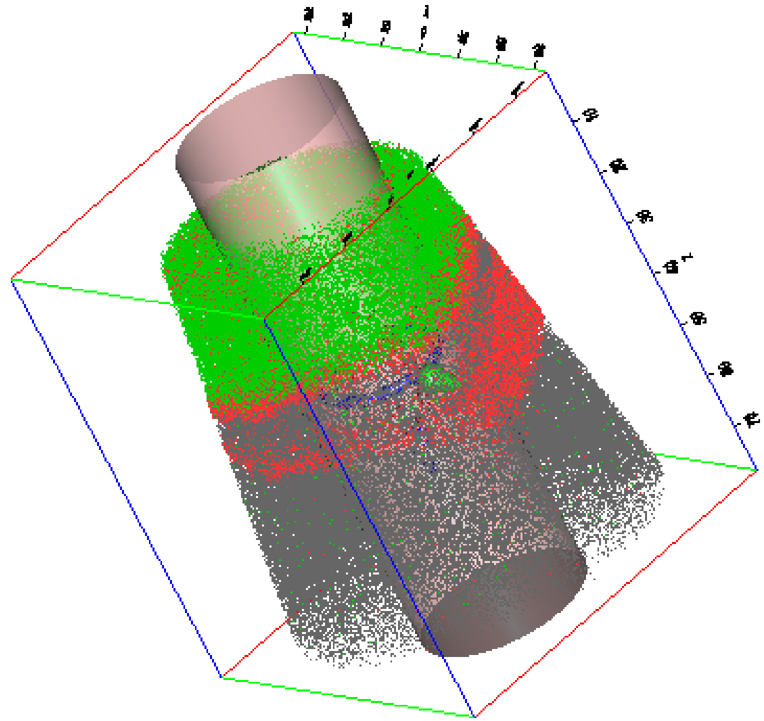

Gay dot: Si atom
Green dot: Ni atom
Red dot: Ge atom

➢ Definition of a volume of interest for data analysis

APT data analysis

Exporting region

Buried Ge islands

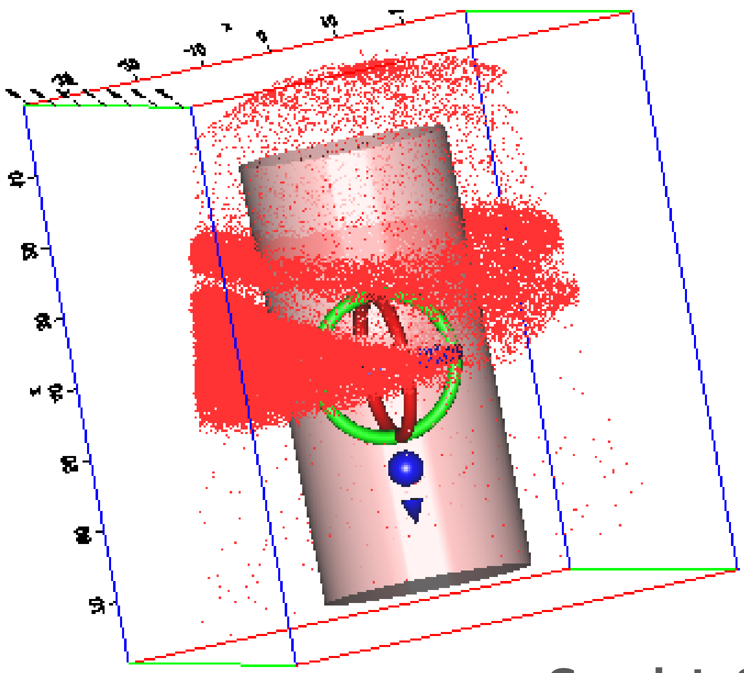

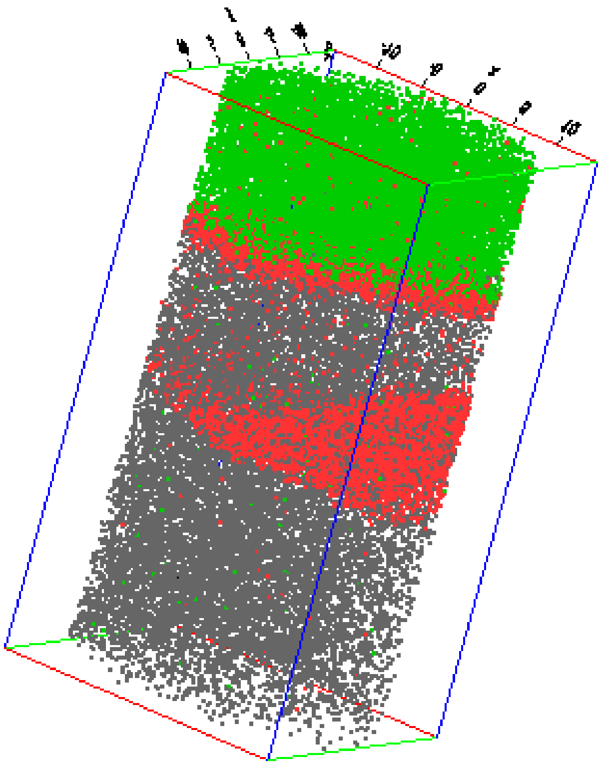

Gay dot: Si atom
Green dot: Ni atom
Red dot: Ge atom

➢ Allows for example to define the mass spectrum of a given volume sample taken from the global APT volume (noise study, peak overlaps…)

APT data analysis

Quantitative measurements: 1D concentration profiles

Buried Ge islands

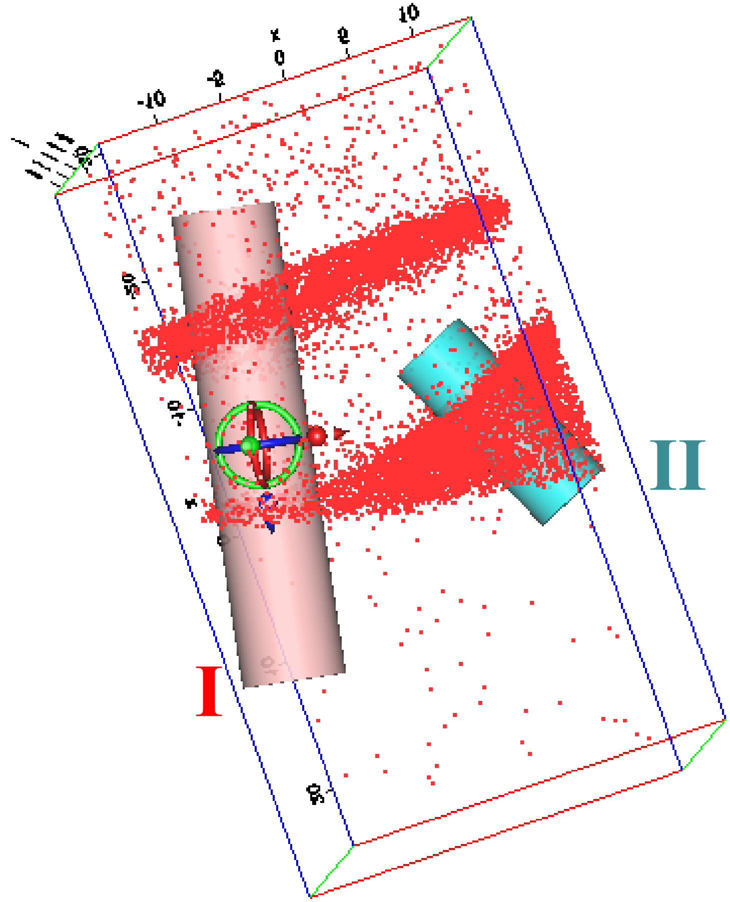

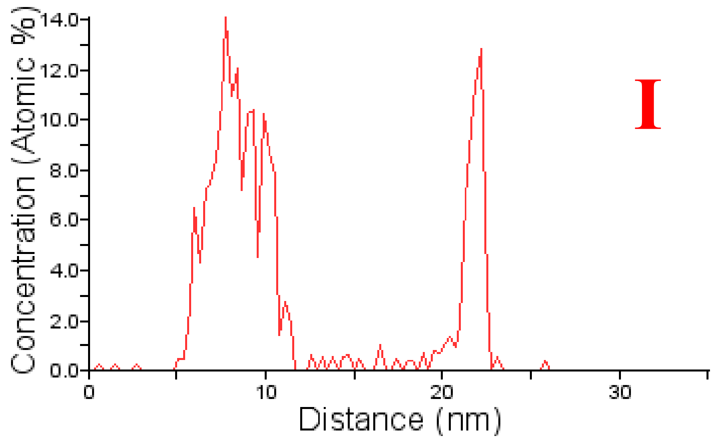

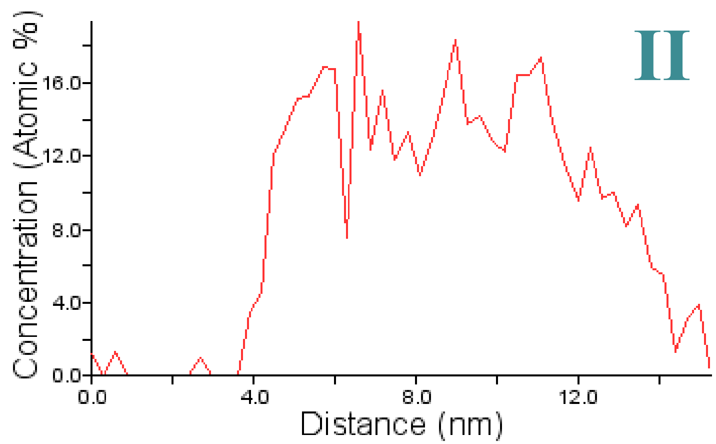

APT data analysis

1D concentration profiles: Examples

Ge(Mn) nano-columns

Purple dot: Mn atom

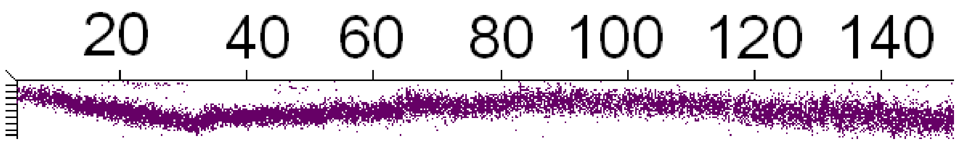

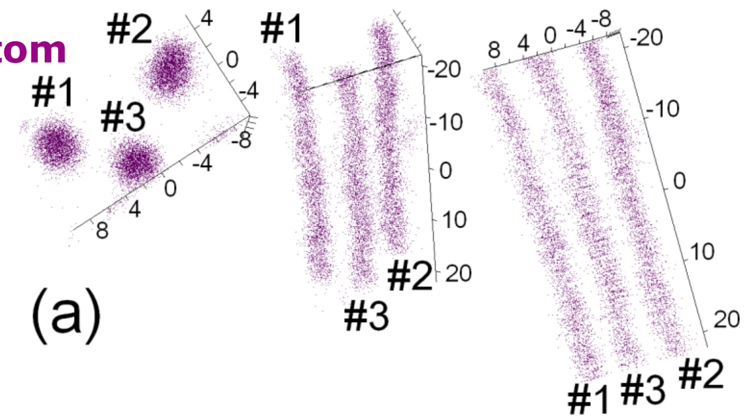

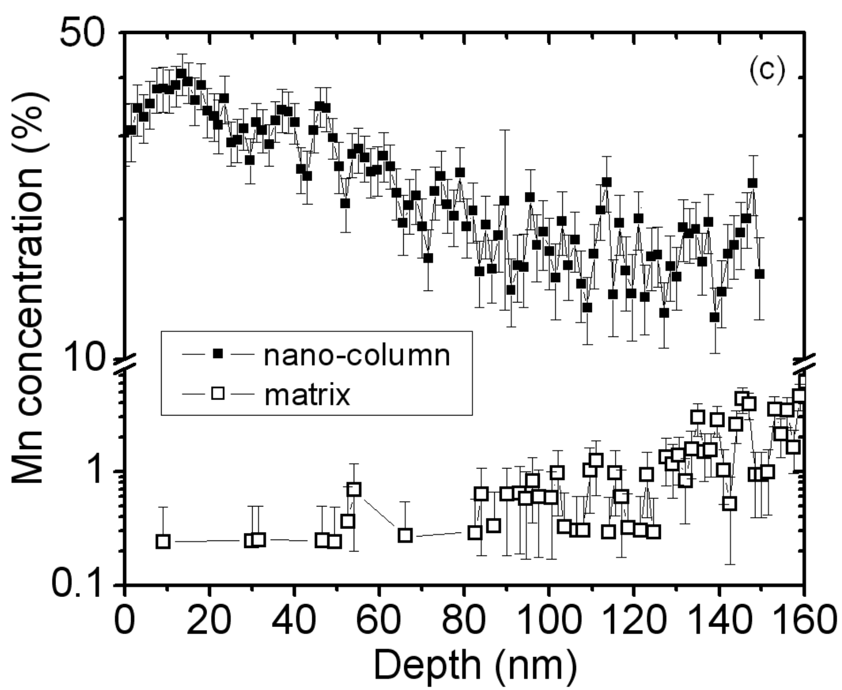

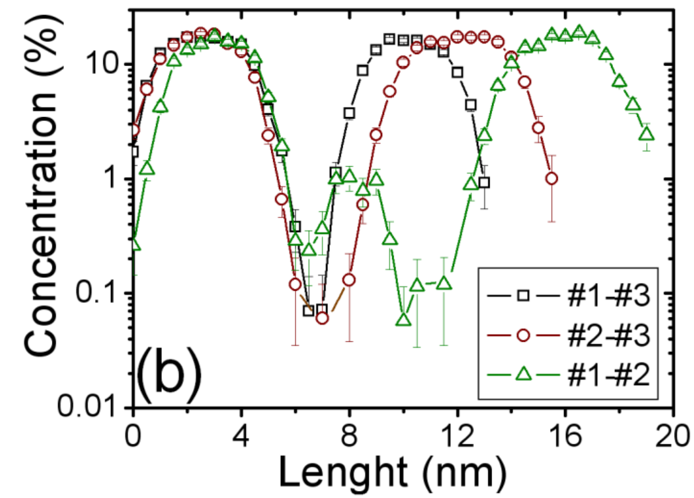

APT data analysis

Quantitative measurements: 2D concentration map

Buried Ge islands

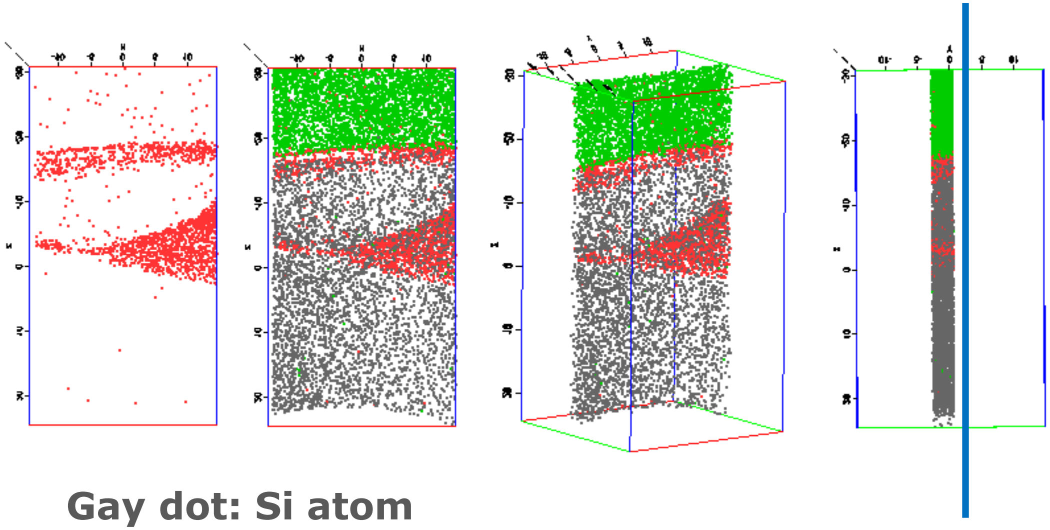

Gay dot: Si atom
Green dot: Ni atom
Red dot: Ge atom

Projection plan

Max (red) = 0.17%
Min (blue) = 0.0%

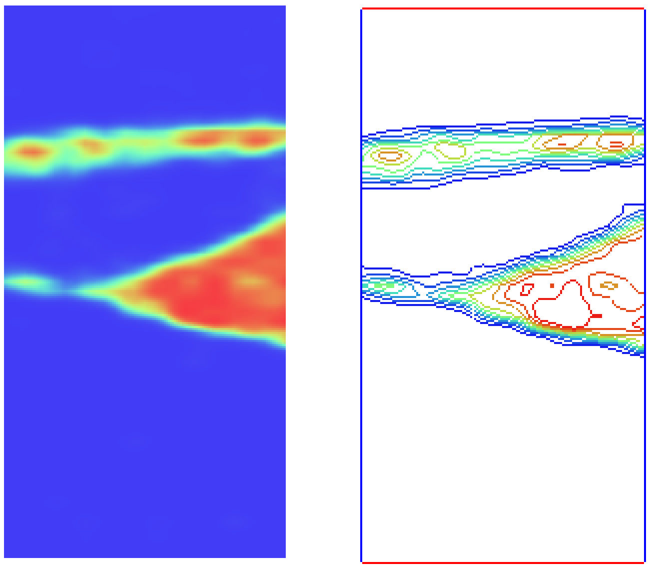

APT data analysis

2D concentration map: Examples

Si clusters in a SiO_2 thin film

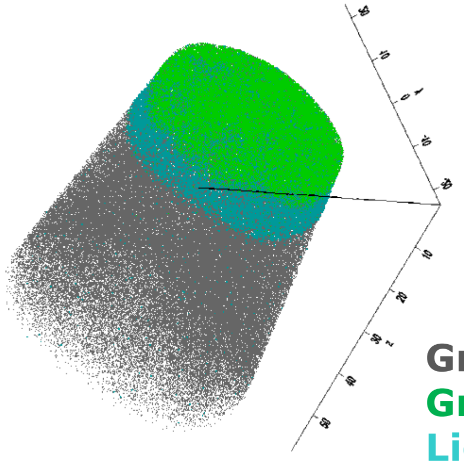

Gray dot: Si atom
Green dot: Ni atom
Light blue: O atom

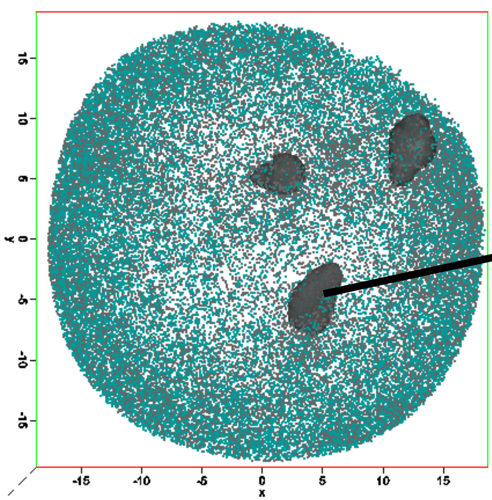

2D Si atom distribution surrounding a single Si cluster

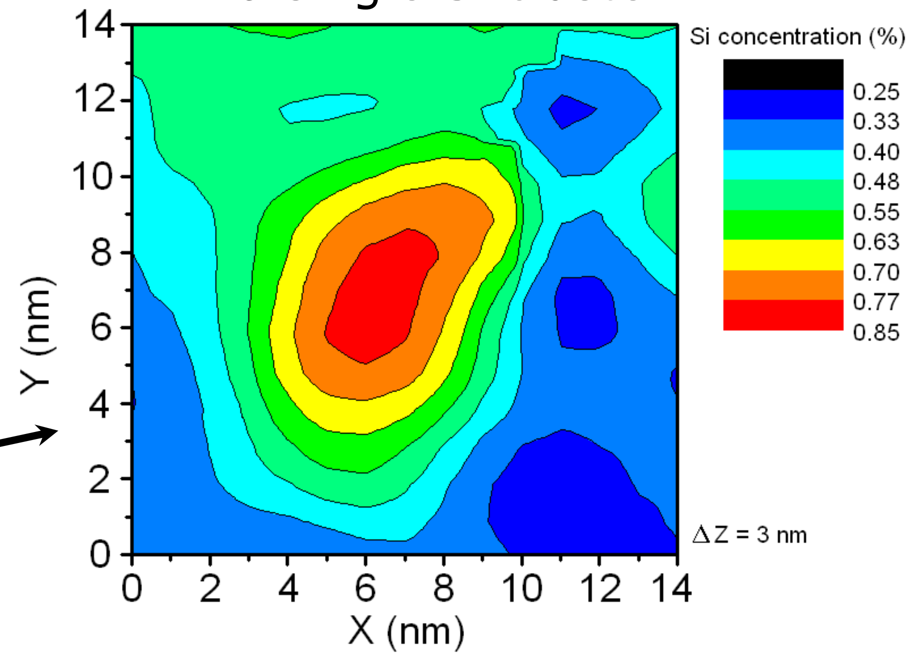

APT data analysis

2D concentration map: Examples

Ge concentration in the core of a Ge "dome" island

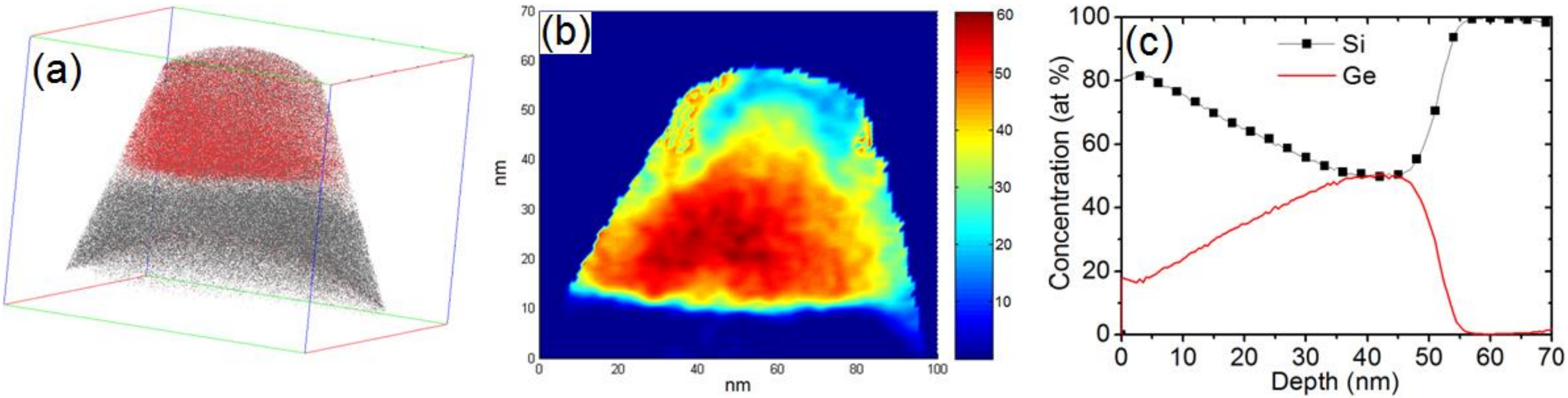

3D 2D 1D

- 1D profile ⇨ Ge concentration in the island core ~ 50%
- 2D map ⇨ Ge concentration in the island core ~ 55%

APT data analysis

Iso-concentration/iso-density surfaces

Buried Ge islands

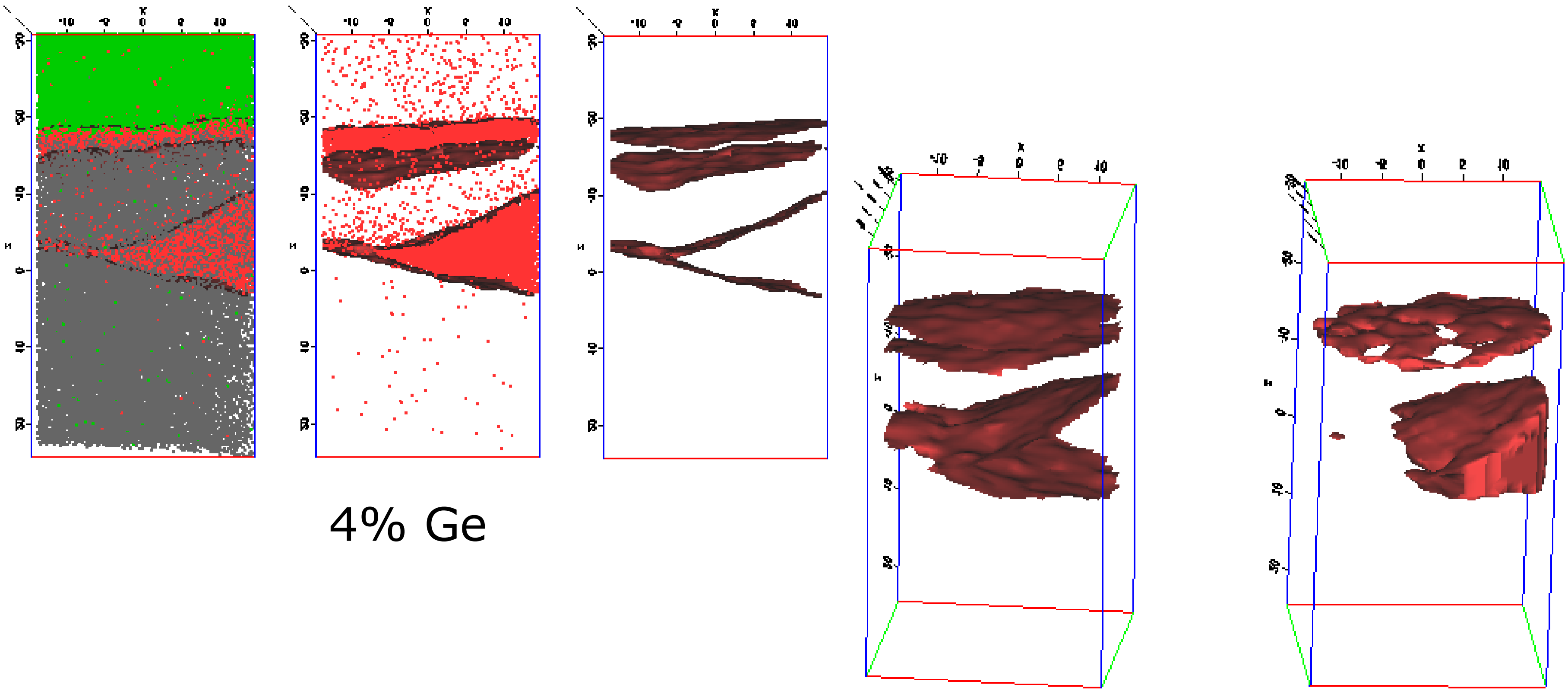

4% Ge

4%

10%

APT data analysis

Iso-concentration surfaces: Examples

Ge(Mn) nano-columns

TEM

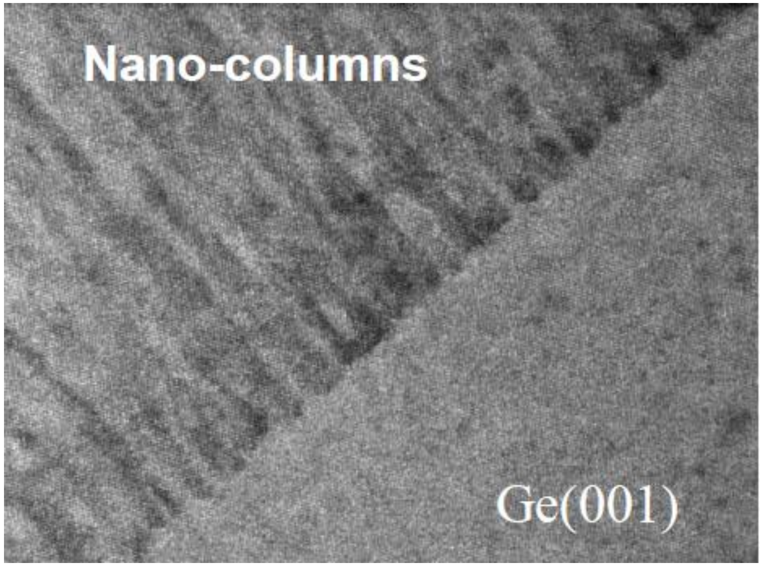

cross-section

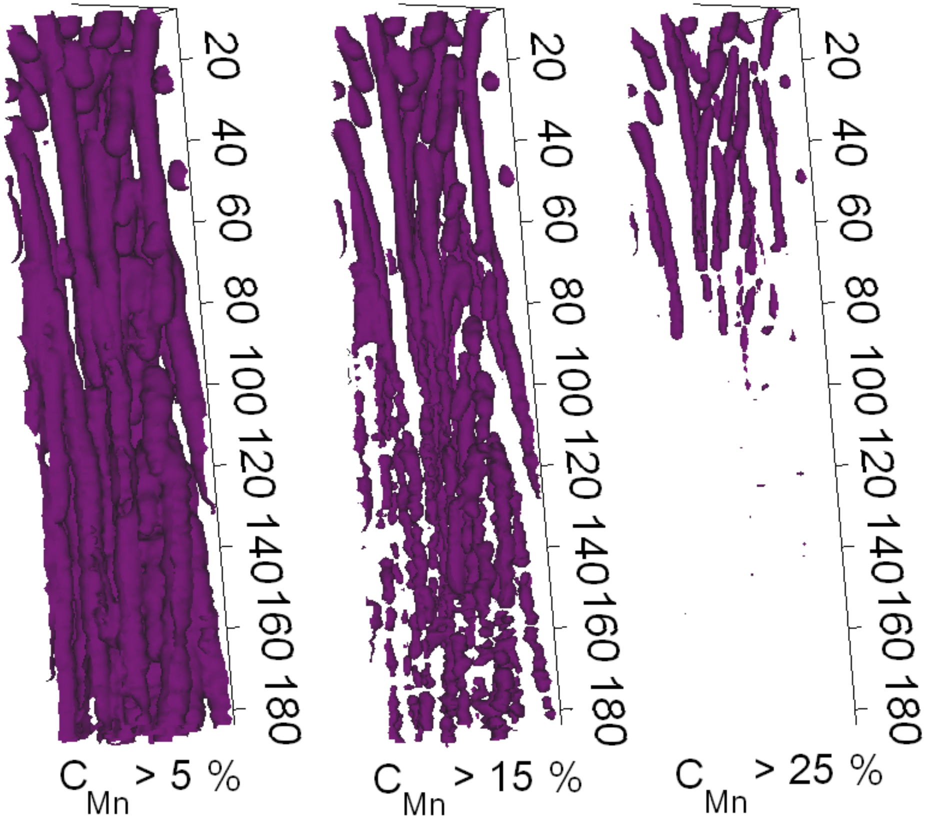

- Concentration gradients

⇨ nano-columns richer in Mn in their core and closer to the surface

APT data analysis

Iso-concentration surfaces: Examples

$Mn_5Ge_3(C)$ layer grown on Ge(111) by reactive diffusion

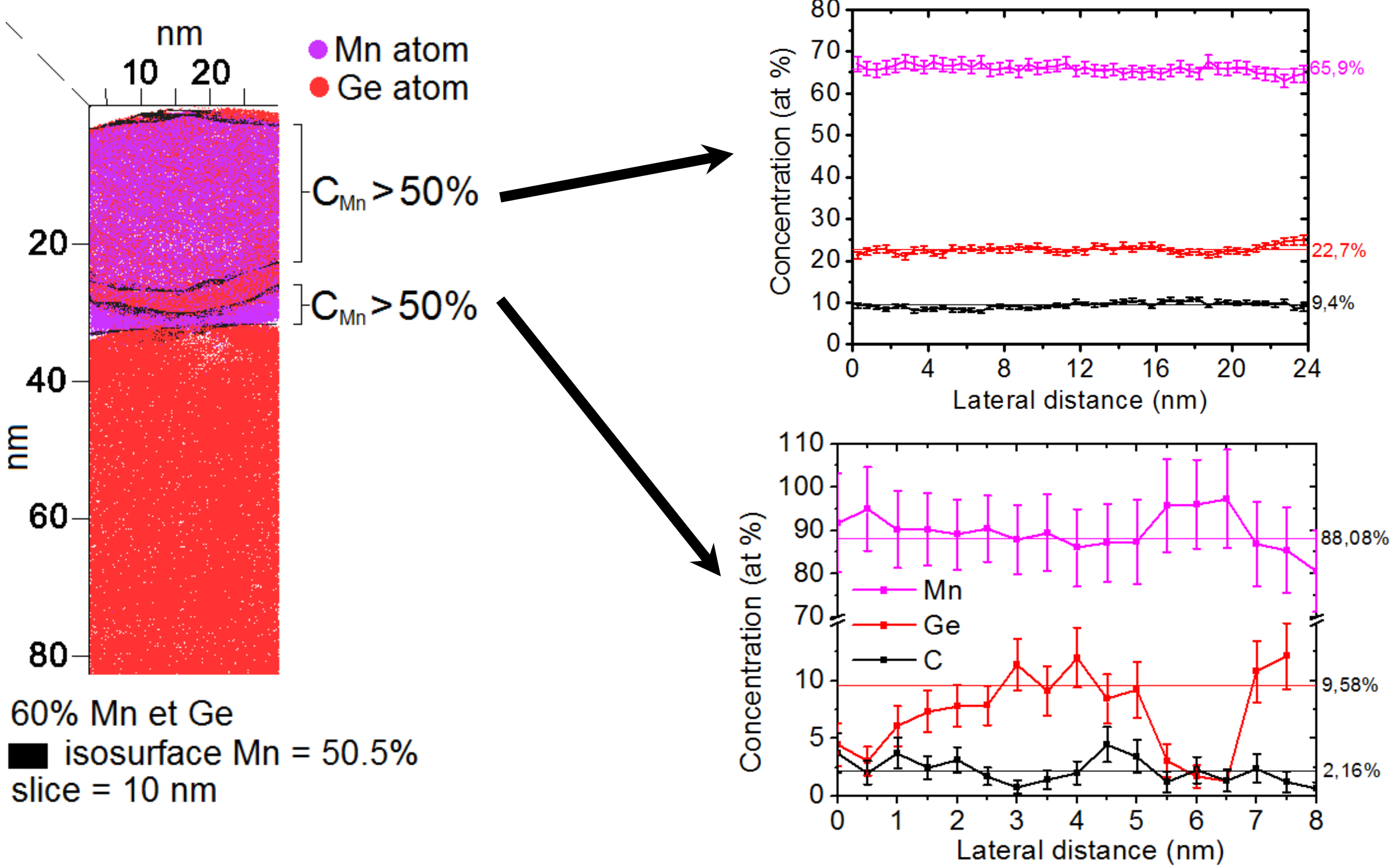

➢ Delimitation of different phases (phase selection for data analysis)

APT data analysis

Iso-surfaces: cluster detection

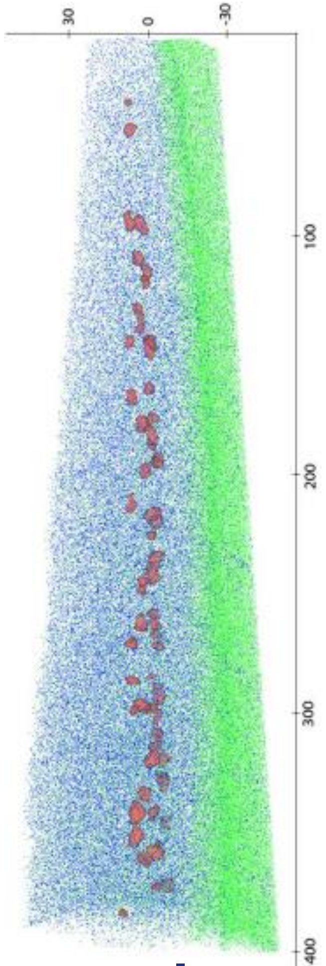

Blue dot: O atom
Green dot: Si atom
Red volumes: silicon-enriched regions in SiO_2 matrix

Si nano-clusters in a SiO_2/Si(001) layer

Blue dot: B atom
Green dot: Ni atom
Black dot: Si atom
Blue volumes: isodensity surfaces = 0.65 B at nm^{-3}

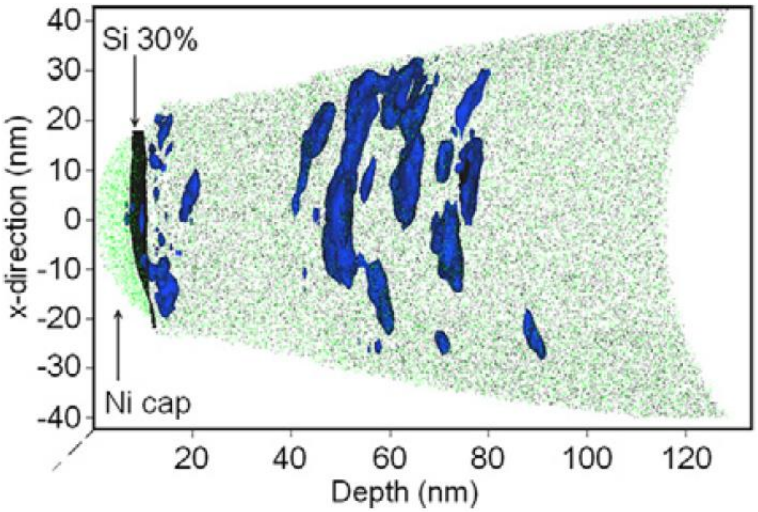

B nano-cluster in a SiO_2/NiSi/SiO_2/Si(001) layer

APT data analysis

Quantitative measurements: proxigram

Buried Ge islands

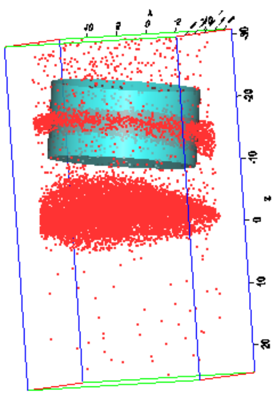

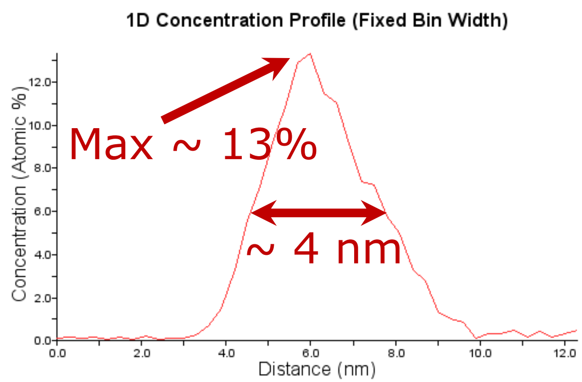

Average composition calculated along the directions perpendicular to the defined iso-surface

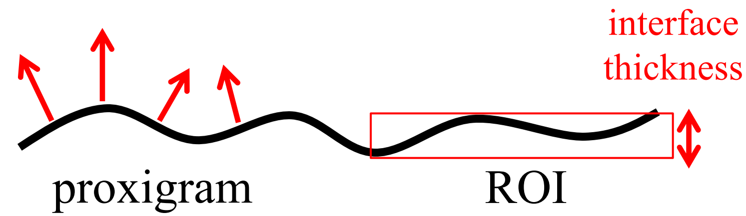

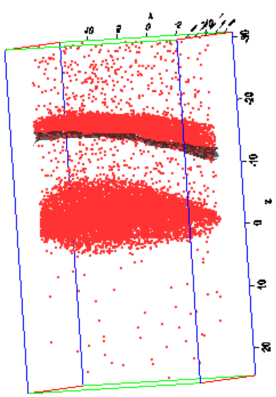

5%

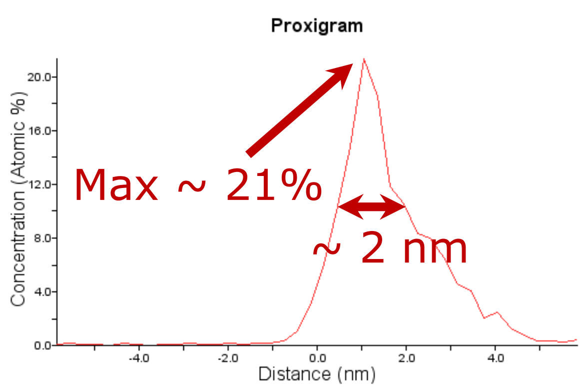

- ➢ Allows the curvature of an interface to be taken into account in the 1D concentration profile

Institut Matériaux Microélectronique Nanosciences de Provence
UMR 6242 CNRS, Universités Paul Cézanne, Provence et Sud Toulon-Var

APT data analysis

Proxigram: Examples
Cluster composition

Mn-Ge nano-clusters in poly-Ge

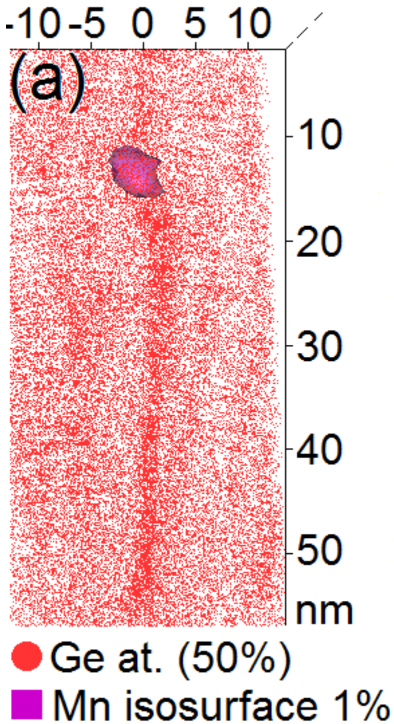

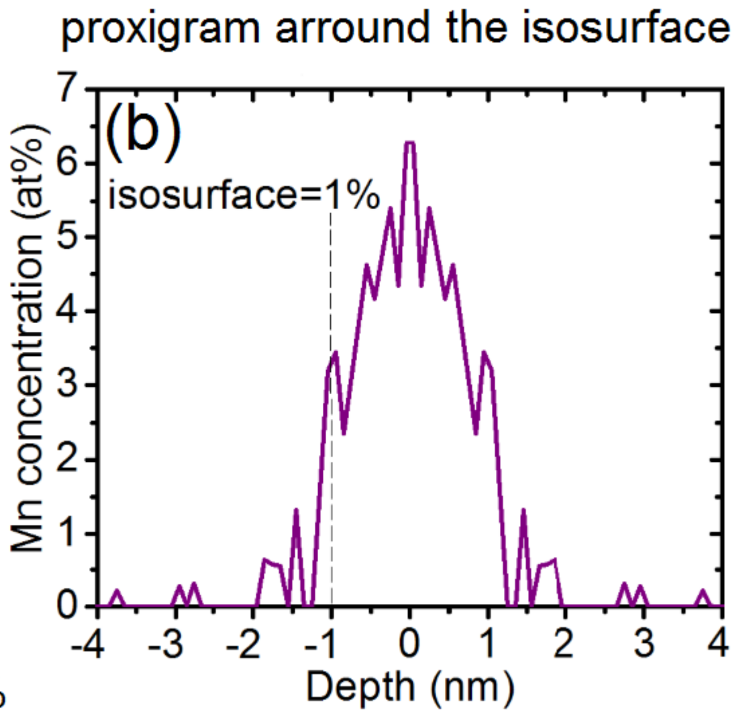

Island average size ~ 2 nm

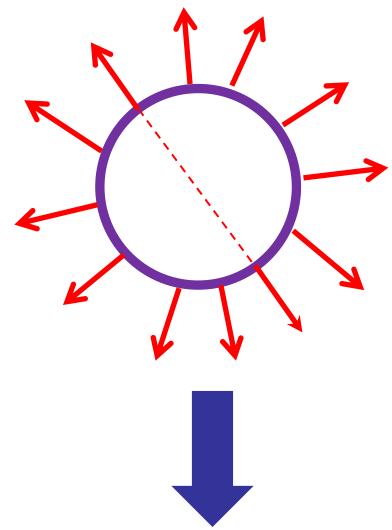

- Average cluster size
- Average cluster composition

Im2np Institut Matériaux Microélectronique Nanosciences de Provence
UMR 6242 CNRS, Universités Paul Cézanne, Provence et Sud Toulon-Var

APT data analysis

Proxigram: Examples
Cluster composition

Si nano-clusters in SiO_2

Plane view

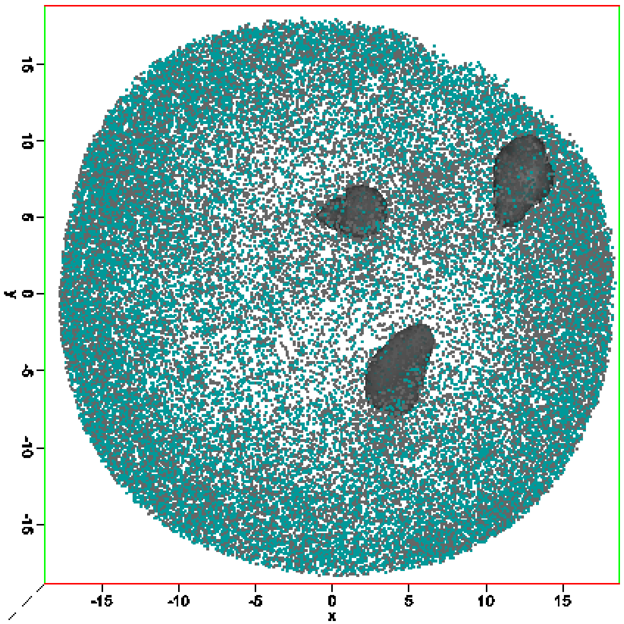

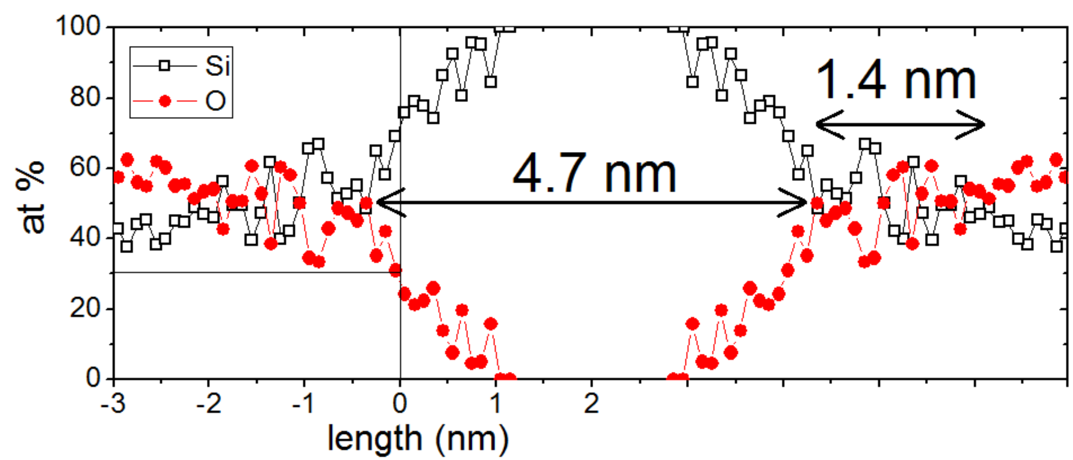

Island average size ~ 5 nm

Si-pure island core ~ 1.5 nm

APT data analysis

Quantitative measurements: atomic radial distribution

Mn-Ge nano-clusters in poly-Ge

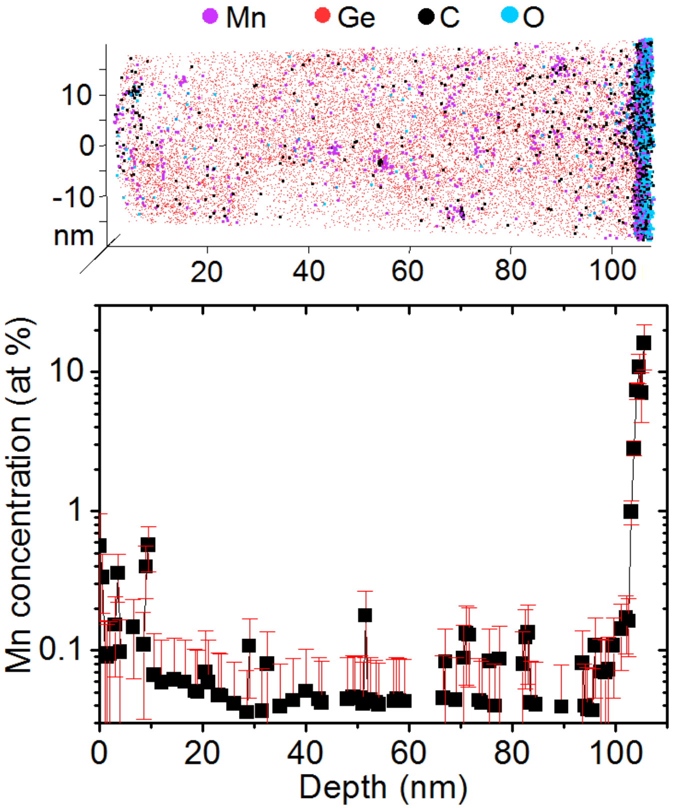

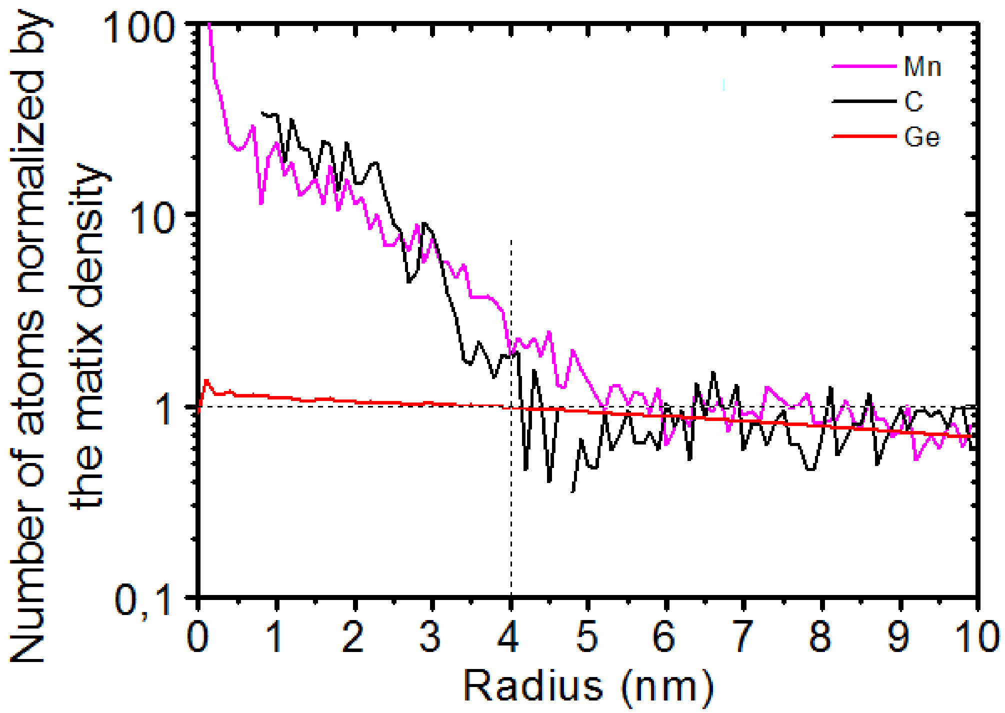

➢ Investigation of atom distribution, here up to 4 nm a Mn atom has ~10 times more Mn and C atoms than Ge atoms in its vicinity

APT data analysis

Quantitative measurements: cluster analysis

W atoms in Si

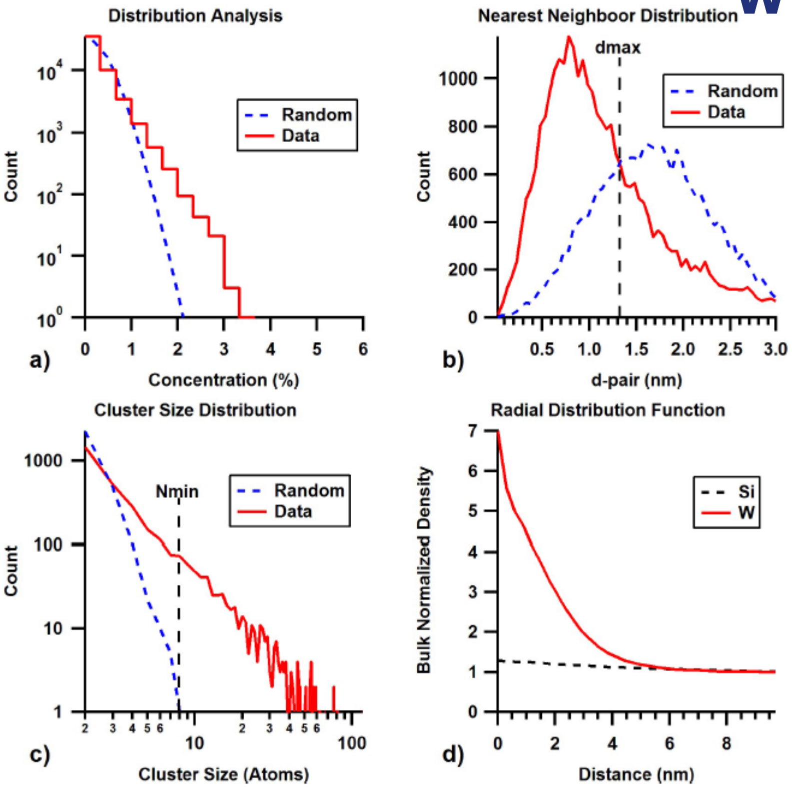

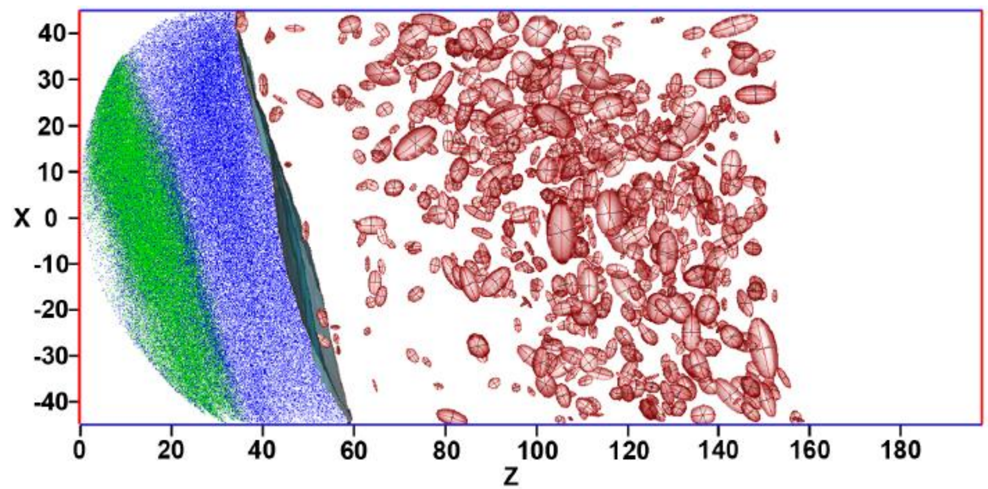

➢ Even if clusters cannot be observed using iso-surfaces, statistical studies can be performed on the atomic distribution in the APT volume lading to the detection of clusters (number, size, composition…)

APT data analysis

Cluster analysis: Examples

Sb atoms in Sb- and P-doped Ge grown by MBE

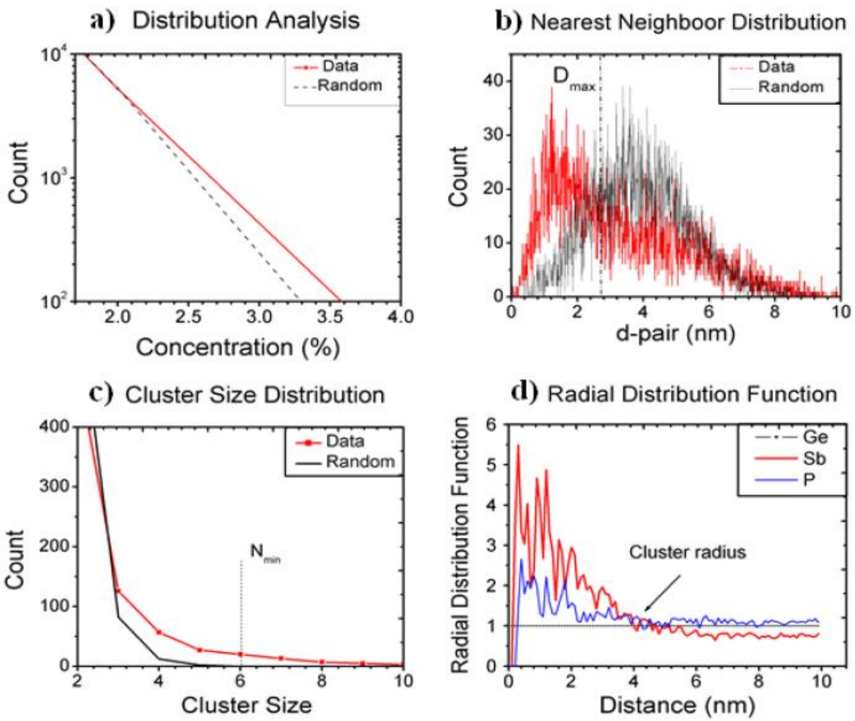

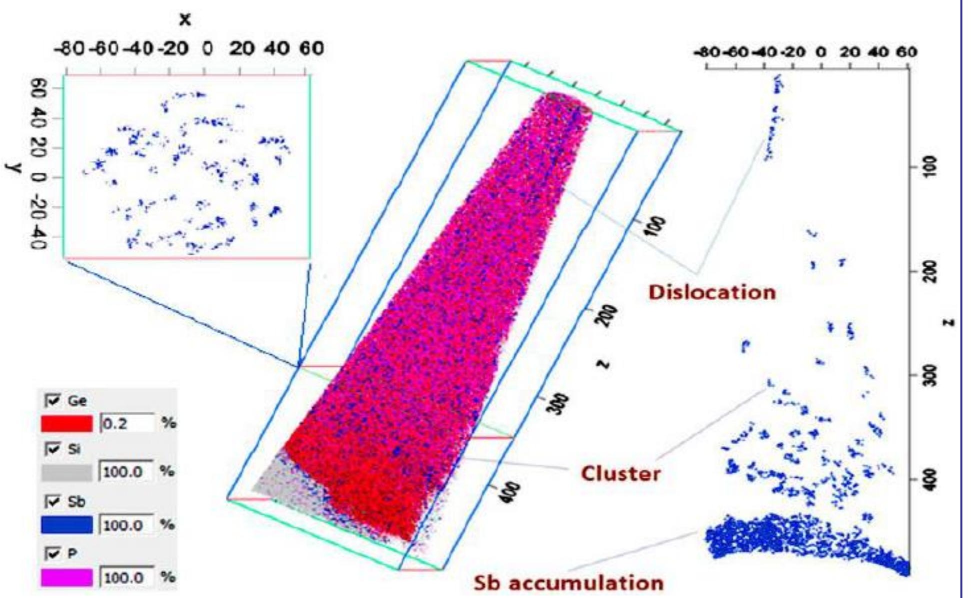

Sb cluster analysis

Tip information			Cluster analysis		
Upper radius	Bottom radius	Height	Number of clusters	Average atom per cluster	Clusters per microtip
20 nm	60 nm	450 nm(*)	83	10	3.4×10^{16} clusters/cm^3

*without taking into account the Sb accumulation at the bottom of the tip

APT: some issues

- Sample fracture due to the stress applied to the tip during electrical or laser pulsing (electrical force and/or temperature diffusion effects), and due to interface weakness in multilayer films
- Detection limit ~ 10^{18} at cm^{-3}: APT allows atomic scale analysis but despite that 50-40% of all the atoms present in the sample are collected, the detection limit is limited by the small size of the probed volumes (10^{19} at cm^{-3} ~ 1 at in 100 nm^3)
- Mass resolution (overlapping peaks in the mass spectrum) can depend on analysis conditions (too high laser energy for example)
- Evaporation of some materials can occur via molecule formation $\Rightarrow$ complex mass spectra (complex ion identification)
- Need references (film thickness, flat interfaces) in order to perform the best 3D reconstruction $\Rightarrow$ best reference = atomic planes
- Reconstruction procedure considers a single evaporation field F (= 1 homogeneous material), but samples can be made of several materials
- Best analysis conditions can be different for different materials (oxides, metals, semiconductors…) $\Rightarrow$ alloys, multilayer films…

APT issues: multiple hits

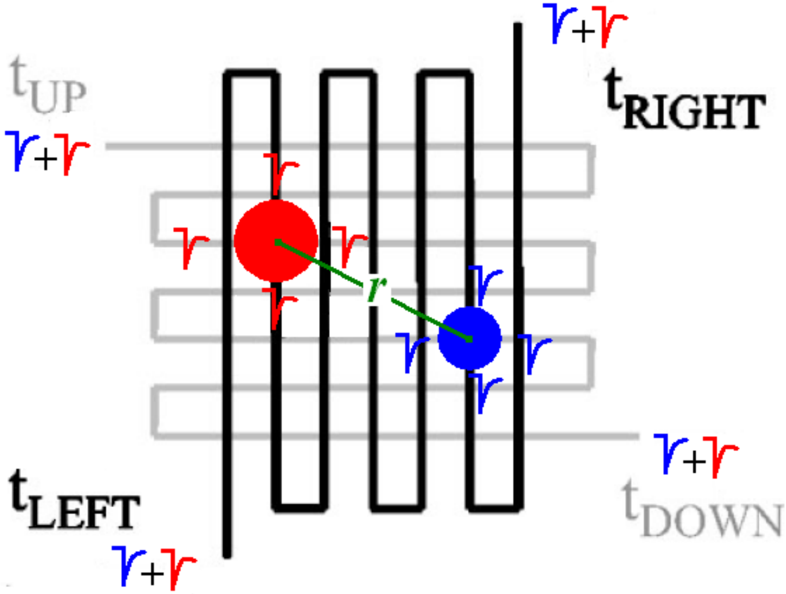

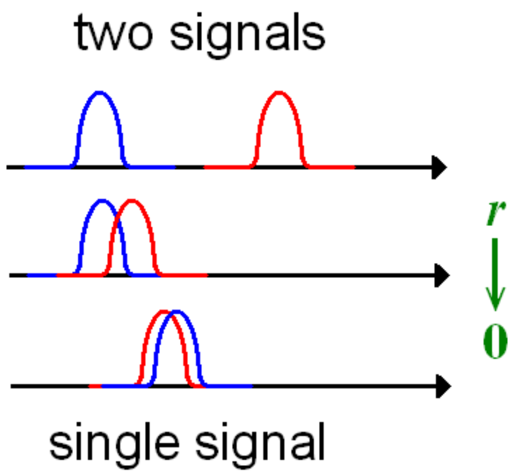

- ➢ Ions from close regions on the tip can arrive at the same time on the line detector
- ➢ If the two hits are enough far apart on the detector, two signals are detected but it is difficult to define which signal belongs to which ion
  ⇒ dedicated algorithms can separate some of the ions
- ➢ If the ions are too close on the detector, a single signal instead of n can be detected on some lines, preventing to differentiate the n ions
  ⇒ a single hit is counted instead of n! ⇒ C = C/n!!

APT issues: surface diffusion

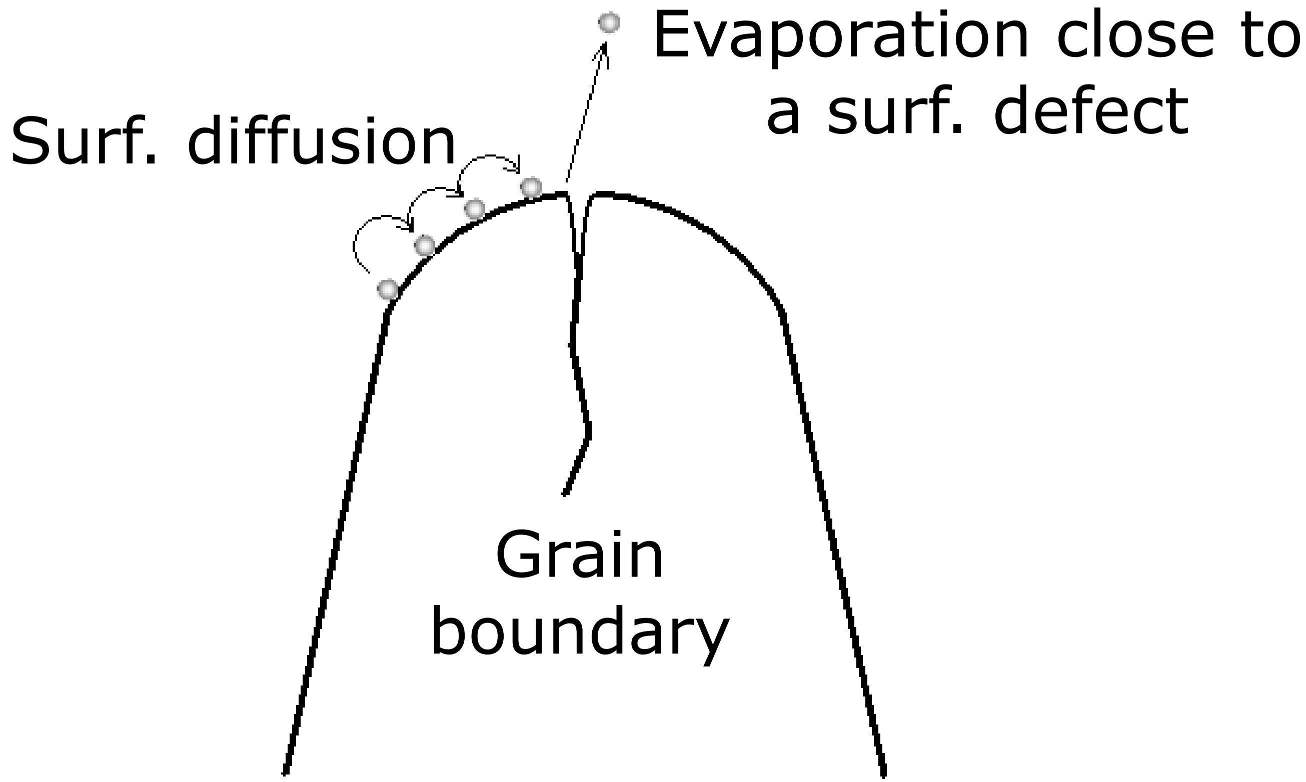

➢ Due to the low temperature of analysis (20-80 K), surface diffusion is not a problem in general, but in some cases some of the atoms may diffuse on the tip surface and evaporate preferentially on sites of smaller curvature radius ⇒ wrong atom distribution

APT issues: local magnification

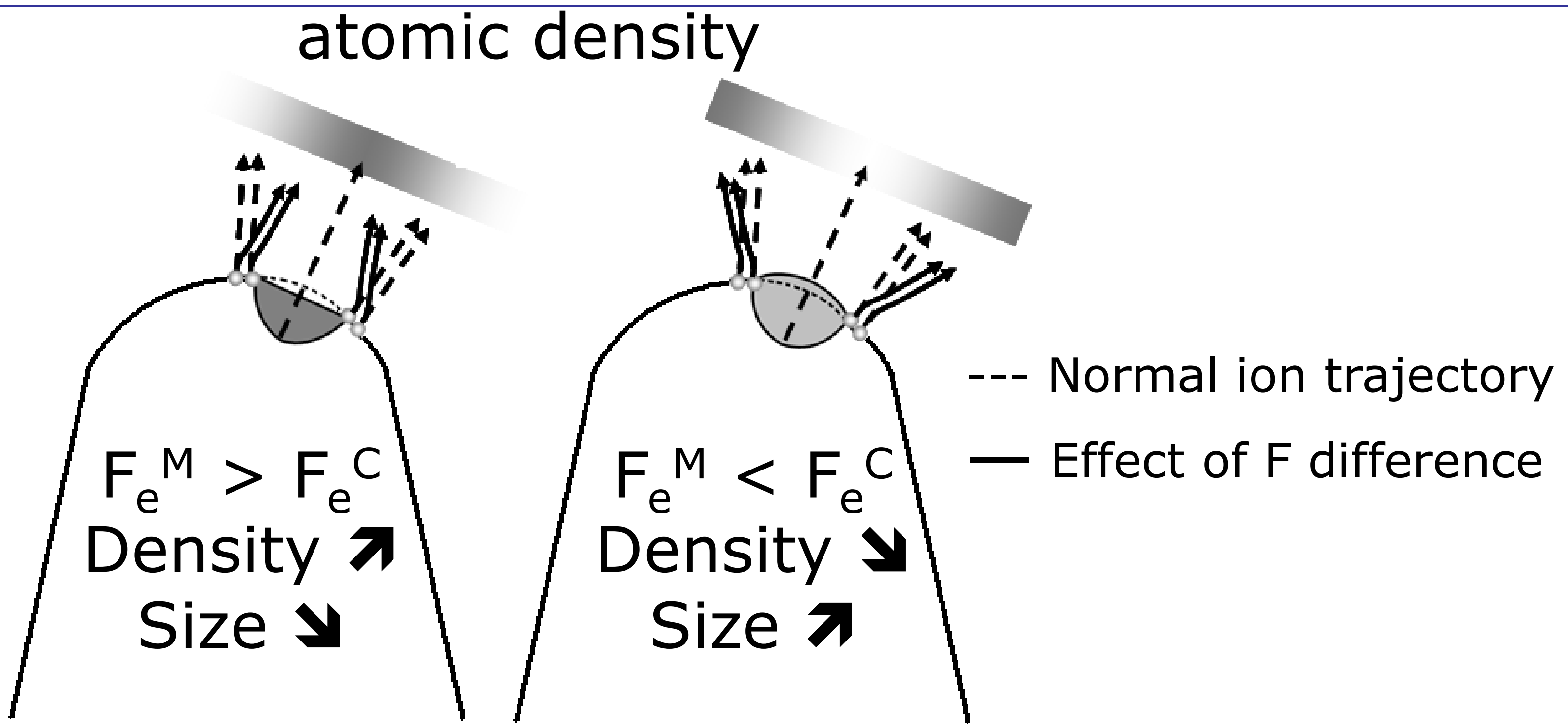

- V = const: evaporation at surface regions of smaller curvature radius
- Regions of higher evap. field (F_e) need smaller radius for evaporation
- Case of an homogeneous matrix with F_e^M containing clusters with F_e^C

$\Rightarrow$ the density of atoms in clusters will be different from in the matrix, and the size of the clusters will not be the real one

APT issues: local magnification

Interfaces between different Mn-Ge phases

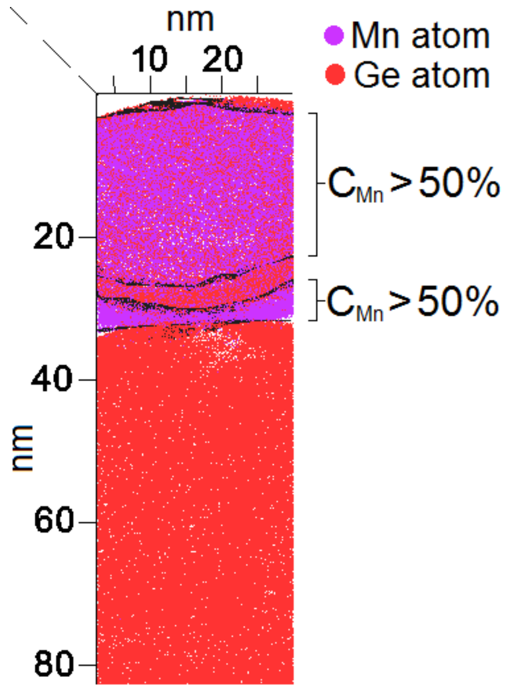

60% Mn et Ge
isosurface Mn = 50.5%
slice = 10 nm

Interface between Si and SiO_2

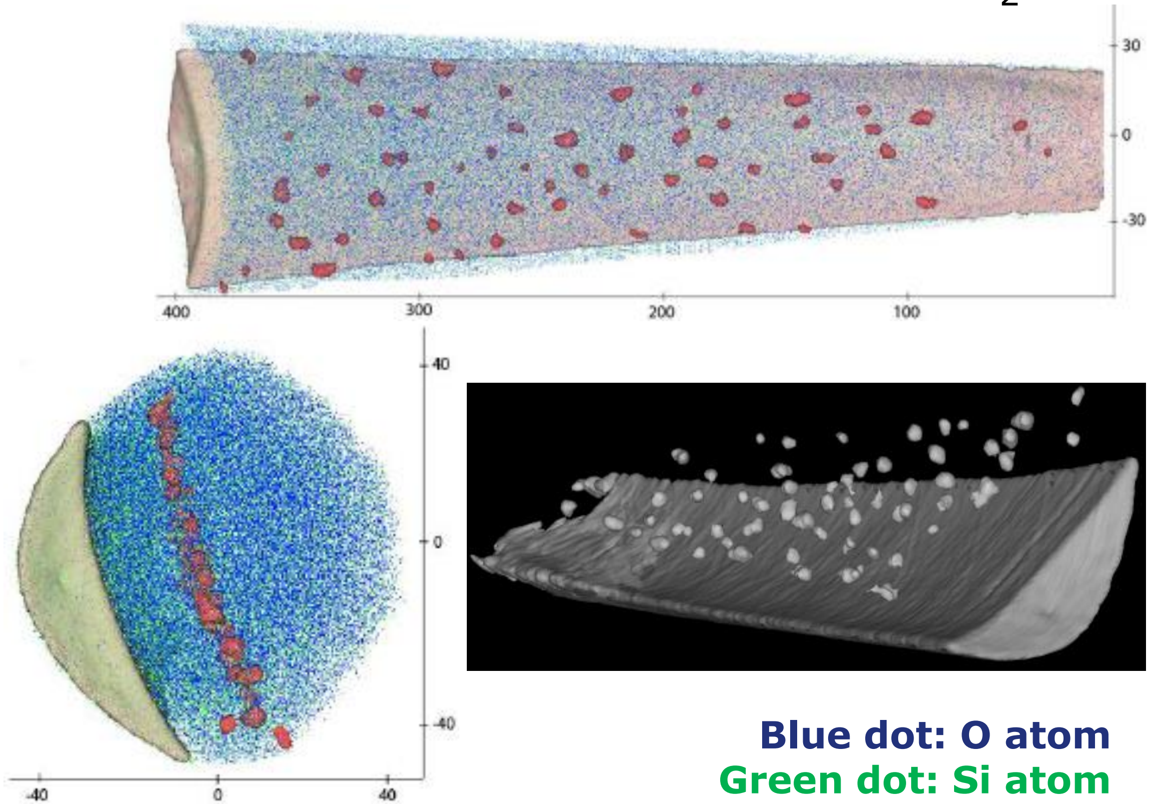

Blue dot: O atom
Green dot: Si atom
Red volumes: Si clusters
Continuous volume: Si substrate

➢ Significant evaporation field difference promotes curved interfaces

APT issues: local magnification

Grain boundary effect in poly-Ge

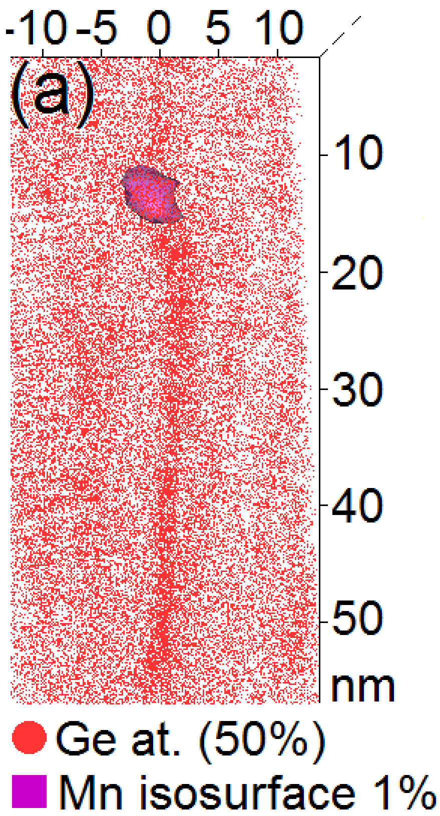

Grain boundary effect in poly-$Ni_2Si(Pt)$

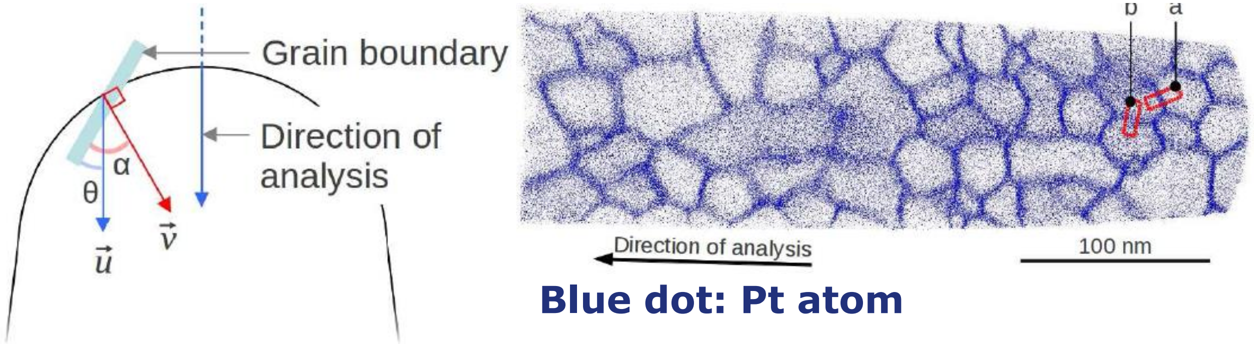

Blue dot: Pt atom

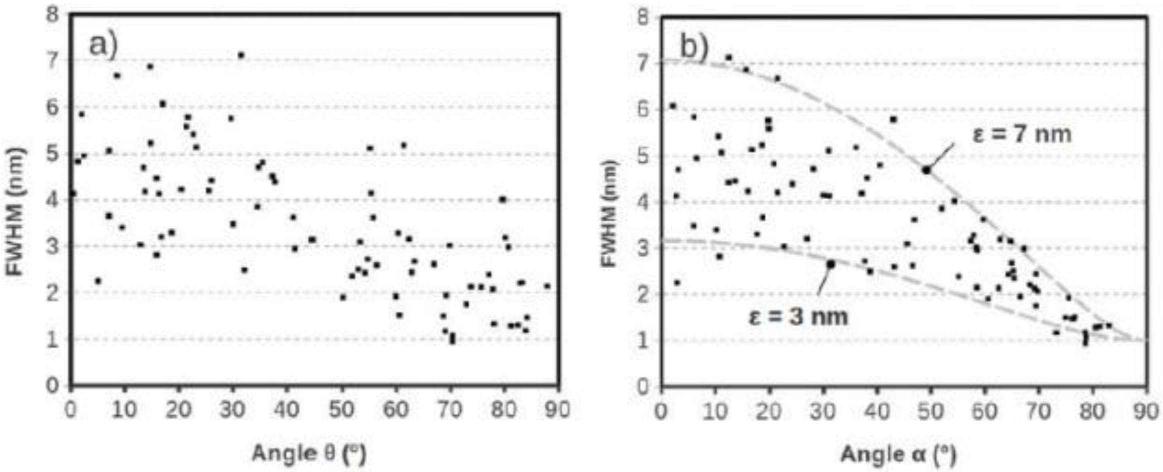

➢ Difference of curvature radius promotes atomic density variations and distance/thickness variations

APT issues: molecules

$Mn_5Ge_3(C)$ layer grown on Ge(111) by reactive diffusion

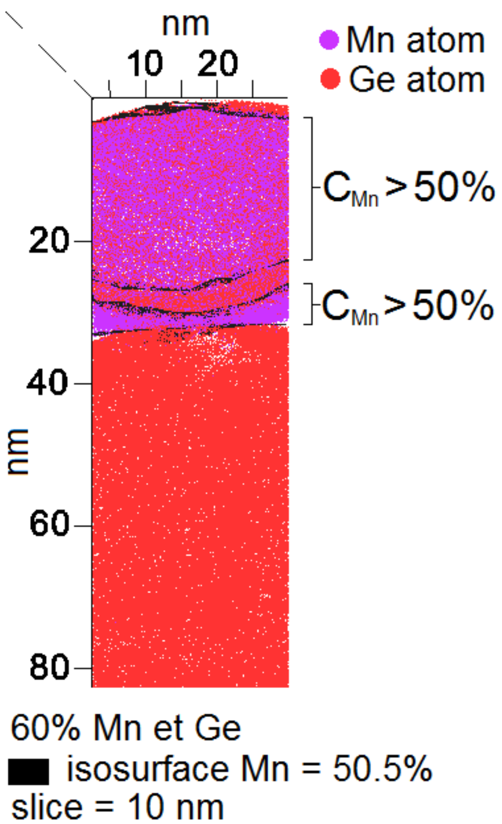

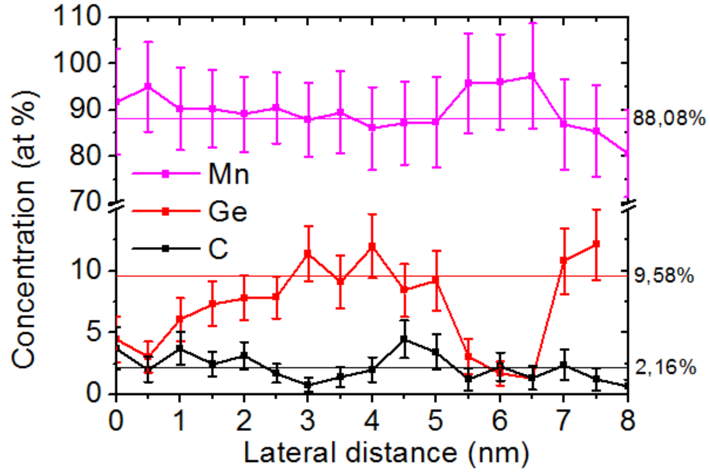

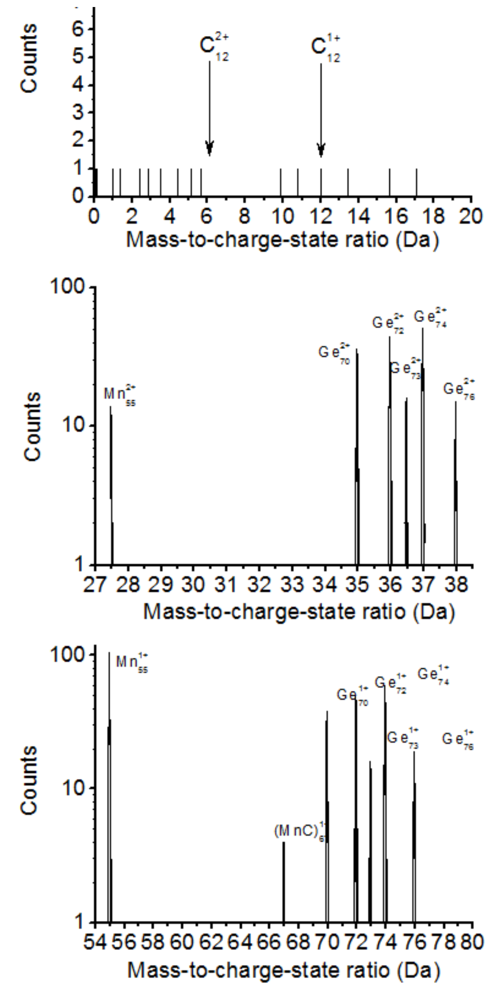

- Inform on atom neighboring (molecules not formed after evaporation)

APT issues: heat flow

Buried Ge islands on Si substrate

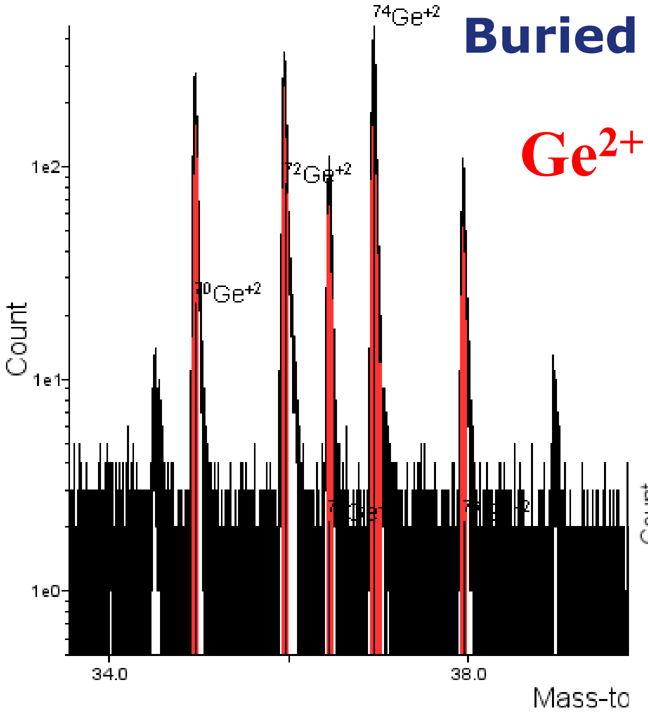

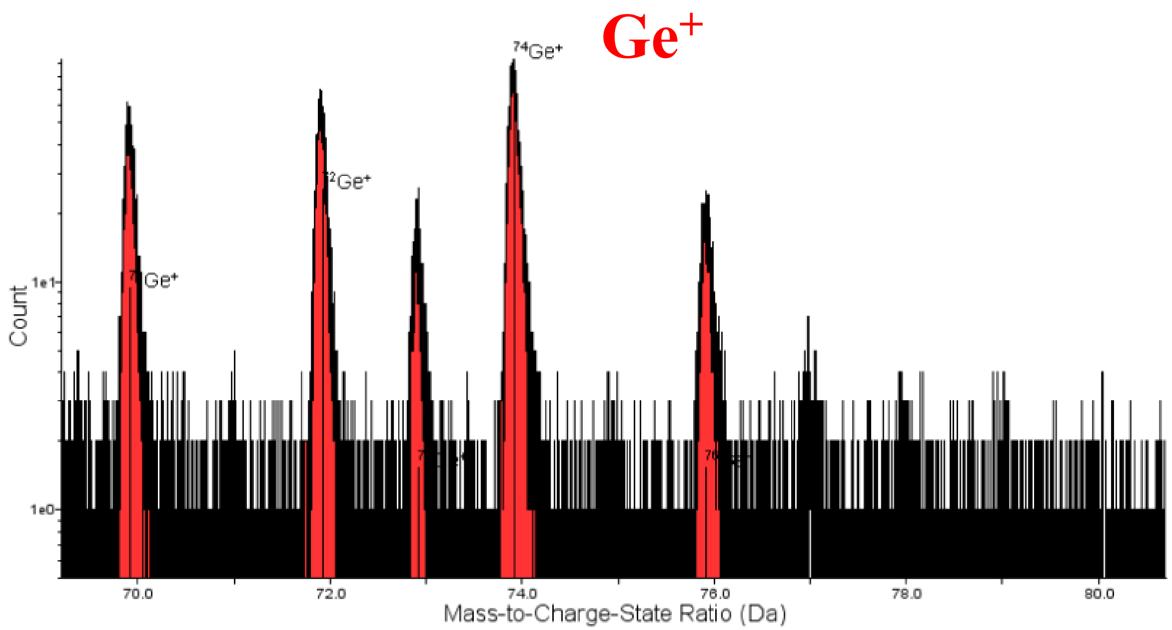

0.5 nJ and 40 K on Si substrate

- Detect Ge^{2+} and Ge^{1+} with a ratio Ge^{2+}/Ge^{1+} ~ 4.44
- No Ge molecules in the mass spectrum
- Background noise ~ 1-2

APT issues: heat flow

Ge layer grown by MBE on SOI

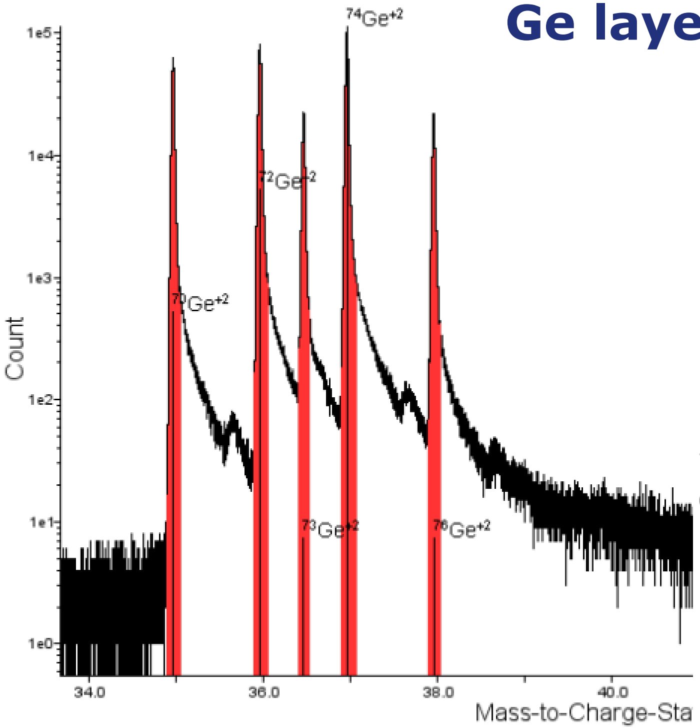

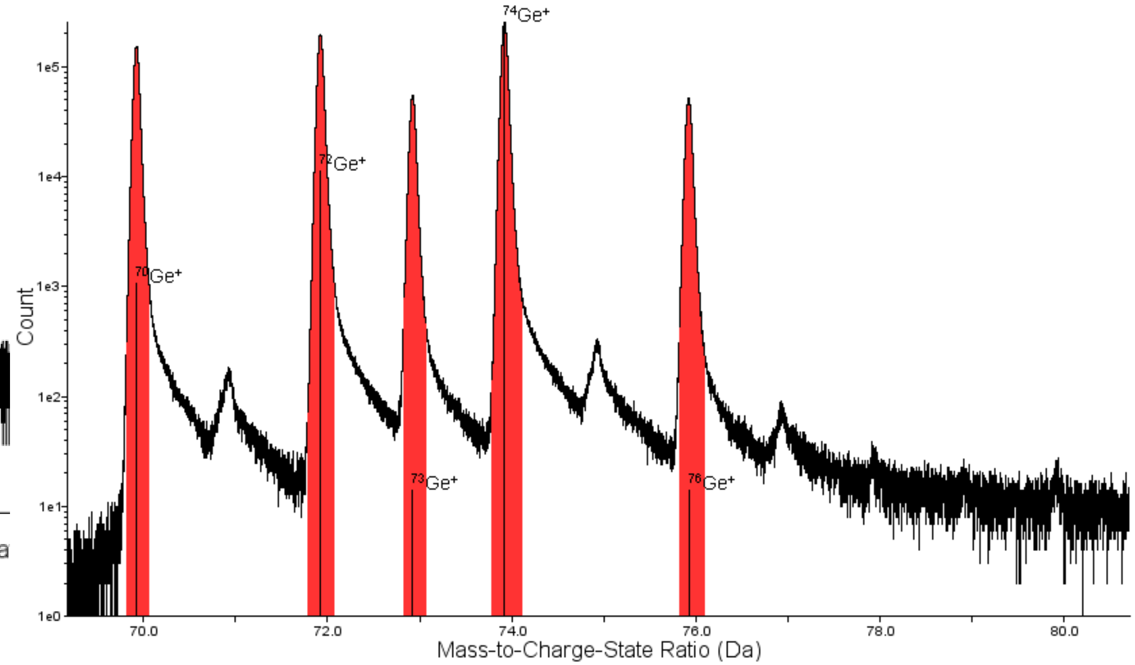

0.2 nJ and 40 K on SOI substrate

- Detect Ge^{2+} and Ge^{1+} with a ratio Ge^{2+}/Ge^{1+} ~ 0.5
- Wider Ge peaks in the mass spectrum
- Higher background noise ~ 6-10

APT issues: heat flow

Ge layer grown by MBE on SOI

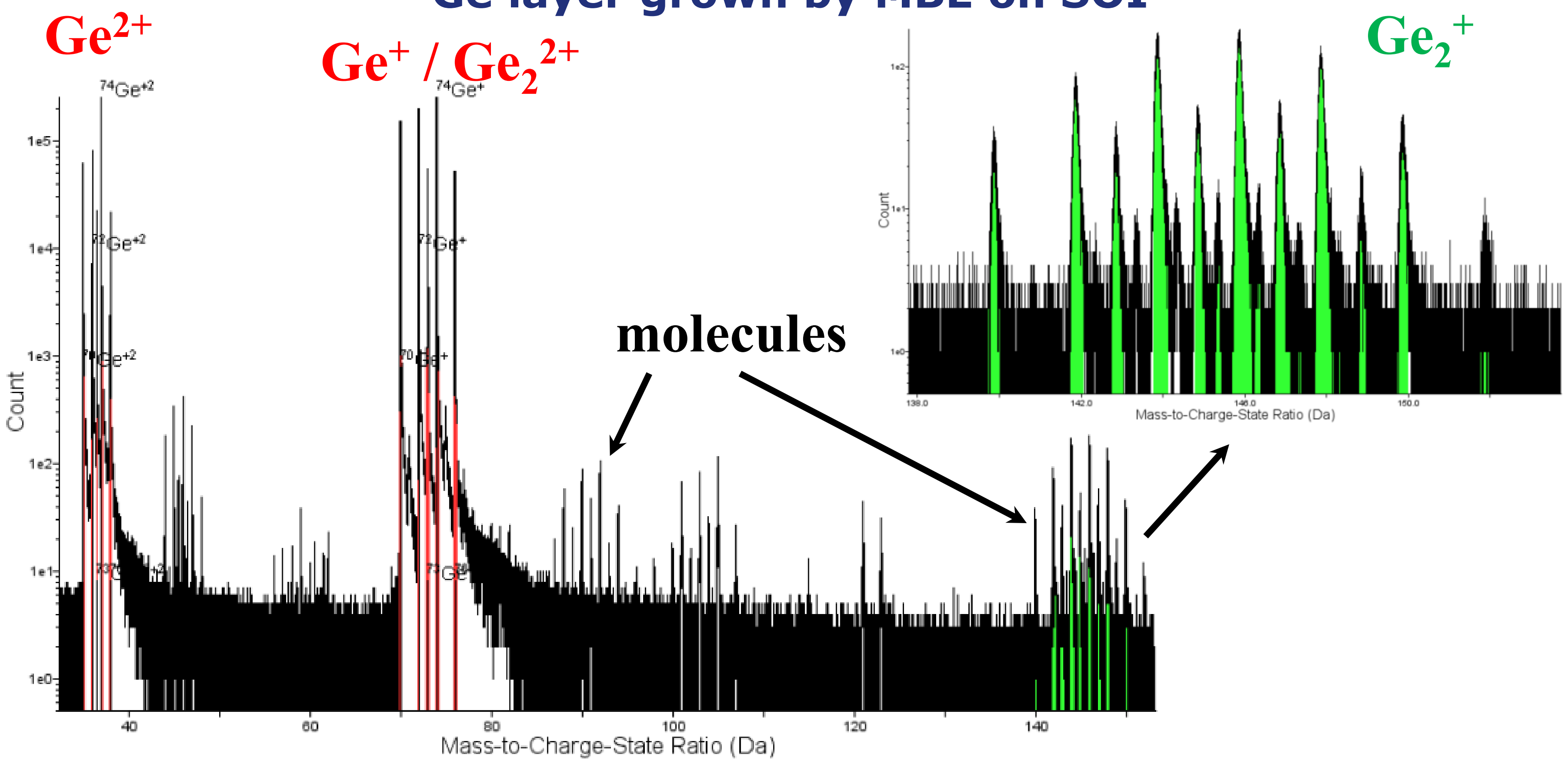

0.2 nJ and 40 K on SOI substrate

- Detect Ge_2 molecules in the mass spectrum

APT issues: heat flow

Ge layer grown by MBE on SOI

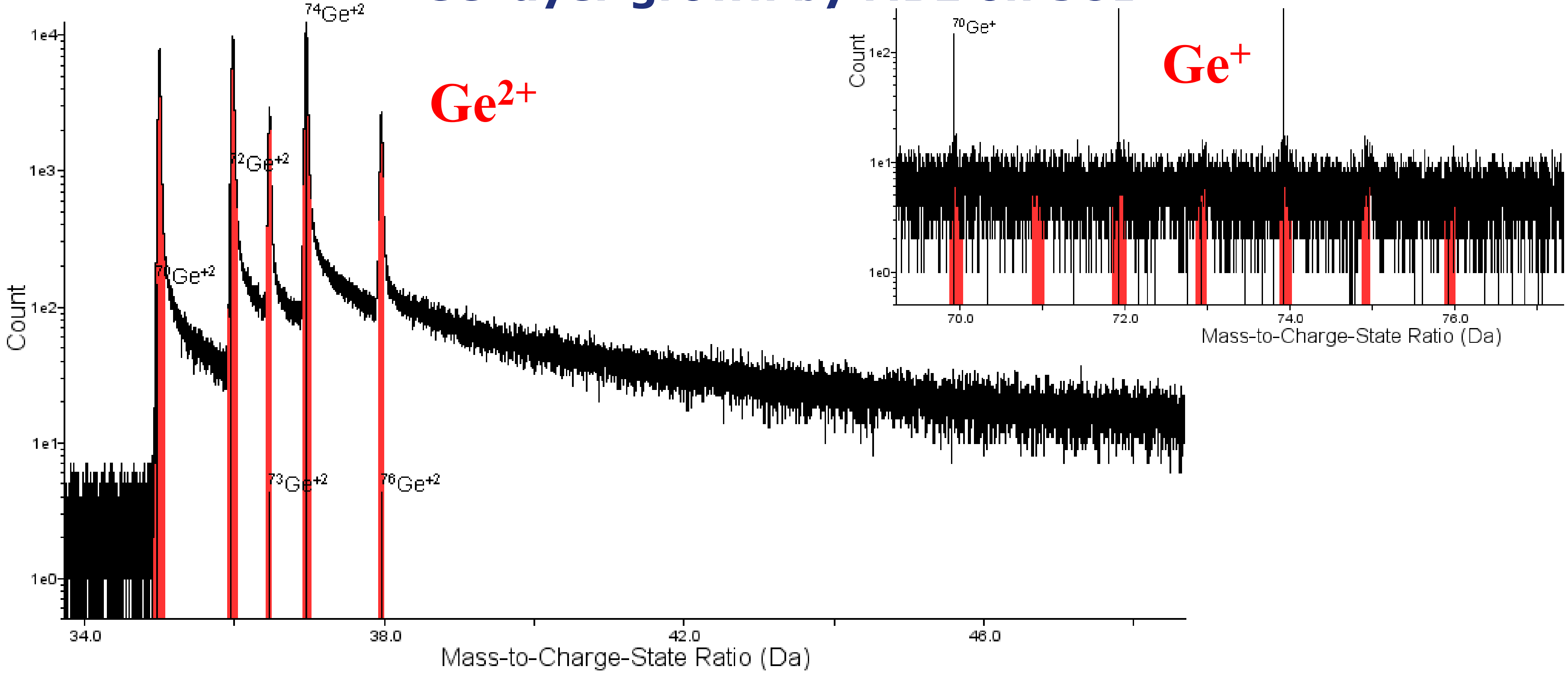

0.03 nJ and 20 K on SOI substrate

- Detect mainly Ge^{2+} with a ratio Ge^{2+}/Ge^{1+} ~ 670
- No more Ge molecules in the mass spectrum
- Background noise stays high ~ 10, specially between peaks ~ 40-100

References

- *The post-ionization of field evaporation ions: a theoretical explanation of multiple charge states*, D. Kingham, Surface Science 116 (1982) 273
- *Étude de la fonction de transfert pointe-image de la sonde atomique tomographique*, F. Vurpillot, PhD thesis (2001)
- *Estimation of the cooling times for a metallic tip under laser illumination*, F. Vurpillot, B. Gault, A. Vella, M. Bouet, and B. Deconihout, Appl. Phys. Lett. 88 (2006) 094105
- *Introduction to the method of the Field Ion Microscopy, the conventional Atom Probe and 3D-Atom Probe*, www.material.physik.uni-goettingen.de
- *Advances in the calibration of atom probe tomographic reconstruction*, B. Gault, M.P. Moody, F. de Geuser, G. Tsafnat, A. La Fontaine, L.T. Stephenson, D. Haley, S.P. Ringer, J. Appl. Phys. 105 (2009) 034913
- *Atom probe tomography*, T.F. Kelly, M.K. Miller, Rev. Sci. Instruments 78 (2007) 031101
- *Design of a delay-line position-sensitive detector with improved Performance*, G. Da Costa, F. Vurpillot, A. Bostel, M. Bouet, B. Deconihout, Rev. Sci. Instruments 76 (2005) 013304
- *Advances in the reconstruction of atom probe tomography data*, B. Gault, D.Haley, F. deGeuser, M.P. Moody, E.A. Marquis, D.J. Larson, B.P. Geiser, Ultramicroscopy 111 (2011) 448
- *Pragmatic reconstruction methods in atom probe tomography*, F. Vurpillot, M. Gruber, G. Da Costa, I. Martin, L. Renaud, A. Bostel, Ultramicroscopy 111 (2011) 1286

Acknowledgements

- Collaborators that participated to the presented APT analyses

Marion Descoins, Ivan Blum, Anthony De Luca, Nicolas Dal Bianco, Jacques Perrin-Toinin, Khalid Hoummada, and Dominique Mangelinck

- Collaborators that provided the presented samples

Claude Alfonso, Isabelle Berbezier, Lisa Michez, Omar Abbes, Luong Minh Anh, Vinh Le Thanh, Enrico Napolitani, and Antoine Ronda